University of Alberta

Examination of Alternative Oxidase Induction in *Neurospora crassa*

by

Michael Sukyoung Chae 

A thesis submitted to the Faculty of Graduate Studies and Research
in partial fulfillment of the requirements for the degree of

Doctor of Philosophy

in

Molecular Biology and Genetics

Department of Biological Sciences

Edmonton, Alberta

Spring 2008

Your file Votre référence
ISBN: 978-0-494-45403-9
Our file Notre référence
ISBN: 978-0-494-45403-9

Abstract

Disruption of the cytochrome-mediated respiratory chain in *Neurospora crassa* results in the induction of alternative oxidase, which is encoded by the nuclear *aod-1* gene. The induction of *aod-1* in response to mitochondrial dysfunction suggests that a retrograde pathway can help coordinate nuclear gene expression with the functional status of mitochondria.

In *Saccharomyces cerevisiae*, a well-characterized retrograde response involves three *RTG* genes, of which only *RTG2* had an obvious homologue in *N. crassa*. To determine if this homologue (named *rtg-2*) was involved in controlling alternative oxidase expression, *rtg-2* knockout strains were examined for their ability to induce the *aod-1* gene. These mutants displayed wild-type expression of alternative oxidase as indicated by the presence and activity of the protein only when exposed to chloramphenicol, which hinders translation of mitochondrial-encoded mRNAs, most of which code for respiratory complex components. Thus, alternative oxidase is not controlled by a pathway involving the homologue of the yeast *RTG2* gene.

To uncover sequence elements required for alternative oxidase induction, various mutations were generated in the upstream region of *aod-1*. Conidia transformed with these mutant constructs were plated on medium containing antimycin A, which inhibits complex III of the respiratory chain so that only cells expressing alternative oxidase will grow. In this manner, I identified an alternative oxidase induction motif (AIM) that consists of two directly repeated CGG triplets separated by seven base pairs. The AIM sequence is required for efficient expression of *aod-1* and resembles sequences known to be bound by Zn(II)2Cys6 binuclear cluster (zinc cluster) transcription factors.

The *aod-2* and *aod-5* genes of *N. crassa* were predicted to encode zinc cluster transcription factors. Electrophoretic mobility shift assays performed using the DNA binding domains of the AOD2 and AOD5 proteins demonstrated that these two fragments synergistically bind the AIM sequence. This binding is dependent on the integrity of the CGG repeats and the spacing between them. Pull-down assays and size-exclusion chromatography showed that the DNA binding domains of AOD2 and AOD5 physically interact. Altogether, my data suggests that an AOD2/AOD5 heterodimer activates alternative oxidase expression by binding to the AIM sequence of the *aod-1*.

Acknowledgements

There have been a number of people that have provided me with support in one form or another. I would like to start by thanking past and present members of the Nargang lab who helped to make my time in the lab so enjoyable. Special thanks go out to Andrea Descheneau, Ian Cleary, Cheryl Nargang, Katie Kessler, Colin Lin and Leanne Hahn whose work allowed me to obtain the data presented in this thesis. Of course, I must thank Frank Nargang for providing me with wisdom, encouragement and guidance. I would also like to thank all of my friends who were always ready with a helping hand whenever I needed it. You guys truly are the best around.

I must also acknowledge members of my family who have helped make me the person that I am today. I would like to start by thanking my in-laws who have welcomed me into their family and have always been so supportive. My sisters, Susan Chae-Bell and Gina Walker, helped raise me and have always treated me so well despite my duties as a younger brother. My parents, Dr. Yeh-Moon Chae and Chung Chae, have always provided me with everything that I ever needed and in most cases, even more. With their support, I always knew that I had a warm bed in which to sleep and a world-class meal. I would like to end by thanking my lovely wife Amy for being so patient and supportive, even though the last year of my degree magically turned into three. My successful graduation is truly the combined efforts of a great many people and I know that I would not have been able to do it without them.

Table of Contents

List of Tables

List of Figures

Abbreviations

A. thaliana	*Arabidopsis thaliana*
ADP	adenosine diphosphate
AIF	apoptosis inducing factor
AIM	alternative oxidase induction motif
AOD2-FLAG	bacterial lysate supernatant containing an N-terminal AOD2 fragment with a FLAG-tag
AOD2-his	bacterial lysate supernatant containing an N-terminal AOD2 fragment with a his-tag
AOD5-FLAG	bacterial lysate supernatant containing an N-terminal AOD5 fragment with a FLAG-tag
AOD5-his	bacterial lysate supernatant containing an N-terminal AOD5 fragment with a his-tag
ATP	adenosine triphosphate
BLAST	basic local alignment search tool
bp	base pair
BSA	bovine serum albumin
bZIP	basic leucine zipper
C. albicans	*Candida albicans*
cDNA	complementary deoxyribonucleic acid
CORR	co-localization for redox regulation
cpm	counts per minute
Cys_I	One of two conserved cysteine residues in the N-terminus of plant alternative oxidase; The more upstream residue
Cys_{II}	One of two conserved cysteine residues in the N-terminus of plant alternative oxidase; The more downstream residue
Da	Dalton
$\Delta\Psi$	membrane potential
DHFR	dehydrofolate reductase
DMSO	dimethylsulfoxide
DNA	deoxyribonucleic acid
dNTP	deoxynucleotide triphosphate
DTT	dithiothreitol
E. coli	*Escherichia coli*
EDTA	ethylenediaminetetraacetic acid
EMS	ethyl methanesulfonate
EMSA	electrophoretic mobility shift assay
$FAD/FADH_2$	flavin adenine dinucleotide
FGSC	Fungal Genetics Stock Center
FMN	flavin mononucleotide
g	grams

G. max	*Glycine max*
GMP	guanine monophosphate
GTP	guanosine triphosphate
HEPES	4-(2-hydroxyethyl)-1-piperazineethanesulfonic acid
hr	hours
IMS	intermembrane space
IPTG	isopropyl-beta-D-thiogalactopyranoside
kbp	kilobase pairs
KCN	potassium cyanide
KDa	kilodalton
LB	Luria-Bertani
μg	micrograms
μl	microliters
M	molar
M. grisea	*Magnaporthe grisea*
MAPK	mitogen-activated protein kinase
MBSU	Molecular Biology Service Unit
MIM	mitochondrial inner membrane
min	minutes
ml	milliliter
mM	millimolar
MOM	mitochondrial outer membrane
MOPS	3-morpholinopropanesulfonic acid
MPT	mitochondrial permeability transition
mRNA	messenger ribonucleic acid
MRR	mitochondrial retrograde regulation
mtDNA	mitochondrial deoxyribonucleic acid
N. aromaticivorans	*Novosphingobium aromaticivorans*
N. crassa	*Neurospora crassa*
N. tabacum	*Nicotiana tabacum*
NAD/NADH + H^+	nicotinamide adenine dinucleotide
NEM	*N*-ethylmaleimide
Ni-NTA	nickel-nitrilotriacetic acid
OD	optical density
P. falciparum	*Plasmodium falciparum*
PAM	presequence translocase-associated protein import motor
PAS	period, aryl hydrocarbon receptor nuclear translocator protein, single-minded
PCR	polymerase chain reaction
PEG	polyethylene glycol
PMSF	phenylmethylsulphonyl fluoride
ρ^0	strains lacking a mitochondrial genome
ρ^+	strains harboring a wild-type mitochondrial genome
RNA	ribonucleic acid
ROS	reactive oxygen species

rpm	revolutions per minute
rRNA	ribosomal ribonucleic acid
RTG	retrograde response
S. cerevisiae	*Saccharomyces cerevisiae*
S. guttatum	*Sauromatum guttatum*
S. pombe	*Schizosaccharomyces pombe*
SAM	sorting and assembly machinery
SC-Ura	synthetic complete medium without uracil
SDS	sodium dodecyl sulfate
SDS-PAGE	sodium dodecyl sulfate polyacrylamide gel electrophoresis
sec	seconds
SHAM	salicylhydroxamic acid
spp.	species
SPS	Ssy1p-Ptr3p-Ssy5
T. brucei	*Trypanosoma brucei*
TCA	tricarboxylic acid
TIM	translocase of the inner mitochondrial membrane
TOB	topogenesis of mitochondrial outer membrane beta-barrel proteins
TOM	translocase of the outer mitochondrial membrane
Tris	tris (hydroxymethyl) aminomethane
tRNA	transfer ribonucleic acid
VECTOR	bacterial lysate supernatant obtained from a strain expressing empty vector
X-gal	5-bromo-4-chloro-3-indoyl-beta-D-galacto-pyranoside

Chapter 1: General Introduction

1.1. Mitochondrial Structure

Mitochondria are multifunctional organelles that are observed in virtually all eukaryotic cells. They are bound by a double membrane, which results in the formation of four major compartments: the mitochondrial outer membrane (MOM), the mitochondrial inner membrane (MIM), the intermembrane space (IMS) and the matrix. The MIM can be further divided into two subclasses, the cristal membranes, which form specialized folds termed cristae, and the inner boundary membrane, which is thought to form contact sites with the outer membrane (FREY *et al.* 2002; VOGEL *et al.* 2006). The folded structure of the cristal membranes is thought to maximize the surface area on which oxidative phosphorylation can occur. The two classes of MIM are separated by cristae junctions, which are believed to form small openings that separate the IMS from the intracristal space. Mitochondria are able to specifically localize proteins and molecules to each of these domains resulting in the formation of compartments and membranes that allow specialized functions to occur in each (LOGAN 2006; VOGEL *et al.* 2006). Mitochondria can be observed in numerous conformations such as the traditional kidney bean shaped structure or as a branching reticulum whose morphology is constantly changing through continual fusion and fission events (HOPPINS *et al.* 2007; SHAW and NUNNARI 2002). The morphology that mitochondria assume is usually related to the developmental stage and cell type in which they are found (CHAN 2006; WESTERMANN and PROKISCH 2002; YAFFE 1999).

1.2. The Origin of Mitochondria

The generally accepted explanation for the origin of mitochondria is known as the endosymbiotic theory (LANG *et al.* 1999; MARGULIS 1970). This theory postulates that mitochondria are remnants of an α-proteobacterium that was engulfed by a primitive host cell. This idea is supported by phylogenetic analyses which suggest that several mitochondrial-encoded proteins and ribosomal RNAs (rRNAs) are very closely related to their counterparts in α-proteobacteria (ANDERSSON *et al.* 2003; GERMOT *et al.* 1996;

GRAY *et al.* 1999; GRAY *et al.* 1989; GUPTA 1995; YANG *et al.* 1985). Initially, it was thought that this endosymbiotic relationship resulted from the host's provision of favored carbon intermediates and protection from harsh environmental conditions in exchange for the energy molecule adenosine triphosphate (ATP) (ANDERSSON *et al.* 2003). However, at its most basic level, this hypothesis seems flawed as it assumes that the mitochondrial ancestor possessed ATP excretion machinery, which is not likely since such systems are not observed in modern day bacteria (ANDERSSON *et al.* 1998; MARTIN and MULLER 1998). In light of this, several additional hypotheses have been proposed that address the origins of the endosymbiotic relationship that gave rise to mitochondria.

The ox-tox hypothesis speculates that the accumulation of oxygen within the atmosphere was the primary driving force behind the symbiotic relationship (ANDERSSON and KURLAND 1999; KURLAND and ANDERSSON 2000). Here, the aerobic endosymbiont employed cellular respiration to remove oxygen molecules which were toxic to the anaerobic host. This relationship was maintained by selective pressure resulting from the accumulation of high oxygen levels in the atmosphere attributed to the increased number of photosynthetic organisms. Another hypothesis, the hydrogen hypothesis, proposes that the host was a hydrogen-dependent anaerobe that became dependent on and eventually engulfed a symbiont, which produced hydrogen and carbon dioxide as waste products of metabolism (MARTIN and MULLER 1998). A similar hypothesis, called the syntrophy hypothesis, also implicates interspecies hydrogen transfer as the driving force of endosymbiosis, but suggests that the mitochondrial predecessor relied on methane produced by the host cell (MOREIRA and LOPEZ-GARCIA 1998). A common feature to all three hypotheses is that they predict that the evolution of the machinery to export ATP from mitochondria occurred after the establishment of the endosymbiotic relationship.

1.2.1. Hydrogenosomes and mitosomes

Several amitochondriate species have been observed that harbor hydrogenosomes or mitosomes, which are believed to have evolved from the same α-proteobacterial ancestor as present-day mitochondria (EMBLEY *et al.* 2003; HACKSTEIN *et al.* 2006; MULLER 1993; TOVAR *et al.* 1999). For instance, hydrogenosomes have been observed in the parasitic protozoan *Trichomonas vaginalis*, while the intestinal parasite *Giardia*

intestinalis is known to carry mitosomes (DOLEZAL *et al.* 2005; REGOES *et al.* 2005). Like mitochondria, both of these organelles are bound by a double membrane. However, virtually all hydrogenosomes and mitosomes examined do not contain DNA, cytochromes or a complete citric acid cycle (BUI *et al.* 1996; LEON-AVILA and TOVAR 2004). Hydrogenosomes synthesize ATP by substrate level phosphorylation, which is accompanied by the production of hydrogen gas (BUI *et al.* 1996). Conversely, mitosomes have lost the ability to generate ATP (AGUILERA *et al.* 2007). The only function common to all three of these organelles appears to be the synthesis of iron-sulphur clusters (EMBLEY *et al.* 2003; TOVAR *et al.* 2003). Thus, it has been recently hypothesized that iron-sulphur cluster production was the driving force behind the original endosymbiosis between the α-proteobacterium and its host cell (LILL and KISPAL 2000; TOVAR *et al.* 2003). Interestingly, the hydrogenosomes of *Nyctotherus ovalis* have recently been shown to possess a genome and functional respiratory complexes I and II suggesting that it may be a "missing link" between mitochondria and hydrogenosomes (BOXMA *et al.* 2005).

1.3. Mitochondrial Genomes

Mitochondria harbor DNA that is believed to have originated from the genome of the α-proteobacterium from which they were derived. While almost all mitochondrial genomes are circular, some organisms such as *Tetrahymena spp.* and *Jakoba spp.* are known to possess linear mitochondrial DNA (mtDNA) (GRAY *et al.* 1999; LANG *et al.* 1999). The size of the mitochondrial genome varies greatly from organism to organism: only 6 kbp in the malaria-causing parasite *Plasmodium falciparum*, but almost 270 kbp in *Arabidopsis thaliana* (GRAY *et al.* 1999; UNSELD *et al.* 1997). The number of mitochondrial genes and the specific products that they encode also vary among mitochondrial genomes (LANG *et al.* 1999). For instance, the mtDNA of *P. falciparum* encodes only three mitochondrial proteins and two rRNA genes, while the 65 kbp mtDNA of *Neurospora crassa* encodes 2 rRNAs, 27 transfer RNAs (tRNAs), 15 known polypeptides and 5 unidentified reading frames (GRIFFITHS *et al.* 1995; LANG *et al.* 1999). The Jakobid protist *Reclinomonas americana* possesses the largest repertoire of

mitochondrial-encoded genes and has thus been termed the "missing link" between present day mitochondria and their bacterial ancestor (LANG *et al.* 1997; PALMER 1997). Conversely, the α-proteobacterium *Rickettsia prowazekii* harbors a highly reduced genome that most resembles the DNA observed in mitochondria (ANDERSSON *et al.* 1998).

1.3.1. Transfer of mitochondrial genes to the nucleus

Variation in the coding capacity among mitochondrial genomes can likely be explained by the differential migration of mitochondrial-encoded genes to the nucleus. For example, *cox2*, which encodes subunit 2 of cytochrome *c* oxidase, is located within the mtDNA of some plants, found in the nuclear genome of others, and in some cases is observed in both (ADAMS *et al.* 1999; COVELLO and GRAY 1992; DALEY *et al.* 2002). These data suggest that migration of the *cox2* gene from the mitochondrial genome to the nucleus is a recent and on-going event. It has been hypothesized that the transfer of DNA from the mitochondria to the nucleus may be favored in evolutionary terms because mitochondria cannot repair mutations through recombination and thus mtDNA rapidly accumulates deleterious mutations (BLANCHARD and LYNCH 2000). While the precise method through which this migration occurs is unknown, DNA transformed into the mitochondria of yeast cells has been observed to spontaneously migrate to the nucleus (THORSNESS and FOX 1990).

Despite the on-going transfer of mtDNA to the nucleus, certain genes have been retained in the mitochondrial genome. The hydrophobicity and the co-localization for redox regulation (CORR) hypotheses have been proposed to explain why certain genes have not been transferred to the nucleus. The hydrophobicity hypothesis suggests that some genes are trapped within the mitochondrial genome because their gene products are extremely hydrophobic (MARTIN and HERRMANN 1998; VON HEIJNE 1986). The hydrophobic nature of these proteins is predicted to interfere with mitochondrial targeting or import, and may even result in cell toxicity. This hypothesis is supported by work in soybean (*Glycine max*) where it was shown that nuclear-encoded Cox2 displayed a reduced local hydrophobicity compared to its mitochondrial-encoded counterpart (DALEY *et al.* 2002). Conversely, the CORR hypothesis postulates that mitochondrial genomes

maintain genes whose expression are subject to redox regulation (ALLEN 2003). As a result, mitochondria can respond more quickly to changes in redox state, an ability that would be lost if these genes were transferred to the nucleus.

1.4. Mitochondrial Protein Import

1.4.1. Import into and across the MOM

Since most mitochondrial proteins are now encoded in the nucleus, mitochondria have evolved import machinery that ensures the delivery of proteins to the appropriate mitochondrial compartment (Figure 1.1) (WIEDEMANN *et al.* 2004). Import of virtually all nuclear-encoded mitochondrial proteins is initiated through interaction with the translocase of the outer mitochondrial membrane (TOM) complex. The TOM complex is comprised of the pore-forming protein Tom40, three receptor proteins Tom20, Tom22 and Tom70, and three small Tom proteins, Tom5, Tom6 and Tom7. The outer membrane receptors Tom20 and Tom22 bind preproteins with an N-terminal signal sequence, consisting of 10-80 amino acids arranged in an amphipathic α-helix (ABE *et al.* 2000; BRIX *et al.* 2000; GRAD *et al.* 1999; NARGANG *et al.* 1998; VON HEIJNE 1989). Alternatively, Tom70 is involved in the recognition of proteins containing cryptic internal targeting sequences (BRIX *et al.* 1999; WIEDEMANN *et al.* 2001). The binding of precursor proteins to the surface receptors of mitochondria is followed by translocation through the general insertion pore, Tom40 (AHTING *et al.* 1999; HILL *et al.* 1998). Tom5, Tom6 and Tom7 are thought to be involved in the assembly and/or stability of the TOM complex, although in yeast, Tom5 is also thought to facilitate the transfer of preproteins from the receptors to Tom40 (ALCONADA *et al.* 1995; DIETMEIER *et al.* 1997; HONLINGER *et al.* 1996; MODEL *et al.* 2001; SHERMAN *et al.* 2005). Once the mitochondrial proteins have passed through the TOM complex, they are directed to the correct mitochondrial sub-compartment by one of several additional import pathways.

While simple outer membrane proteins can be inserted into the MOM by the TOM complex alone, those with a more complex conformation must interact with the topogenesis of mitochondrial outer membrane beta-barrel proteins (TOB) complex,

Figure 1.1. Mitochondrial protein import machinery. Nuclear-encoded mitochondrial proteins are targeted to mitochondria by an N-terminal amphipathic α-helix, which is ultimately removed to give the mature protein sequence, or through cryptic internal sequences which are part of the mature protein. Virtually all of these proteins initiate their import by interacting with the TOM complex, which inserts simple outer membrane proteins directly into the MOM or transfers proteins destined for other mitochondrial compartments to additional pathways of import. β-barrel proteins of the MOM must be passed from the TOM complex to the TOB complex to ensure their proper assembly within the outer membrane. The transfer of proteins from the TOM complex to the TOB complex is facilitated by two complexes within the IMS composed of Tim8/Tim13 or Tim9/Tim10, which are believed to act as chaperones. A disulphide relay system involving Mia40 and Erv1 has been shown to be required for the import of small IMS proteins that contain cysteine residues in common motifs. Proteins bound for the matrix or inner membrane proteins adopting a simple conformation are passed from the TOM complex to the TIM23 complex. Tim21 appears to coordinate the association of the TIM23 complex with either the TOM complex or the ATP-dependent presequence translocase-associated protein import motor (PAM) complex. Import of matrix-bound proteins is achieved using the PAM complex. The N-terminal presequence is then removed by the mitochondrial processing peptidase (MPP). MIM proteins that contain several transmembrane domains, such as the carrier proteins, are passed from the TOM complex to the TIM22 complex, a transfer that is again facilitated by the chaperones Tim8/Tim13 and Tim9/Tim10. The TIM22 complex inserts the proteins into the MIM. Inner membrane proteins encoded by the mitochondrial genome are inserted into the MIM by the Oxa1 protein through a process known as mitochondrial export. The Oxa1 protein can also export a small class of MIM proteins which have passed through the TOM and TIM23 complexes and function in the MIM. The numbers indicated in each protein subunit of the various complexes indicates their approximate molecular mass.

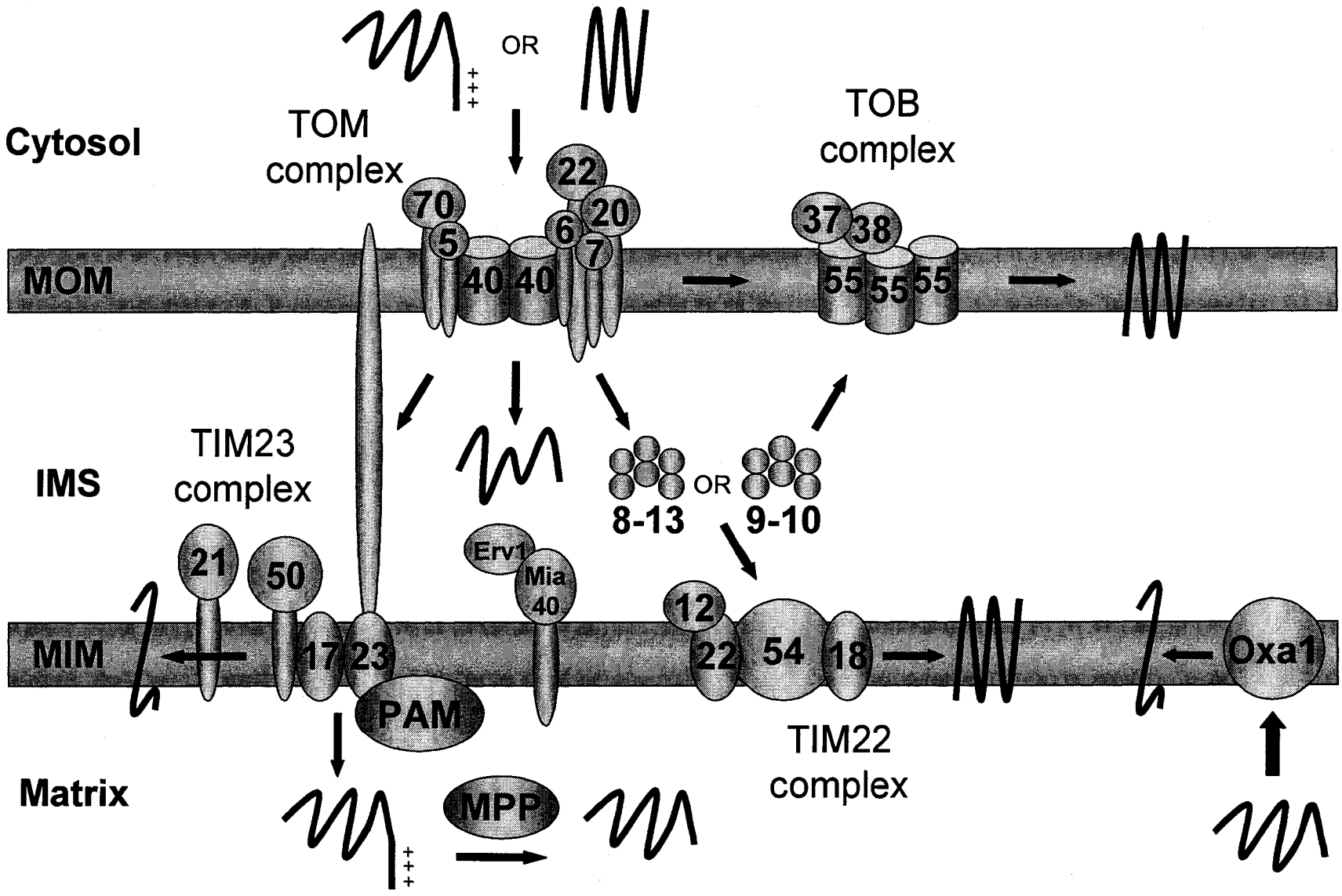
Cytosol
TOM complex
OR
TOB complex
22
70
20
6
5
7
37
38
MOM
40
40
55
55
55
IMS
TIM23 complex
8-13
OR
9-10
21
50
Erv1
Mia 40
12
MIM
17
23
22
54
18
Oxa1
PAM
TIM22 complex
Matrix
MPP

which is also known as the sorting and assembly machinery (SAM) complex. The TOB/SAM complex consists of three core proteins, Tom37 (Sam37/Mas37), Tom38 (Sam35/Tob38) and Tob55 (Sam50/Omp85) (GENTLE *et al.* 2004; HABIB *et al.* 2005; HABIB *et al.* 2007; HOPPINS *et al.* 2007b; ISHIKAWA *et al.* 2004; KOZJAK *et al.* 2003; MILENKOVIC *et al.* 2004; PASCHEN *et al.* 2005; WAIZENEGGER *et al.* 2004; WIEDEMANN *et al.* 2003). Although the precise mechanisms are unclear, the TOB/SAM complex assembles β-barrel proteins, such as Tom40 and porin, into the MOM.

It was originally thought that proteins destined for the IMS were simply imported through the TOM complex. However, recent evidence has shown that the import of small cysteine-rich IMS proteins requires Mia40 and Erv1 (ALLEN *et al.* 2005; CHACINSKA *et al.* 2004; MULLER *et al.* 2007; RISSLER *et al.* 2005; TERZIYSKA *et al.* 2007). These two proteins localize to the IMS and are involved in a disulphide relay system that is required for the import of certain IMS proteins (BIHLMAIER *et al.* 2007; GABRIEL *et al.* 2007; MESECKE *et al.* 2005; TERZIYSKA *et al.* 2007).

1.4.2. Import into and across the MIM

Mitochondrial proteins destined for the matrix or the MIM are transferred from the TOM complex to one of two translocases of the mitochondrial inner membrane (TIM). The TIM23 complex, which contains Tim23, Tim50, Tim17 and Tim21, recognizes proteins containing N-terminal presequences and inserts them directly into the MIM or imports them into the mitochondrial matrix (STOJANOVSKI *et al.* 2006). As preproteins exit the TOM complex, they are sequestered to the TIM23 complex by Tim50 (MEINECKE *et al.* 2006; MOKRANJAC *et al.* 2003; YAMAMOTO *et al.* 2002). The transfer of preproteins from the TOM complex to the TIM23 complex requires Tim21, which tethers the two complexes together during early import (CHACINSKA *et al.* 2005; VAN DER LAAN *et al.* 2006; WIEDEMANN *et al.* 2007). However, Tim21 is believed to dissociate from the TIM23 complex during translocation of matrix-bound, but not MIM, proteins (WIEDEMANN *et al.* 2007). The pore of the TIM23 complex is believed to be formed by Tim23, although Tim17 may be necessary for pore formation and/or function (MARTINEZ-CABALLERO *et al.* 2007; MOKRANJAC and NEUPERT 2005). The movement of matrix proteins through the TIM23 complex requires both membrane potential ($\Delta\Psi$)

and the ATP-dependent presequence translocase-associated protein import motor (PAM) complex (BAUER *et al.* 1996; TRUSCOTT *et al.* 2003). Once in the matrix, the N-terminal presequence is cleaved by the mitochondrial processing peptidase (LUCIANO and GELI 1996).

The TIM22 complex, which includes Tim22, Tim18, Tim54 and Tim12, is generally responsible for the import of hydrophobic MIM proteins that carry multispanning membrane domains and internal targeting sequences (KERSCHER *et al.* 1997; KERSCHER *et al.* 2000; KOVERMANN *et al.* 2002; SIRRENBERG *et al.* 1996). Two small Tim complexes Tim8/Tim13 and Tim9/Tim10 are thought to act as chaperones, shuttling the hydrophobic proteins from the TOM complex to the TIM22 complex (CURRAN *et al.* 2002a; CURRAN *et al.* 2002b; DAVIS *et al.* 2000; PASCHEN *et al.* 2000). Tim12 is required for the docking of the small Tim complexes, which allows for subsequent translocation through the MIM pore that is formed by Tim22 (BAUD *et al.* 2007; KOVERMANN *et al.* 2002). The insertion of proteins into the MIM by the TIM22 complex is dependent on $\Delta\Psi$, but does not require ATP-dependent machinery (KOVERMANN *et al.* 2002; REHLING *et al.* 2003). The functions of Tim18 and Tim54 are currently unknown.

1.4.3. Mitochondrial protein export

Some proteins are transferred from the mitochondrial matrix to the MIM through the process of mitochondrial protein export. This includes a few nuclear-encoded proteins that have been imported through the TOM and TIM23 complexes, as well as several mitochondrial-encoded gene products synthesized within the mitochondrial matrix. This pathway of protein transport is referred to as "export" since it occurs in the opposite direction of the major import pathways. Mitochondrial export is facilitated by the translocase encoded by the nuclear *oxa-1* gene (FIUMERA *et al.* 2007; HERRMANN and BONNEFOY 2004; HERRMANN and NEUPERT 2003; NARGANG *et al.* 2002; SAKAMOTO *et al.* 2000; STUART 2002).

1.5. Mitochondrial Function

1.5.1. Metabolism

Although mitochondria are best known for their role in ATP production, they are also involved in several other important cellular processes. In many species, mitochondria are involved in the breakdown of fatty acids through the process of β-oxidation (BARTLETT and EATON 2004). Mitochondria also participate in the urea cycle as well as the biosynthesis of heme, arginine and ketone bodies (HEGARDT 1999; HENTZE *et al.* 2004; NASSOGNE *et al.* 2005; WU and MORRIS 1998). Calcium signaling is also controlled in part by mitochondria, which can store and release calcium ions (GIACOMELLO *et al.* 2007; SZABADKAI *et al.* 2006).

1.5.2. Production of iron-sulphur clusters

The assembly of iron-sulphur clusters also occurs within mitochondria. Iron-sulphur cluster are cofactors that are able to transport electrons, catalyze enzymatic reactions and regulate protein function (GERBER and LILL 2002; LILL and MUHLENHOFF 2005; ROUAULT and TONG 2005; ZHENG *et al.* 1998). The iron-sulphur clusters synthesized in mitochondria are incorporated into proteins that reside in mitochondria, the cytosol and the nucleus (KISPAL *et al.* 1999). The manner through which iron-sulphur clusters are produced is highly conserved as demonstrated by the remarkable similarity between the assembly machinery observed in mitochondria of eukaryotes and modern day bacteria (LILL and KISPAL 2000; SCHILKE *et al.* 1999). To date, there are ten proteins that are thought to be involved in the assembly of iron-sulphur clusters (LILL and MUHLENHOFF 2005).

Generation of iron-sulphur clusters in mitochondria requires a sulphur donor and a scaffolding protein on which the iron-sulphur cluster is formed. In yeast, these functions are performed by the proteins Nfs1p and Isu1p, respectively (MUHLENHOFF *et al.* 2003; YUVANIYAMA *et al.* 2000). Initiation of iron-sulphur cluster synthesis involves the transfer of a sulphur atom from Nfs1p to a cysteine residue of Isu1p (LILL and MUHLENHOFF 2005). Yfh1p, or its human homologue frataxin, then delivers reduced iron to sulphur-bound Isu1p (GERBER *et al.* 2003; YOON and COWAN 2003). Although the specific mechanisms have not been uncovered, additional factors, such as ferredoxin

(Yah1p), ferredoxin reductase (Arh1p) and glutaredoxin (Grx5p) are believed to be involved in the maturation of iron sulfur clusters or the transfer of these cofactors to the appropriate targets (LANGE *et al.* 2000; LI *et al.* 2001a; RODRIGUEZ-MANZANEQUE *et al.* 2002).

The importance of the iron-sulphur cluster assembly machinery is emphasized by the high degree of conservation observed between prokaryotes and eukaryotes. In fact, proteins containing iron-sulphur clusters are involved in many important cellular processes such as oxidative phosphorylation, cytosolic ribosome biogenesis and mitochondrial heme production (ATAMNA *et al.* 2002; BARROS *et al.* 2002; KISPAL *et al.* 2005; LILL and MUHLENHOFF 2005; YARUNIN *et al.* 2005). Mutation of iron-sulphur cluster assembly factors in *Saccharomyces cerevisiae* results in cell death or extremely slow growth phenotypes (LILL and MUHLENHOFF 2005). In humans, Friedreich's ataxia is caused by loss of frataxin, which results in the formation of abnormal iron-sulphur clusters and the accumulation of iron within mitochondria (PUCCIO and KOENIG 2000; ROUAULT and TONG 2005).

1.5.3. The Krebs cycle

Reactions of the Krebs cycle, which is also called the citric acid or tricarboxylic acid (TCA) cycle, are catalyzed by enzymes that reside in the mitochondrial matrix (Figure 1.2). The Krebs cycle is a key component of carbohydrate metabolism, converting pyruvate to other useful organic molecules, and coupling these reactions to energy production. Pyruvate, which is formed through glycolytic reactions in the cytosol, is imported into mitochondria where it is irreversibly converted to acetyl-CoA by pyruvate dehydrogenase (PLAXTON 1996; TOVAR-MENDEZ *et al.* 2003). Acetyl-CoA can then enter the Krebs cycle where it is eventually converted to carbon dioxide and energy-rich molecules (PITHUKPAKORN 2005). Each molecule of acetyl-CoA that enters the Krebs cycle results in the formation of one molecule of guanosine triphosphate (GTP), three molecules of $NADH + H^+$ and one molecule of reduced flavine adenine dinucleotide ($FADH_2$) (PITHUKPAKORN 2005; VAN HELLEMOND *et al.* 2005). $NADH + H^+$ and $FADH_2$ transfer electrons to the respiratory chain thereby facilitating the production of ATP molecules.

Figure 1.2. The Krebs cycle. The Krebs cycle begins when a molecule of acetyl-CoA combines with oxaloacetate to generate the six carbon molecule citrate. Through a series of reactions catalyzed by various enzymes, citrate is converted back to oxaloacetate, allowing the cycle to initiate again. Each molecule of acetyl-CoA that enters the Krebs cycle results in the generation of two molecules of carbon dioxide, one molecule of GTP, one molecule of $FADH_2$ and three molecules of $NADH + H^+$. $FADH_2$ and $NADH + H^+$ pass their electrons to the cytochrome-mediated respiratory chain thereby facilitating further energy production.

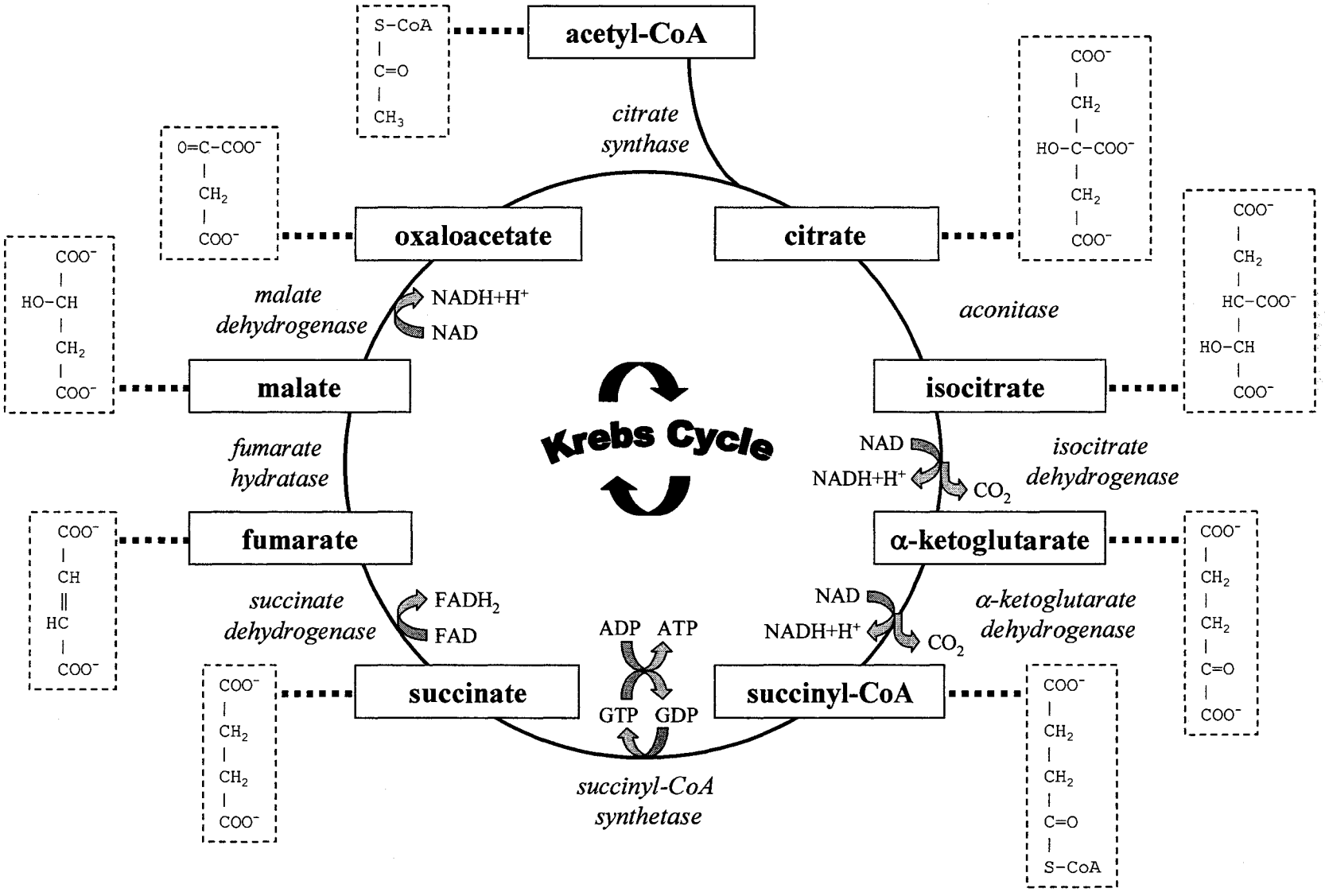
acetyl-CoA
citrate synthase
oxaloacetate
citrate
malate dehydrogenase
NADH+H+
NAD
aconitase
malate
isocitrate
Krebs Cycle
fumarate hydratase
NAD
NADH+H+
CO2
isocitrate dehydrogenase
fumarate
α-ketoglutarate
succinate dehydrogenase
FADH2
FAD
ADP ATP
GTP GDP
NAD
NADH+H+
CO2
α-ketoglutarate dehydrogenase
succinate
succinyl-CoA
succinyl-CoA synthetase

Although the Krebs cycle is integral to energy production, several of its intermediates are also involved in other biosynthetic pathways. The amino acids glutamate and aspartate are produced through the transamination of the Krebs cycle intermediates α-ketoglutarate and oxaloacetate, respectively (LANOUE *et al.* 2001; NISSIM *et al.* 2003). The Krebs cycle can also participate in fatty acid biosynthesis through its production of citrate, which is transported to the cytosol and then converted to the fatty acid precursor acetyl-CoA (AOSHIMA 2007; VAN HELLEMOND *et al.* 2005). The Krebs cycle intermediate succinyl-CoA is required for production of aminolevulinic acid, which is the first step in the synthesis of porphyrins (FUKUDA *et al.* 2005). Porphyrins can interact with iron atoms to form molecules of heme. Malate, another substrate synthesized within the Krebs cycle, can be exported to the cytosol where it can be used to regenerate pyruvate, which can subsequently be used for gluconeogenesis (JITRAPAKDEE *et al.* 2006; MACDONALD 1995).

Although intermediates of the Krebs cycle can be consumed by other biosynthetic pathways, they can also be replenished through anaplerotic reactions. For example, pyruvate can be directly converted to oxaloacetate by the enzyme pyruvate carboxylase (JITRAPAKDEE *et al.* 2006; OWEN *et al.* 2002). This bypasses the reaction catalyzed by pyruvate kinase, an enzyme that is under strict adenylate control (TURPIN *et al.* 1990; VANLERBERGHE and ORDOG 2002). In addition, fatty acid oxidation can replenish the acetyl-Co-A molecules required to convert oxaloacetate to citrate, which is the first reaction of the Krebs cycle (BUTOW and AVADHANI 2004).

1.5.4. Oxidative phosphorylation

The process of oxidative phosphorylation involves five complexes that are located in the MIM: NADH:ubiquinone oxidoreductase (Complex I), succinate:ubiquinone oxidoreductase (Complex II), ubiquinol:cytochrome *c* oxidoreductase (Complex III), ferrocytochrome *c*:oxygen oxidoreductase (Complex IV) and ATP synthase (Complex V) (HATEFI 1985; JOSEPH-HORNE *et al.* 2001). In respiratory competent cells, the reduced electron carriers, $NADH + H^+$ and $FADH_2$, donate their electrons to complexes I and II, respectively (Figure 1.3). From here, electrons are shuttled through ubiquinone, complex III, cytochrome *c* and finally to complex IV, where they are passed to molecular oxygen,

Figure 1.3. The electron transport chain. Initiation of the electron transport chain occurs when electron carriers, NADH + H+ and $FADH_2$, transfer their electrons to complexes I and II, respectively. NADH + H+ can also donate electrons to external (ND_{EX}) and internal (ND_{IN}) alternative NADH dehydrogenases. From here, the electrons are shuttled through ubiquinone (Q), complex III, cytochrome *c* (*c*), and finally to complex IV, where they are accepted by molecular oxygen, along with four hydrogen ions, to form water. Proton pumping, which occurs at complexes I, III and IV creates a chemiosmotic gradient that is used by ATP synthase (complex V) to produce ATP molecules. When oxidative phosphorylation is inhibited by antimycin A (star) at complex III or cyanide (triangle) at complex IV, alternative oxidase (AOD) is produced. Alternative oxidase accepts electrons from ubiquinol, and donates them directly to oxygen. Since alternative oxidase bypasses complexes III and IV, net ATP production is decreased. However, oxidation of ubiquinol by alternative oxidase allows recycling of electron carriers and ATP production to continue via complex I.

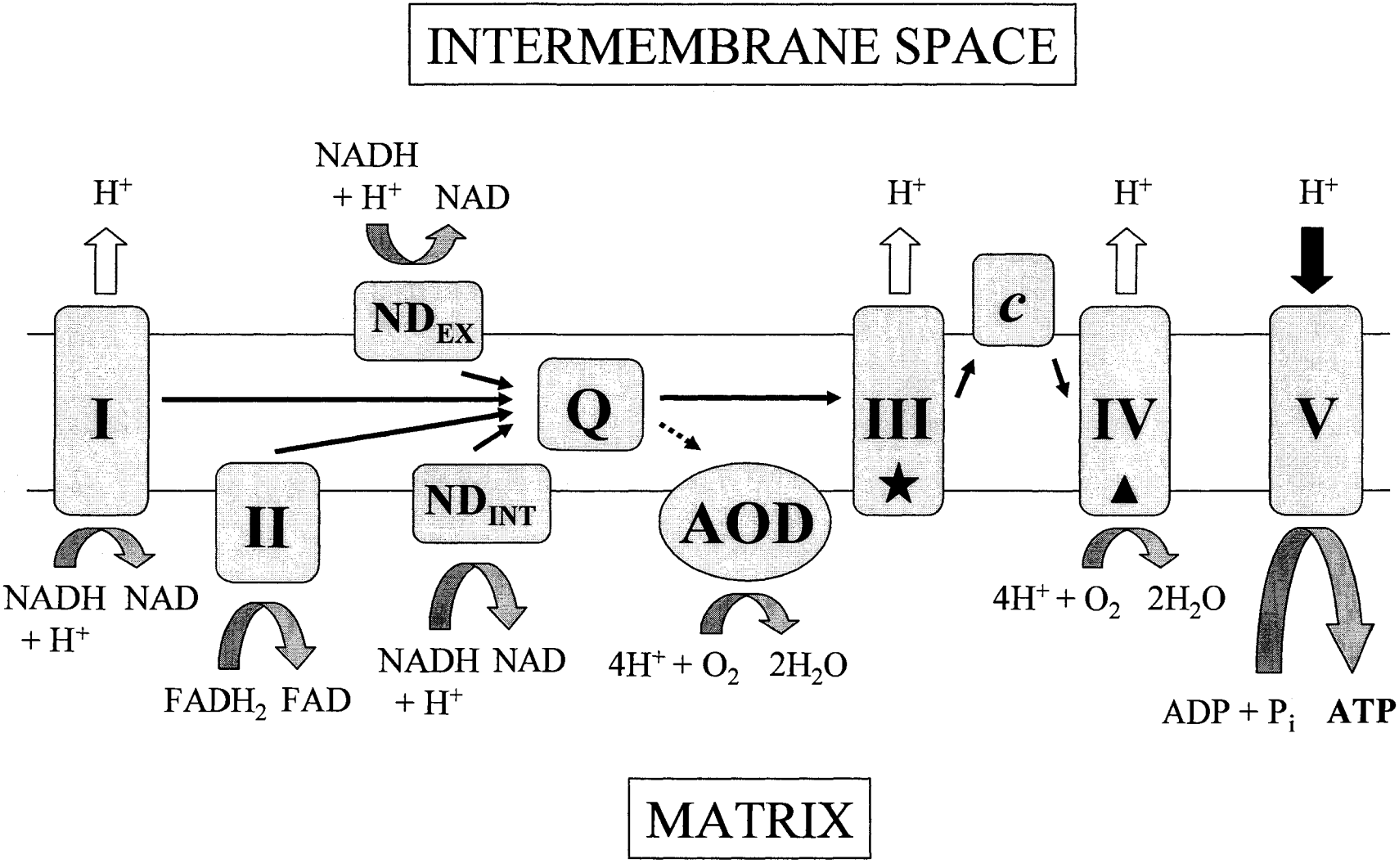
INTERMEMBRANE SPACE
NADH
+ H+ NAD
H+
H+
H+
H+
NDEX
c
I
Q
III
IV
V
II
NDINT
AOD
NADH NAD
+ H+
FADH2 FAD
NADH NAD
+ H+
4H+ + O2 2H2O
4H+ + O2 2H2O
ADP + Pi ATP
MATRIX

along with four hydrogen ions to form water. The movement of electrons through the electron transport chain enables complexes I, III and IV to pump protons from the mitochondrial matrix to the IMS, creating a chemiosmotic gradient across the MIM. This potential energy is harnessed by ATP synthase to generate ATP.

In addition to the five respiratory complexes mentioned above, plants and fungi possess alternative NADH dehydrogenases (JOSEPH-HORNE *et al.* 2001; KERSCHER 2000). These enzymes are able to transfer electrons from cytosolic or mitochondrial $NADH + H^+$ to ubiquinone and thus are considered to be non-energy conserving since they bypass proton pumping through complex I (KERSCHER *et al.* 2007). Some organisms such as *S. cerevisiae* do not possess complex I and thus the oxidation of $NADH + H^+$ occurs exclusively through alternative NADH dehydrogenases (FRIEDRICH *et al.* 1995; JOSEPH-HORNE *et al.* 2001). *N. crassa* has a functional complex I and at least three non-protein pumping NADH dehydrogenases (JOSEPH-HORNE *et al.* 2001). Examination of *N. crassa* strains mutant for alternative NADH dehydrogenases suggests that these enzymes may be involved in spore germination and hyphal branching (CARNEIRO *et al.* 2004; DUARTE *et al.* 2003).

Electron flow through the cytochrome-mediated respiratory chain can be impeded through exposure to various chemicals. Inhibitors such as rotenone, antimycin A and cyanide can block the electron transport chain through their interactions with complex I, III, or IV, respectively (PAPA *et al.* 1975; SINGER and RAMSAY 1994; VAN BUUREN *et al.* 1972; ZHANG *et al.* 1998). In addition, electron transport can be obstructed indirectly through the addition of chloramphenicol, which hinders translation of mitochondrial-encoded proteins, most of which are components of respiratory complexes (SCHLUNZEN *et al.* 2001). The presence of inhibitors impedes electron flow, which results in a cessation of proton pumping and accumulation of the reduced forms of all respiratory complexes and electron carriers preceding the blocked site.

1.5.5. Apoptosis

Apoptosis is a method of programmed cell death that permits the safe disposal of unwanted cells and is required for the development and maintenance of multicellular organisms (ANTIGNANI and YOULE 2006; GREEN 2005; XU and SHI 2007). The process

of apoptosis is regulated by both pro-apoptotic and anti-apoptotic members of the Bcl-2 family, although the molecular mechanisms through which this regulation is achieved are not entirely characterized (TSUJIMOTO and SHIMIZU 2007). It is thought that the interplay between pro-apoptotic and anti-apoptotic factors such as Bax and Bcl-2, respectively, helps regulate the mitochondrial permeability transition (MPT) (MARTINOU and GREEN 2001; SHIMIZU *et al.* 1998; TSUJIMOTO and SHIMIZU 2007). The MPT is associated with increased permeability of mitochondrial membranes, which results in the loss of $\Delta\Psi$, mitochondrial swelling and subsequent rupture of the MOM. Deterioration of the MOM results in cytoplasmic localization of several pro-apoptotic factors that include an apoptosis inducing factor (AIF), cytochrome *c* and Smac/DIABLO. AIF is imported into the nucleus where it promotes chromatin condensation and the fragmentation of genomic DNA (JOZA *et al.* 2001; SUSIN *et al.* 1999). Cytochrome *c* induces oligomerization of the apoptotic protease activating factor, which promotes formation of the apoptosome (MATAPURKAR and LAZEBNIK 2006). Smac/DIABLO binds to and sequesters caspase inhibitors resulting in the activation of caspases and eventual cell death (VERHAGEN and VAUX 2002).

1.6. Mitochondrial Dysfunction

1.6.1. Human disease

Disruption of mitochondrial function has been associated with numerous human diseases (DETMER and CHAN 2007; PETROZZI *et al.* 2007; PIECZENIK and NEUSTADT 2007). For example, a mutation in the mitochondrial-encoded $tRNA^{Leu,UUR}$ gene results in maternally inherited diabetes and deafness (MAASSEN *et al.* 2006). This mutation is proposed to interfere with the synthesis of mitochondrial-encoded proteins, which leads to altered cytosolic ATP/ADP ratios and a gradual decrease in insulin production. Dysfunctional mitochondria have also been implicated in neurodegenerative diseases such as Parkinson's, Huntington's and Alzheimer's (PETROZZI *et al.* 2007). The precise role of mitochondria in these neurodegenerative diseases remains controversial, but is

thought to result from improper activation of apoptosis or from oxidative damage resulting from impaired energy metabolism.

Most tumor cells do not possess a functional apoptotic pathway and thus mitochondrial dysfunction has also been linked to the progression of cancer. In fact, studies in the human prostate cancer cell line PC-3 have shown that overexpression of the pro-apoptotic factors Bax or Bad could cause malignant cells to activate apoptosis (LI *et al.* 2001b). Furthermore, when PC-3 cells were subjected to chemical treatments which down-regulate the anti-apoptotic factor Bcl-X_L, their ability to undergo apoptosis was restored. These data suggest that tumor cells become immortalized because they are unable to activate the MPT due to improper regulation by Bcl-2 family members. Consequently, reactivation of the apoptotic pathway in tumor cells has been a major focus in the development of numerous cancer treatments (COSTANTINI *et al.* 2000; CULLEN *et al.* 2007; DENIAUD *et al.* 2006). Recently, it has been shown that the chemical dichloroacetate can initiate apoptosis specifically in cancer cells, resulting in the targeted execution of malignant cells (BONNET *et al.* 2007).

1.6.2. Mitochondria, reactive oxygen species (ROS) and ageing

Mitochondria are known to generate a large amount of ROS through inefficient oxidative phosphorylation, most of which originate from the respiratory complexes I and III (BALABAN *et al.* 2005). ROS such as superoxide anions (O_2^-), hydroxide ions (OH^-) and hydrogen peroxide (H_2O_2) are able to oxidize proteins, lipids and nucleic acids and can therefore be highly detrimental to the cell when present in high concentrations (KAKKAR and SINGH 2007; ORRENIUS 2007). In fact, considerable evidence suggests that the production of ROS within mitochondria contributes to the process of ageing (BARJA 2004; TRIFUNOVIC *et al.* 2004). *Drosophila* mutants lacking copper/zinc superoxide dismutase and/or catalase displayed greater sensitivity to oxidative stress and died at a younger age (GRISWOLD *et al.* 1993; PHILLIPS *et al.* 1989; WOODRUFF *et al.* 2004). Conversely, overexpression of the same proteins in fruit flies enhanced resistance to oxidative damage and correlated with a longer lifespan (ORR and SOHAL 1993; ORR and SOHAL 1994). Similarly, mice expressing high levels of human catalase exhibited lower amounts of oxidative damage and lived longer (SCHRINER *et al.* 2005). Restriction of

caloric intake by ~40% in vertebrates has also been shown to reduce ROS production and increase lifespan (BARJA 2004; GREDILLA *et al.* 2001a; GREDILLA *et al.* 2001b; LOPEZ-TORRES *et al.* 2002). It was later shown that lowering levels of ROS and increasing mean and maximum lifespan could be achieved by reducing dietary protein by 40%, without changing caloric intake (SANZ *et al.* 2004). This suggested that protein restriction and not caloric restriction was a key determinant in the ageing process. Subsequent research demonstrated that the decrease in ROS generation and the increase in lifespan resulting from caloric and protein restriction likely stem from a decrease in methionine ingestion, although the mechanisms behind this are currently unknown (SANZ *et al.* 2006).

The mitochondrial theory of ageing was originally postulated to explain the correlation between mitochondrial ROS production and ageing. This theory suggested that ROS can mutate mtDNA, which can lead to further disruption of the respiratory chain, resulting in additional ROS production. The accumulation of mutations within mtDNA generates severely dysfunctional mitochondria that may facilitate the ageing process. Consistent with this theory, the frequency of mutation in mtDNA of mammalian tissues has been shown to increase with age (KHRAPKO *et al.* 2004; LEE and WEI 2007; MELOV *et al.* 1997; OZAWA 1999). Further work demonstrated that "mutator mice" expressing a proof-reading-deficient mitochondrial DNA polymerase display higher frequencies of mtDNA mutation and premature ageing phenotypes (KUJOTH *et al.* 2005; TRIFUNOVIC *et al.* 2004). However, other mice strains have exhibited a premature ageing phenotype even though they demonstrate normal rates of mtDNA mutation or have appeared healthy despite harboring a large number of mutations within their mitochondrial genome (HASTY *et al.* 2003; KHRAPKO and VIJG 2007; LOMBARD *et al.* 2005; VERMULST *et al.* 2007). In addition, the number of mutations contained within the mtDNA of the mutator mice were more than one order of magnitude higher than what was observed in the tissues of aged humans or mice (KHRAPKO *et al.* 2006; VERMULST *et al.* 2007). Clearly, more research is required to uncover the correlation between mitochondrial mutations, mitochondrial ROS production, and the process of ageing.

1.7. The Retrograde Response

When mitochondria become dysfunctional, the cell elicits a retrograde response that results in the altered expression of numerous nuclear-encoded genes (BISWAS *et al.* 2005; BUTOW and AVADHANI 2004; EPSTEIN *et al.* 2001; LIU and BUTOW 2006). This phenomenon is thought to occur in an attempt to minimize cellular damage that could potentially result from prolonged mitochondrial defects and is believed to be mediated by several distinct retrograde response signaling pathways.

1.7.1. The *RTG*-mediated retrograde response

The best characterized retrograde response pathway has been described in *S. cerevisiae* where the expression of the peroxisomal isoform of citrate synthase, encoded by *CIT2*, was shown to be elevated 6-30 fold in ρ^0 cells compared to isochromosomal ρ^+ cells (LIAO *et al.* 1991). Under conditions where the respiratory chain and Krebs cycle become stalled, there is inefficient recycling of electron carriers and the cell is depleted of Krebs cycle intermediates, some of which are precursors for other important metabolites including the amino acids aspartate and glutamate. Increased expression of the nuclear *CIT2* gene helps elevate levels of peroxisomal citrate, which is subsequently shuttled to the mitochondria where it can be used to replenish essential Krebs cycle intermediates (KAPLAN *et al.* 1996; LIAO *et al.* 1991; TOLBERT 1981). Subsequent research has shown that the expression of several additional genes are also controlled by this pathway of retrograde regulation (CHELSTOWSKA and BUTOW 1995; EPSTEIN *et al.* 2001). This retrograde pathway was originally defined by three *RTG* (retrograde) genes and is discussed in further detail in Chapter 2.

1.7.2. ROS as signaling molecules

Although ROS generated by mitochondria are capable of damaging various cellular components, they can also function in both external and internal signaling pathways. In human lung fibroblasts, the binding of TGF-β1 to cell surface receptors has been shown to induce production of extracellular H_2O_2 through the function of a plasma membrane-associated NADH oxidase (THANNICKAL *et al.* 2000; THANNICKAL and FANBURG 1995). The ROS generated through the interaction of TGF-β1 with its receptor was shown to induce apoptosis in neighboring epithelial cells, a phenomenon that was

prevented through addition of catalase to the cell culture (WAGHRAY *et al.* 2005). These data, combined with results obtained from additional studies in rat and mice, suggest that H_2O_2 functions in a TGF-β1-mediated pathway that inhibits cell growth or induces apoptosis (THANNICKAL and FANBURG 2000; WAGHRAY *et al.* 2005).

Although the majority of cellular ROS is produced through inefficient oxidative phosphorylation, many growth factors, hormones and cytokines have also been shown to induce formation of ROS. These molecules can regulate gene expression by interacting with several mitogen-activated protein kinase (MAPK) signal transduction pathways (BAE *et al.* 1997; CHAPPLE 1997; DEYULIA *et al.* 2005; RHEE *et al.* 2005; SUNDARESAN *et al.* 1996; TURPAEV 2002; VALKO *et al.* 2006). For example, ROS has been shown to oxidize specific cysteine residues of protein kinase C and numerous protein tyrosine phosphatases resulting in the activation or repression of enzyme function, respectively, both of which lead to initiation of MAPK pathways (WU 2006). ROS can also activate MAPK cascades through indirect activation of kinases. Under normal physiological conditions, the serine protein kinase JNK is bound and inactivated by a reduced form of the ROS scavenging enzyme glutathione-S-transferase (ADLER *et al.* 1999; ZHAO and WANG 2006). ROS-induced oxidation of glutathione-S-transferase causes it to dissociate from JNK, which produces an active kinase that initiates downstream MAPK pathways. The mammalian apoptosis signal-regulating kinase (ASK1) is also regulated by ROS. In this system, it is now believed that multimers of reduced ASK1 are oxidized by H_2O_2, resulting in the formation of disulphide bonds between adjacent subunits and production of a functional enzyme (NADEAU *et al.* 2007). In addition, the antioxidant enzyme thioredoxin is also thought to add another element of redox control by maintaining ASK1 in its reduced form when the induction of downstream MAPK pathways is not required. Stimulation of MAPK signal transduction cascades by ROS leads to the activation of numerous transcription factors including AP-1 and NF-κB, which have received much attention due to their role in cell proliferation and cancer (GOPALAKRISHNAN and TONY KONG 2007; MATTHEWS *et al.* 2007; ORANGE *et al.* 2005; VALKO *et al.* 2006).

Recent evidence in mice has shown that two transcription coactivators, PGC-1α and PGC-1β, may also be involved in a ROS-induced signaling pathway (ST-PIERRE *et al.* 2006; VALLE *et al.* 2005; WU *et al.* 1999). The PGC-1 proteins associate with a wide

range of transcription factors to regulate various aspects of energy metabolism including mitochondrial biogenesis and function (LIANG and WARD 2006). Northern-blot analysis has shown that exposure to ROS results in elevated levels of PGC-1α and PGC-1β transcript, which correlates with increased expression of downstream targets (ST-PIERRE *et al.* 2006). There is also evidence that PGC-1α and PGC-1β are involved in the activation of a nuclear-encoded antioxidant defense system as cells lacking either or both of these proteins display lower levels of ROS scavengers such as glutathione peroxidase, catalase and superoxide dismutase when exposed to H_2O_2 (ST-PIERRE *et al.* 2006). These data provide evidence of a PGC-1-mediated retrograde response pathway that may be induced by ROS and can simultaneously enhance mitochondrial biogenesis, modulate respiration and induce antioxidant enzymes, although the precise molecular mechanisms which regulate this pathway are currently unknown.

1.8. Alternative Oxidase

All higher plants as well as several fungal, protist and animal species express an alternative oxidase, which is a nuclear-encoded mitochondrial protein (CHAUDHURI *et al.* 2006; JOSEPH-HORNE *et al.* 2001; LI *et al.* 1996; MCDONALD and VANLERBERGHE 2004; VANLERBERGHE and MCINTOSH 1997; VEIGA *et al.* 2003). Insensitive to antimycin A, cyanide and the effects of chloramphenicol, alternative oxidase accepts electrons from ubiquinol and donates them, along with four hydrogen ions, directly to molecular oxygen, forming water (Figure 1.3). Alternative oxidase can be inhibited by exposure to aromatic hydroxamic acids such as salicylhydroxamic acid (SHAM) (SCHONBAUM *et al.* 1971). The consequence of alternative oxidase function is a reduction in net ATP production as electron flow bypasses complexes III and IV, which are both involved in proton pumping. However, alternative oxidase restores the movement of electrons through the respiratory chain, allowing the recycling of electron carriers and continued synthesis of ATP through the $\Delta\Psi$ produced by proton pumping at complex I (LAMBOWITZ *et al.* 1972b).

1.8.1. Alternative oxidase is present in many forms of life

For many years it was thought that alternative oxidase was only present in higher plants, fungi and protists. However, recent genome sequencing projects have led to the discovery of alternative oxidase in over 60 prokaryotic species including the α-proteobacterium *Novosphingobium aromaticivorans*, which was the first prokaryote shown to encode alternative oxidase (McDonald *et al.* 2003; McDonald and Vanlerberghe 2005; Stenmark and Nordlund 2003). To assess the functionality of the alternative oxidase gene identified in *N. aromaticivorans*, a standard complementation assay was performed. These experiments showed that the *N. aromaticivorans* alternative oxidase gene could rescue a *hemA Escherichia coli* mutant, confirming that the exogenous alternative oxidase protein was fully functional (Stenmark and Nordlund 2003). Further genomic analysis uncovered putative alternative oxidase genes in several animal species including a mollusk (*Crassostrea gigas*), a nematode (*Meloidogyne hapla*) and two chordate species (*Ciona intestinalis* and *Ciona savignyi*) (McDonald and Vanlerberghe 2004).

Recently, a new theory concerning the evolutionary origins of alternative oxidase has been suggested based on the identification of an alternative oxidase gene in an α-proteobacterium (Atteia *et al.* 2004; Finnegan *et al.* 2003; McDonald *et al.* 2003). This hypothesis suggests that the alternative oxidase present in eukaryotes is derived from the original endosymbiont that eventually evolved into present day mitochondria. This idea is supported by phylogenetic analysis that demonstrated a close relationship between the alternative oxidase of higher plants and bacteria (McDonald and Vanlerberghe 2005).

1.8.2. Alternative oxidase structure

Comparison of alternative oxidase protein sequences from several species identified two conserved E-X-X-H iron binding motifs resembling those occurring in binuclear iron proteins (Siedow *et al.* 1995). Members of this protein family contain a four-helix bundle harboring two E-X-X-H motifs, which coordinate binding of two central iron atoms. Alternative oxidase was proposed to adopt a similar conformation, with the enzyme exposed to the mitochondrial matrix and anchored to the MIM by two transmembrane domains located at the N-terminus of the protein (Figure 1.4, panel A)

Figure 1.4. Alternative oxidase structural models. **(A)** The Siedow, Umbach and Moore model (SIEDOW *et al.* 1995). In this model, four alpha-helices (cylinders) present in the mitochondrial matrix surround two iron atoms (spheres), which are thought to be bound by conserved iron binding E-X-X-H motifs present on helices 1 and 4. The alpha-helices are numbered as described by Siedow *et al.* The four helix bundle is anchored to the MIM by two transmembrane domains (cuboids). **(B)** The Andersson and Nordlund model (ANDERSSON and NORDLUND 1999). This model suggests that the alternative oxidase protein is monotopically bound to the MIM, interacting with only one leaflet of the lipid bilayer. The advantages of this structural model are that the four predicted alpha-helices are much longer than in the previous conformation and the E-X-X-H motifs which interact with the iron atoms are placed on helices 2 and 4. These adaptations produce an alternative oxidase structure that is in better agreement with structural data obtained from other members of the di-iron binuclear protein family to which alternative oxidase belongs.

A

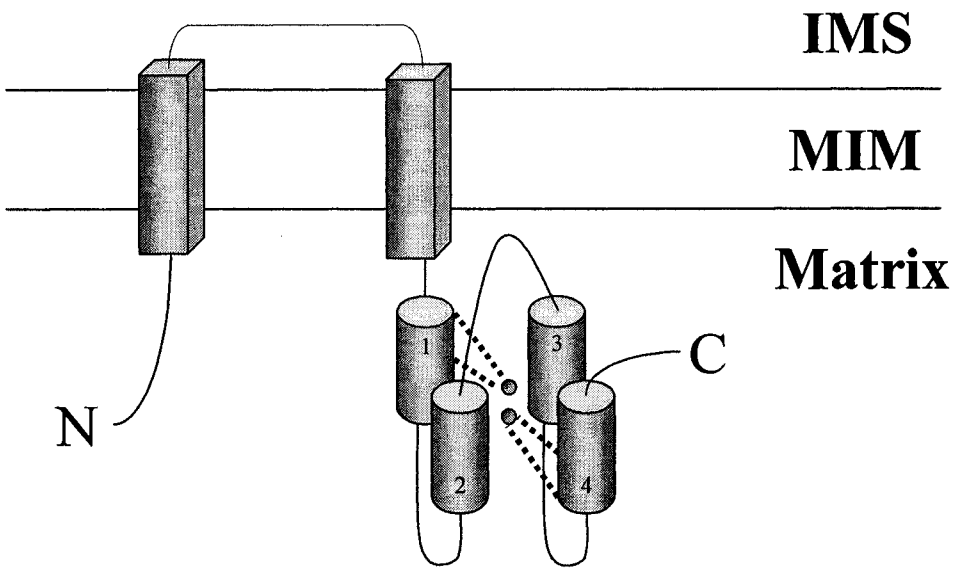

B

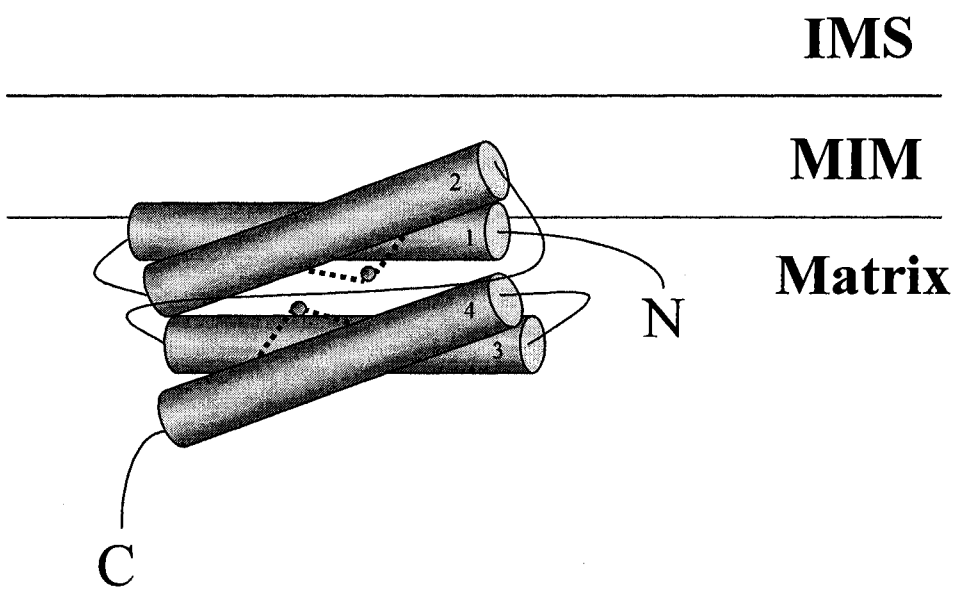

(SIEDOW *et al.* 1995). However, the α-helices predicted by this model were fairly short, each consisting of only 10-11 amino acid residues instead of the 30-35 observed in other binuclear iron proteins. In addition, although the E-X-X-H motifs are normally positioned on helices 2 and 4 of the four-helix bundle, this model placed the iron-binding residues on helices 1 and 4 (ANDERSSON and NORDLUND 1999). Because of these inconsistencies, a new model was proposed in which alternative oxidase was predicted to be monotopically bound, interacting with only one leaflet of the MIM bilayer (Figure 1.4, panel B) (ANDERSSON and NORDLUND 1999). This adaptation produced larger α-helices (27-30 amino acids) and placed the E-X-X-H iron binding motifs on helices 2 and 4. A structural characterization of the chloroplast di-iron binuclear protein encoded by the *IMMUTANS* gene of *A. thaliana* led to the repositioning of a conserved tyrosine in the alternative oxidase structural model, bringing it closer to the di-iron center (BERTHOLD *et al.* 2000). The α-helical bundle of alternative oxidase is thought to form a hydrophobic pocket from the MIM to the di-iron center of the molecule. It is thought that this hydrophobic pocket acts as a channel between ubiquinol and alternative oxidase, thereby promoting the transfer of electrons (ANDERSSON and NORDLUND 1999).

Mutational analysis has confirmed the importance of the conserved E-X-X-H iron binding motifs of the Andersson and Nordlund model and the above mentioned tyrosine residue. Alteration of the conserved glutamate or histidine residues of the *Trypanosoma brucei* alternative oxidase impaired protein function, and rendered the protein unable to rescue a *hemA E. coli* mutant (AJAYI *et al.* 2002). Furthermore, the antimycin A insensitive growth displayed by *Schizosaccharomyces pombe* strains expressing *Sauromatum guttatum* alternative oxidase is abolished when the conserved glutamate or tyrosine residues are mutated (ALBURY *et al.* 2002). More recently, an additional glutamate in close proximity to an essential tyrosine residue has been shown to be indispensable for alternative oxidase function in *S. guttatum* and thus defined a novel conserved $E(X)_6Y$ motif (NAKAMURA *et al.* 2005). Random mutations introduced into the *A. thaliana* alternative oxidase through error-prone polymerase chain reaction (PCR) produced several SHAM-resistant proteins (BERTHOLD 1998). These mutants possessed missense mutations which were predicted to be in close proximity to the di-iron binding site, suggesting that SHAM likely interferes with the transfer of electrons.

1.9. Regulation of Alternative Oxidase

1.9.1. The alternative oxidase gene family

In many plant and several fungal species, alternative oxidase is encoded by multiple, differentially regulated genes. Members of this gene family are separated into two categories based on their expression patterns and amino acid sequence. The first category consists of alternative oxidase proteins that are only induced under stressful conditions while the second represents those proteins whose expression is either constitutive or developmentally regulated (CLIFTON *et al.* 2006; CONSIDINE *et al.* 2002; FINNEGAN *et al.* 1997; SAISHO *et al.* 1997). For example, the two alternative oxidase genes in *C. albicans* demonstrate different expression patterns as AOX1a is expressed constitutively while AOX1b is inducible (HUH and KANG 2001). However, mutation of either isoform renders cells sensitive to the respiratory chain inhibitor cyanide, suggesting that the function(s) performed by the constitutively expressed alternative oxidase is integral to the growth and/or development of *C. albicans*. Of the three alternative oxidase isoforms observed in *G. max*, only Aox1 was shown to be inducible (DJAJANEGARA *et al.* 2002). Conversely, Aox3 was constitutively expressed at relatively high levels while Aox2 was not detectible under any of the conditions examined. *Zea mays* possesses three inducible forms of alternative oxidase. While the levels of all three forms are elevated through exposure to antimycin A, Aod2 and Aod3 are also induced by the respiratory chain inhibitors rotenone and cyanide, respectively (KARPOVA *et al.* 2002). Additionally, although Aod2 and Aod3 are observed in all cells, Aod1 displays tissue-specific expression being absent in ear shoots but highly expressed in young tassels.

Interestingly, only the inducible form of alternative oxidase has been observed in monocot plant species such as *S. guttatum*, *Z. mays*, *Triticum aestivum* and *Oryza sativa* (CONSIDINE *et al.* 2002; ITO *et al.* 1997; RHOADS and MCINTOSH 1993b). Conversely, both types of alternative oxidase protein have been identified in the dicot species *G. max*, *N. tabacum* and *A. thaliana* and are expected to be present in all dicot plants (CLIFTON *et*

al. 2006; CONSIDINE *et al.* 2002; DJAJANEGARA *et al.* 2002; FINNEGAN *et al.* 1997; SAISHO *et al.* 1997; VANLERBERGHE and MCINTOSH 1992a; VANLERBERGHE and MCINTOSH 1992b; VANLERBERGHE and MCINTOSH 1994). In addition, phylogenetic analysis placed the alternative oxidase protein present in monocots in a single group that was distinguishable from the two different types of alternative oxidase in dicots (BORECKY *et al.* 2006; CONSIDINE *et al.* 2002). The discrepancy between which isoforms of alternative oxidase are present in monocot and dicot species is thought to result from the different physiological role of each form in the two divisions of plants. However, additional research will be required to confirm whether or not this hypothesis is accurate.

1.9.2. Stimulation of alternative oxidase expression and activity

The expression and activity of the inducible form of alternative oxidase can be regulated through exposure to a wide variety of molecules and/or environmental conditions, and is dependent on the organism in which the protein is observed. Respiratory inhibitors such as antimycin A and cyanide have been shown to induce alternative oxidase in all plant and fungal species examined thus far (JOSEPH-HORNE *et al.* 2001; JUSZCZUK and RYCHTER 2003; VANLERBERGHE and MCINTOSH 1997). In plants, but not fungi, activation of the alternative oxidase protein can be stimulated by exposure to the organic molecule pyruvate (JUSZCZUK and RYCHTER 2003; MILLAR *et al.* 1993; RHOADS and MCINTOSH 1992; UMBACH and SIEDOW 2000; UMBACH *et al.* 1994). The alternative oxidase of wheat, soybean and tobacco plants is induced by environmental stresses including drought, cold temperatures or heat shock, while such induction is not observed in fungi (JUSZCZUK and RYCHTER 2003; MIZUNO *et al.* 2007; PASTORE *et al.* 2007; RIBAS-CARBO *et al.* 2005; VANLERBERGHE and MCINTOSH 1992b). Plants have also been shown to induce alternative oxidase in response to pathogen attack or exposure to salicylic acid (CHIVASA *et al.* 1997; MAXWELL *et al.* 1999; ORDOG *et al.* 2002; RHOADS and MCINTOSH 1992; RHOADS and MCINTOSH 1993b; SIMONS *et al.* 1999). Hydrogen peroxide has been shown to induce expression of alternative oxidase in many plant species and some fungal species such as *C. albicans*, although ROS-mediated induction of alternative oxidase has not yet been observed in *N. crassa* (MAXWELL *et al.* 2002; POLIDOROS *et al.* 2005; VANLERBERGHE and MCLNTOSH 1996; WAGNER 1995).

Exposure to mononucleotides, particularly AMP, ADP and GMP, has been shown to stimulate alternative oxidase activity in fungal species such as *N. crassa* and *Pichia stipitis* (MICHEA-HAMZEHPOUR and TURIAN 1987; SAKAJO *et al.* 1997; UMBACH and SIEDOW 2000; VANDERLEYDEN *et al.* 1980). The mechanisms of alternative oxidase regulation are discussed in more detail below.

1.9.3. Regulating the levels of alternative oxidase transcript

In numerous organisms including *A. thaliana, N. tabacum, G. max, N. crassa* and *Magnaporthe grisea*, Northern analysis has shown that exposure to certain chemicals and/or environmental conditions allows transcripts of the inducible alternative oxidase to accumulate (DJAJANEGARA *et al.* 2002; DOJCINOVIC *et al.* 2005; GRAY *et al.* 2004; MAXWELL *et al.* 2002; SAISHO *et al.* 1997; TANTON *et al.* 2003; VANLERBERGHE and MCINTOSH 1994; VANLERBERGHE and MCLNTOSH 1996; YUKIOKA *et al.* 1998). The elevated amounts of *aod-1* mRNA observed under such conditions seems to correlate with increased protein levels and/or function (DJAJANEGARA *et al.* 2002; MAXWELL *et al.* 2002; VANLERBERGHE and MCINTOSH 1994). Thus, *aod-1* transcript levels are regulated in response to conditions encountered by the cell.

Nuclear run-on experiments in *M. grisea* and *N. crassa* have shown that exposure to respiratory inhibitors dramatically increases the rate of alternative oxidase transcription, which suggests that the accumulation of alternative oxidase mRNA may be regulated at the level of transcription (TANTON *et al.* 2003; YUKIOKA *et al.* 1998). However, a readily detectible amount of constitutive transcription was also observed in these run-on experiments even though accumulation of mRNA and protein are only observed when the respiratory chain is blocked. Similar experiments conducted in *T. brucei* showed that both the procyclic and bloodstream forms exhibit comparable transcription rates despite the fact that alternative oxidase mRNA and protein are more abundant in the bloodstream form (CHAUDHURI *et al.* 1998; CHAUDHURI *et al.* 2002). Therefore, in some organisms, control of alternative oxidase production may at least partially occur through post-transcriptional mechanisms. Additional work demonstrated that exposure to the protein synthesis inhibitor cycloheximide in both *T. brucei* and *M. grisea* resulted in the accumulation of alternative oxidase mRNA without changing the

rate of transcription (CHAUDHURI *et al.* 2002; YUKIOKA *et al.* 1998). This suggests that cycloheximide treatment prevents production of an mRNA degradation factor, which increases the half-life of alternative oxidase mRNA. Thus, in these organisms, alternative oxidase expression appears to be regulated by transcript stability.

1.9.4. Post-translational regulation of alternative oxidase

Identification of alternative oxidase homodimers in *G. max*, *S. guttatum* and *Vigna radiate* suggested that in higher plants, alternative oxidase activity may be regulated post-translationally (UMBACH and SIEDOW 1993). Further investigation revealed that in these plant species, the subunits of the alternative oxidase homodimer can be held together through either covalent or non-covalent interactions. By measuring oxygen uptake in the presence of DTT and diamide, which are reducing and oxidizing agents, respectively, the non-covalently associated dimer was shown to have significantly higher levels of activity (UMBACH and SIEDOW 1993). Additional experiments in *G. max* showed that treating mitochondria with the sulfhydryl reacting compound iodoacetate also resulted in the predominance of the non-covalently bound enzyme and correlated with increased alternative oxidase activity (UMBACH and SIEDOW 1996).

Analysis of the alternative oxidase protein sequence of several plant species identified two conserved cysteine residues in the N-terminal tail of the plant protein (UMBACH and SIEDOW 1993; VANLERBERGHE and MCINTOSH 1997). It was hypothesized that one or both of these residues, later named Cys_I and Cys_{II}, were involved in regulating alternative oxidase dimerization (BERTHOLD *et al.* 2000). Consistent with this model, the N-terminal tail of the plant alternative oxidase is completely absent in the fungal version of the protein, which functions as a monomer (UMBACH and SIEDOW 2000). Experiments in *N. tabacum* and *A. thaliana* demonstrated that converting Cys_I to an alanine residue inhibited formation of the covalently-associated homodimer, while this form of alternative oxidase was still observed when Cys_{II} was mutated in a similar fashion (RHOADS *et al.* 1998; VANLERBERGHE *et al.* 1998). These data suggested that formation of a disulphide bond between Cys_I residues in different alternative oxidase molecules inactivates the homodimeric complex. However, the Cys_I to alanine substitution in the alternative oxidase of both *N. tabacum* and *A. thaliana*

rendered the enzyme inactive even though it was present in its non-covalently bound form (RHOADS *et al.* 1998; VANLERBERGHE *et al.* 1998). Furthermore, in whole root and leaf extracts of *Poa annua* and *A. thaliana*, respectively, the non-covalently associated homodimer was observed at relatively high levels even though enzyme activity was low (MILLENAAR *et al.* 1998; SIMONS *et al.* 1999). Thus, although regulation of disulphide bond formation between alternative oxidase subunits is involved in regulating alternative oxidase at the post-translational level, additional mechanisms must exist to control activity of the enzyme. It was hypothesized that reduction of the disulphide bond present in the covalently associated alternative oxidase homodimer enabled the Cys_I residues of each subunit to interact with an activating molecule such as pyruvate.

Numerous studies in several plant species have shown that alternative oxidase can be activated by α-keto carboxylic acids such as pyruvate (DAY *et al.* 1994; MILLAR *et al.* 1993; UMBACH *et al.* 2006; UMBACH *et al.* 1994; VANLERBERGHE *et al.* 1998; VANLERBERGHE *et al.* 1999). In fact, the accumulation of pyruvate, which occurs when cytochrome-mediated respiration is inhibited and the Krebs cycle becomes stalled, may be required for activation of alternative oxidase in higher plants. Furthermore, treating mitochondria of *G. max* with the sulfhydryl reacting compounds iodoacetate or *N*-ethylmaleimide (NEM) rendered alternative oxidase insensitive to pyruvate, suggesting that these chemicals interacted with the same cysteine residue as α-keto carboxylic acids (UMBACH and SIEDOW 1996). A pyruvate-insensitive form of alternative oxidase was also generated when Cys_I was converted to glutamate (RHOADS *et al.* 1998). Surprisingly, this change resulted in constitutive activity of alternative oxidase. This was thought to occur as the glutamate side chain resembles the thiohemiacetal adduct that is predicted to form between pyruvate and Cys_I, and is believed to activate alternative oxidase. Recently, it has been shown that Cys_{II} may also contribute to alternative oxidase regulation through its interaction with the α-keto carboxylic acid glyoxylate, although this function requires that Cys_I is in its reduced state (UMBACH *et al.* 2006). Taken together, these data suggest that formation of disulphide bridges between cysteine residues on adjacent homodimer subunits can inactivate alternative oxidase by preventing α-keto carboxylic acids from binding Cys_I and/or Cys_{II}.

1.10. Alternative Oxidase Function

Electron flow through the alternative pathway bypasses two sites of proton pumping, resulting in the conversion of potential energy to heat. Thus, the function of alternative oxidase is considered to be energetically wasteful. In support of this idea, the expression of *S. guttatum* alternative oxidase in *S. pombe* resulted in dramatic decreases in both fungal growth rates and growth yields (AFFOURTIT *et al.* 1999). Similar experiments in *S. cerevisiae* suggest that impaired growth results from the loss of potential energy resulting from the preferred flow of electrons through alternative oxidase instead of complex III (MATHY *et al.* 2006). However, the highly conserved nature of alternative oxidase suggests that it must perform some integral function within the cell that has been selected for throughout evolution.

The alternative respiratory pathway is activated in thermogenic tissues of many plant species (BREIDENBACH *et al.* 1997; SEYMOUR 2001; WATLING *et al.* 2006). The use of different oxygen isotopes in respiration experiments distinguished between electron flow through the two respiratory pathways and showed that the bulk of floral thermogenesis in the sacred lotus (*Nelumbo nucifera*) occurred through the function of alternative oxidase (WATLING *et al.* 2006). The heat generated from engagement of the alternative pathway is also thought to maintain the fluidity of mitochondrial membranes in plant species exposed to cold climates (BREIDENBACH *et al.* 1997; MOYNIHAN *et al.* 1995). In *S. guttatum*, the heat released through alternative oxidase function is required for the volitalization of aromatic compounds which attracts pollinating insects (MEEUSE 1975; VANLERBERGHE and MCINTOSH 1997).

Alternative oxidase is also thought to be involved in the biosynthesis of carbon metabolites and regulating growth based on nutrient availability. Reduced flow of electrons through the cytochrome-mediated respiratory pathway can hinder the Krebs cycle, which limits production of several important carbon metabolites (AFFOURTIT *et al.* 2001; LAMBOWITZ *et al.* 1972b). Induction of alternative oxidase maintains Krebs cycle flux and thus allows for the continued production of essential carbon skeletons. Furthermore, the loss of alternative oxidase in nitrogen-starved *N. tabacum* resulted in the accumulation of carbohydrates, a phenotype that was not observed in wild-type cells

(SIEGER *et al.* 2005). Since alternative oxidase function results in a net decrease in energy production, its induction can also serve to uncouple ATP synthesis from the progression of the Krebs cycle. Consequently, alternative oxidase may permit the production of Krebs cycle intermediates even when there are high cytosolic ATP/ADP ratios, a condition which generally represses ATP synthesis (AFFOURTIT *et al.* 2001; LAMBERS 1982; PARSONS *et al.* 1999; SLUSE and JARMUSZKIEWICZ 1998).

The induction of alternative oxidase is also hypothesized to play a role in defense mechanisms. Evolution of the alternative respiratory pathway in fungal pathogens ensures their survival in the presence of cyanide or nitric oxide, which are released as part of the hypersensitivity response in plants species (HUANG *et al.* 2002; VANLERBERGHE and MCINTOSH 1997). Conversely, elevated levels of alternative oxidase in *A. thaliana* plants infected with *Pseudomonas syringae* or in tobacco mosaic virus-infected *N. tabacum* suggest that it may also be involved in the defense mechanism of plants (LENNON *et al.* 1997; SIMONS *et al.* 1999). In support of this hypothesis, the increased resistance of *N. tabacum* plants to the tobacco mosaic virus after exposure to salicylic acid was inhibited by SHAM (CHIVASA *et al.* 1997; MURPHY *et al.* 1999). However, further evidence showed that *N. tabacum* plants lacking alternative oxidase could still mount an effective response to viral attack (ORDOG *et al.* 2002). Furthermore, overexpression of alternative oxidase did not seem to influence overall resistance of the plant. How alternative oxidase is able to confer viral resistance to plant species is not known.

Evidence has also implicated alternative oxidase in protecting the cell from the damaging effects of ROS. When the cytochrome-mediated respiratory chain is fully engaged, significant amounts of ROS are generated at respiratory complexes I and III. The induction of alternative oxidase siphons electrons away from these complexes thereby minimizing ROS production (MAXWELL *et al.* 2002). Treatment of procyclic *T. brucei* cells with SHAM resulted in a dramatic increase in ROS production and elevated levels of an iron-containing superoxide dismutase (FANG and BEATTIE 2003). Wild-type *N. tabacum* and *A. thaliana* plants expressing exogenous sense or anti-sense alternative oxidase mRNA were shown to display reduced or increased levels of ROS, respectively, when exposed to antimycin A (MAXWELL *et al.* 1999; UMBACH *et al.* 2002). Transgenic

plants harboring the sense mRNA also displayed lower levels of two ROS scavengers, superoxide dismutase and glutathione peroxidase. The induction of alternative oxidase in *N. tabacum* has been shown to minimize ROS generation during periods of high phosphate uptake when the cytochrome-mediated respiratory chain is fully engaged (PARSONS *et al.* 1999; YIP and VANLERBERGHE 2001). Additionally, *N. tabacum* plants lacking alternative oxidase displayed higher than normal expression of salicylic acid-binding catalase and glutathione peroxidase when exposed to a phosphate-limiting environment (SIEGER *et al.* 2005). Conditions which inhibit the function of other ROS scavengers such as catalase and superoxide dismutase have also been shown to induce expression of alternative oxidase (HWANG *et al.* 2003; RHOADS and MCINTOSH 1992; RHOADS and MCINTOSH 1993a; WAGNER 1995). Conversely, removal of alternative oxidase in transgenic *N. tabacum* plants leads to a dramatic increase in the expression of anti-oxidant defense enzymes (AMIRSADEGHI *et al.* 2006). However, the observed changes in the transcript levels of the ROS scavengers in this experiment was strain specific, which suggests that although alternative oxidase is likely involved in mediating ROS production, more research is required to determine the exact mechanism of its function.

Recent evidence has also implicated alternative oxidase in programmed cell death. *N. tabacum* plants lacking alternative oxidase display greater sensitivity to hydrogen peroxide and salicylic acid, two chemicals known to promote fragmentation of DNA, which is indicative of an activated apoptotic pathway (ROBSON and VANLERBERGHE 2002; VANLERBERGHE *et al.* 2002). The presence of alternative oxidase inhibitors caused cold-shocked *T. brucei* cells to undergo a process that resembled programmed cell death of multicellular organisms, as demonstrated through TUNEL analysis (TSUDA *et al.* 2005). Furthermore, overexpression of alternative oxidase in *T. brucei* reduces the occurrence of the programmed cell death-like phenomenon that is normally triggered when cells are grown in high-density cultures (TSUDA *et al.* 2006). However, treatment of *G. max* plants with the apoptotic inducing herbicide dinitro-*o*-cresol was shown to reduce levels of alternative oxidase protein, implying that activation of apoptosis does not necessarily correlate with induction of the alternative pathway (ARANHA *et al.* 2007).

1.11. Alternative Oxidase in *N. crassa*

In *N. crassa*, alternative oxidase is encoded by the nuclear *aod-1* gene and is usually expressed only when the normal cytochrome-mediated respiratory chain is disrupted. Inhibition of the standard chain can be achieved through exposure to respiratory inhibitors such as antimycin A, cyanide and oligomycin, copper deprivation or through mutations affecting components of the electron transport chain (LAMBOWITZ and SLAYMAN 1971; LAMBOWITZ *et al.* 1972a; LI *et al.* 1996; SCHWAB 1973). The *aod-1* gene in *N. crassa* encodes a 362 amino acid protein with a predicted molecular weight of 41.4 kDa, which is reduced to 34.7 kDa upon cleavage of the mitochondrial targeting sequence. As is the case with most fungal alternative oxidases, *N. crassa* AOD1 functions as a monomer and does not contain the N-terminal tail that is conserved in higher plants (UMBACH and SIEDOW 2000). In addition, the alternative oxidase of *N. crassa* is not stimulated by the α-keto carboxylic acids pyruvate or glyoxylate, but is activated by mononucleotides, particularly guanine monophosphate (GMP) (UMBACH and SIEDOW 2000).

The actual alternative oxidase protein of *N. crassa* was first observed as a radiolabeled protein that accumulated after exposure to the ATP synthase (complex V) inhibitor, oligomycin (BERTRAND *et al.* 1983). To isolate mutants of the alternative pathway, a screen was performed which selected for strains that became sensitive to antimycin A after exposure to *N*'-nitro-*N*-nitrosoguanidine (BERTRAND *et al.* 1983). This screen generated several mutant strains belonging to two complementation groups, which were later named *aod-1* and *aod-2*. Since the radiolabeled alternative oxidase protein could still be observed in 19 of the 20 *aod-1* mutants, but was not present in the four *aod-2* mutants, AOD1 was deemed to be the structural protein. These results were later confirmed using a monoclonal antibody developed against the alternative oxidase from *S. guttatum* (ELTHON *et al.* 1989; LAMBOWITZ *et al.* 1989). It was later shown that the single *aod-1* mutant strain that was deficient for the alternative oxidase protein contained a frameshift mutation which inserted a premature stop codon (LI *et al.* 1996).

Nuclear run-on experiments in *N. crassa* have demonstrated that alternative oxidase is transcribed at a low constitutive rate despite that fact that transcript and protein are not typically observed under normal growth conditions (TANTON *et al.* 2003). However, the addition of antimycin A to the growth medium resulted in a dramatic increase in the rate of alternative oxidase transcription, suggesting that in *N. crassa*, a major contributing factor in regulation occurs at the level of transcription. Although evidence suggests that the production of alternative oxidase protein in *N. crassa* correlates with increased transcription rates and accumulation of *aod-1* mRNA, post-transcriptional regulatory mechanism also exist. Northern analysis has shown that some strains accumulate considerable levels of *aod-1* mRNA under non-inducing conditions even though alternative oxidase protein and cyanide-resistant respiration were not observed (DESCHENEAU *et al.* 2005; TANTON *et al.* 2003). The molecular mechanisms by which this post-transcriptional regulation is achieved are not understood.

Since the initial discovery of *aod-1* and *aod-2*, several other *N. crassa* genes have been identified that may be involved in respiration through the alternative pathway. A second alternative oxidase structural gene, *aod-3*, was identified through a BLAST analysis of the *N. crassa* genome (TANTON *et al.* 2003). The *aod-3* gene is predicted to encode a 376 amino acid protein with 55% identity to AOD1. Since *aod-3* does not appear to be induced by chloramphenicol and because there is no evidence of cyanide-resistant respiration in *aod-1* mutant strains, the function of AOD3 is unknown. Conceivably, it could be involved in early development, conidiation, or the sexual cycle of the organism.

A large-scale EMS mutagenesis was performed with a strain carrying a reporter gene fused to 3 kbp of *aod-1* upstream sequence in an attempt to uncover genes involved in the regulation of alternative oxidase. This screen identified three novel genes, *aod-4*, *aod-5*, and *aod-7*, along with the previously identified *aod-2* gene, that were required for the induction of alternative oxidase (DESCHENEAU *et al.* 2005). The recent cloning of *aod-2* and *aod-5* has identified their protein products as belonging to the Zn(II)2Cys6 binuclear cluster (zinc cluster) family of transcription factors (CHAE *et al.* 2007b). The *aod-2* and *aod-5* transcripts are constitutively expressed, although their levels appear to decrease slightly after exposure to antimycin A. Additionally, both proteins contain a

putative PAS domain, which is a common module in many transcription factors that may play a role in their activation and/or dimerization. A more detailed description of zinc cluster transcription factors and PAS domains can be found in Chapter 3.

1.12. Objectives of This Study

The primary goal of the research presented in this thesis was to elucidate how mitochondrial dysfunction is first detected and to identify the pathway(s) involved in the communication of such defects to the nucleus. In an attempt to reveal how this retrograde regulation arises, I hoped to characterize the signals that lead to the expression of alternative oxidase in the filamentous fungus *N. crassa*, and how these signals are transmitted to their sites of action. Acquiring such information may lead to a better understanding of how the functional state of organelles such as mitochondria can regulate the expression of nuclear-encoded genes.

In chapter 2 of this thesis, I describe my attempt to determine if the *RTG* system which has been characterized in *S. cerevisiae* is involved in the regulation of alternative oxidase expression in *N. crassa*. Chapter 3 illustrates my efforts to uncover an activating sequence element(s) within the *aod-1* gene promoter and to characterize the role of two zinc cluster proteins, AOD2 and AOD5, in alternative oxidase induction.

Chapter 2: A *Neurospora crassa* Homologue of the *Saccharomyces cerevisiae* Retrograde Response Gene *RTG2* is not Required for the Induction of Alternative Oxidase

2.1. Introduction

2.1.1. Identification of the *RTG* genes in *S. cerevisiae*

The discovery of increased *CIT2* expression in *S. cerevisiae* strains that contained no mtDNA suggested that the peroxisomal citrate synthase encoded by this gene may be regulated by a retrograde regulation pathway that communicated mitochondrial dysfunction to the nucleus. To uncover genes involved in the retrograde regulation of *CIT2*, an EMS mutagenesis was performed on yeast cells carrying the *LacZ* gene fused to 607 bp of sequence upstream of the *CIT2* coding sequence (LIAO and BUTOW 1993). ρ^0 cells possessing a dysfunctional retrograde response pathway were identified as those that remained white when grown on medium containing 5-bromo-4-chloro-3-indolyl-beta-D-galacto-pyranoside (X-gal). Using this method three retrograde response (*RTG*) genes were identified and cloned (JIA *et al.* 1997; LIAO and BUTOW 1993). *RTG1* and *RTG3* encode helix-loop-helix transcription factors with molecular weights of 19 kDa and 54 kDa, respectively. Only Rtg3p has been shown to contain a transcriptional activation domain (JIA *et al.* 1997; LIAO and BUTOW 1993; ROTHERMEL *et al.* 1997). These two transcription factors form a heterodimeric complex that binds to a unique R (for retrograde) box sequence element (GTCAC) found within the promoters of numerous retrograde-regulated genes including *CIT2* (LIAO and BUTOW 1993). Fluorescence microscopy has shown that Rtg1p is required to sequester Rtg3p within the cytoplasm until the retrograde response is elicited (SEKITO *et al.* 2000). Upon activation of this retrograde pathway, Rtg3p is partially dephosphorylated and the Rtg1p/Rtg3p heterodimer localizes to the nucleus. Both of these events require Rtg2p whose precise function is not known. Rtg2p is a 66 kDa cytoplasmic protein that has an N-terminal ATP binding domain and resembles bacterial polyphosphatases known to hydrolyze transcriptional regulators such as ppGpp and pppGpp (KOONIN 1994).

2.1.2. Phenotypes of the *RTG* mutants

Yeast strains carrying null mutations of any of the three *RTG* genes are viable and respiratory competent as shown by their ability to metabolize non-fermentable carbon sources (JIA *et al.* 1997; LIAO and BUTOW 1993). However, all three *RTG* mutants display growth phenotypes that are typical of strains possessing compromised Krebs and glyoxylate cycles, suggesting that the *RTG* genes may help regulate the interaction between the two metabolic pathways (LIAO and BUTOW 1993). For instance, none of the *RTG* mutants can grow in medium where acetate is the sole carbon source. In addition, when grown on medium where ammonium sulfate is the only source of nitrogen, the *RTG* mutants display aspartate and glutamate auxotrophy. These amino acids are synthesized from Krebs cycle intermediates which become limiting under such growth conditions, and are normally maintained through enhancement of the glyoxylate cycle. The failure of the *RTG* mutants to upregulate the glyoxylate cycle likely results from their inability to enhance expression of numerous nuclear genes such as *CIT2*, *POX1*, *CTA1* and *PMP27*, which encode proteins required for peroxisome function or biogenesis, (CHELSTOWSKA and BUTOW 1995; JIA *et al.* 1997) and cytosolic pyruvate carboxylase (*PYC1*), which converts pyruvate to oxaloacetate (EPSTEIN *et al.* 2001).

2.1.3. Additional proteins in the *RTG*-mediated response pathway

Since the initial discovery of the *RTG* genes, several additional proteins have been implicated in the *RTG*-mediated retrograde response. Mks1p acts as a negative regulator of the *RTG* pathway by promoting the phosphorylation of Rtg3p, which prevents migration of the Rtg1p/Rtg3p activating complex to the nucleus (DILOVA *et al.* 2004). Regulation of Mks1p is achieved through its interaction with other members of the *RTG* pathway. In its inactive form, Mks1p is dephosphorylated and bound to Rtg2p, while its activation is achieved through hyperphosphorylation and interaction with two functionally redundant 14-3-3 proteins, Bmh1/2p (LIU *et al.* 2003). Furthermore, any unbound Mks1p is targeted by Grr1p, a component of the SCF^{Grr1} E3 ubiquitin ligase, which promotes its ubiquitination and eventual degradation (LIU *et al.* 2005). Lst8p is a negative regulator of the *RTG* pathway and is part of two TOR kinase complexes,

TORC1 and TORC2 (CHEN and KAISER 2003; LIU *et al.* 2001). Although the exact role of these complexes in retrograde regulation is not known, the TOR kinase signaling pathway is involved in regulating cell growth in response to nutrient availability (JACINTO and HALL 2003). Regulation of the *RTG* pathway by Lst8p seems to occur both downstream and upstream of Rtg2p. Although it is uncertain how Lst8p functions downstream of Rtg2p, its upstream function involves activation or assembly of the SPS amino acid sensing system, which inhibits Rtg2p function when external levels of glutamine and glutamate are high.

2.1.4. Variation in the retrograde response

There is evidence suggesting that *RTG*-mediated changes in gene expression can be influenced by the carbon source present in the growth medium. Microarray analysis has shown that for some genes, the amount of transcript observed in ρ^0 yeast cells seemed to vary depending on whether the yeast cells were grown in the presence of glucose or raffinose (EPSTEIN *et al.* 2001; TRAVEN *et al.* 2001). Similarly, Northern-blot analysis has demonstrated that the increase in *CIT2* mRNA correlating with the loss of mtDNA is much more pronounced when strains are grown on raffinose and not glucose (KIRCHMAN *et al.* 1999). It is now believed that the altered expression of some, but not all, genes observed when ρ^0 cells were grown in glucose-containing medium may be a consequence of glucose derepression, which accompanies the diauxic shift, and thus may not result from activation of the retrograde response (BUTOW and AVADHANI 2004; LIU and BUTOW 2006). This would explain why similar changes in gene expression were not observed when ρ^0 strains were grown in raffinose.

The expression of *CIT2* mRNA can also be influenced by genetic background. When grown in the presence of raffinose, the *CIT2* mRNA abundance in the yeast strain A364A is 9.4-fold greater in petites compared to isochromosomal grandes, while only a 1.5-fold increase is observed in another strain, W303-1A (KIRCHMAN *et al.* 1999). Surprisingly, when these strains are cultured in media containing glucose, the loss of mtDNA is actually accompanied by a slight decrease in *CIT2* mRNA levels. Conversely, the strains YPK9 and SP1-1 display higher amounts of *CIT2* transcript in ρ^0 cells versus isochromosomal ρ^+ cells when grown in the presence of either sugar. It has been

hypothesized that expression of *CIT2* as well as other retrograde-regulated genes may be controlled by several parallel retrograde pathways and thus the amount of *CIT2* transcript observed is dependent on the interaction between them (BUTOW and AVADHANI 2004).

2.1.5. Objectives of this research

The purpose of the research described in this chapter was to determine whether homologues of the genes involved in the *RTG*-mediated pathway of retrograde regulation that exists in *S. cerevisiae* are also present in *N. crassa* and if so, to determine if they are involved in the induction of alternative oxidase when the cytochrome mediated respiratory chain is blocked.

2.2. Materials and Methods

2.2.1. Strains and growth conditions

Growth of *N. crassa* strains was carried out as previously described (DAVIS and DE SERRES 1970). Briefly, vegetative growth of *N. crassa* strains was achieved by growth in Vogel's medium containing 1.5% sucrose and the appropriate nutritional supplements. When solid media were required, agar (Invitrogen, Burlington, ON) was added at 1.25% (w/v). In the absence of antibiotics, strains were typically grown for 12-14 hr at 30°C. Liquid media were inoculated to a final concentration of 1×10^6 conidia per ml, and aerated by shaking in baffled flasks. Induction of alternative oxidase was achieved through addition of chloramphenicol to the growth medium, at a final concentration of 2.0 mg/ml. Cultures grown in the presence of chloramphenicol generally required 16-18 hr to achieve the required level of growth. To determine growth rates in a nitrogen-limiting medium, ammonium sulphate (0.25%) was added to minimal medium made with a nitrogen-free Vogel's stock. All *N. crassa* strains used in these experiments are listed in Table 2.1.

Table 2.1. *N. crassa* strains used in these experiments

Strain Name	Genotype	Origin or Source
9718	*Δmus-51::bar*$^+$*; a*	FGSC[1]
9719	*Δmus-52::bar*$^+$*; a*	FGSC
Rtg-2KO18-2	*Δmus-51::bar*$^+$*; Δrtg-2::hph*$^+$*; a*	This study
Rtg-2KO19-5	*Δmus-52::bar*$^+$*; Δrtg-2::hph*$^+$*; a*	This study
NCN251-5	*A*	Nargang lab
7207	*aod-1; pan-2; A*	H. Bertrand

[1] Fungal Genetics Stock Center (University of Kansas Medical Center, Kansas City)

2.2.2. BLAST searches and sequence alignment

The protein sequences of the three *RTG* genes of *S. cerevisiae* were obtained from the *Saccharomyces* Genome Database (www.yeastgenome.org). These sequences were subsequently used as queries in BLAST searches of the *N. crassa* Database at the Broad Institute. Alignment of *S. cerevisiae* and *N. crassa* RTG2 protein sequences was achieved using the ClustalW (1.82) algorithm.

2.2.3. Construction of *N. crassa rtg-2* knockouts

The procedure for constructing knockouts in *N. crassa* was modified from previously described protocols (COLOT *et al.* 2006; NINOMIYA *et al.* 2004) and is described in steps in sections 2.2.3.1 to 2.2.3.6 below.

2.2.3.1. Production of DNA fragments for gene replacement

Three DNA fragments were amplified using six of the primers listed in Table 2.2. These fragments were used to develop a construct that was used to delete the *N. crassa rtg-2* gene. MCHA15 and MCHA16 were used to produce a 1082 bp fragment, while an 1123 bp fragment was synthesized using MCHA17 and MCHA18. These fragments corresponded to the 5' and 3' flanking regions of *rtg-2*, respectively. Both reactions were performed using 25 µl of 1.1X PCR mix (50 mM KCl; 10 mM Tris-Cl, pH 8.5; 1.5 mM $MgCl_2$; 0.1 mg/ml BSA; 0.2 mM dNTPs), 0.5 µl of each primer (10 µM), 0.5 µl of template DNA (10 ng/µl of pMOcosX DNA isolated from cells obtained from well H9 of the 96-well plate designated as X18 of the *Neurospora* genomic library (ORBACH 1994)) and 0.5 µl of *Taq/Pfu* (2.4U *Taq*/0.06U *Pfu*). In addition, a 1492 bp hygromycin resistance cassette was amplified from the plasmid pCSN44 (STABEN *et al.* 1989) using the primers *hph*F and *hph*R (Table 2.2). This reaction was carried out using 50 µl of 1.1X PCR mix, 0.5 µl of each primer (0.1 µg/µl), 1.0 µl of template DNA (10 ng/µl) and 0.5 µl of *Taq/Pfu* (2.4U *Taq*/0.06U *Pfu*). All three PCR reactions were carried out under the following conditions: 94°C for 5 min, 35 cycles of 60°C for 30 sec, 72°C for 4 min, 98°C for 20 sec, followed by 10 min at 72°C. The products were resolved on an agarose gel, and the fragments of interest were purified (QIAquick gel extraction kit protocol, but

Table 2.2. Primers used in these experiments

Primer Name	Sequence (5' → 3')	Comments
MCH12	ACACTCGTCGACCCATACCAGCAATAGGC	RTG2 fusion protein cloning primer; for antibody production; top strand; *Sal* I site is underlined
MCH13	TCTCAAAAGCTTCGCAAGTTGTTCAACAG C	RTG2 fusion protein cloning primer; for antibody production; bottom strand; *Hin*d III site is underlined
MCHA15	GTAACGCCAGGGTTTTCCCAGTCACGACG CGACATCTCATTGATAAAAT	*rtg-2* knockout construct primer; *rtg-2* upstream region; top strand
MCHA16	ACCGGGATCCACTTAACGTTACTGAAATC ATCACTCCAGGAGGAACTTG	*rtg-2* knockout construct primer; *rtg-2* upstream region; bottom strand
MCHA17	CGTTCTATAGTGTCACCTAAATCGTATGT GGCACGCAGAGAGAGCAAGA	*rtg-2* knockout construct primer; *rtg-2* downstream region; top strand

Table 2.2. Continued

Primer Name	Sequence (5' → 3')	Comments
MCHA18	GCGGATAACAATTTCACACAGGAAACAGC TCGACTAACGCGATCTTCAC	*rtg-2* knockout construct primer; *rtg-2* downstream region; bottom strand
*hph*F	ACATACGATTTAGGTGACACTATAGAACG CCGTCGACAGAAGATGATATTGAAGGAGC C	hygromycin resistance cassette primer; top strand
*hph*R	AGCTGACATCGACACCAACG	hygromycin resistance cassette primer; bottom strand

using Qiagen QIAprep spin miniprep columns, and 6 M NaI (pH 7.5) instead of the Qiagen buffer QG; Qiagen, Mississauga, ON).

The vector pRS416 was digested with *Xba* I and *Xho* I, subjected to gel electrophoresis, and the desired fragment was purified through gel extraction. pRS416 is a yeast shuttle vector that can be used to manipulate DNA in *S. cerevisiae*, but can also be maintained in *E. coli* (SIKORSKI and HIETER 1989). This plasmid or derivates of it can be selected for in yeast and *E. coli* by using the URA3 nutritional marker or the ampicillin resistance gene, respectively.

2.2.3.2. Transformation of yeast

The three DNA fragments generated by PCR and the digested pRS416 (as described in 2.2.3.1) possess homologous terminal sequences enabling the generation of a circular plasmid through homologous recombination in *S. cerevisiae* (Figure 2.1, panel A). To generate competent yeast cells for transformation, 50 ml of YPAD (1% yeast extract; 2% peptone; 0.01% adenine hemisulfate; 2% glucose) was inoculated with 1 ml of a freshly grown culture of strain FY2 (*ura3*-52) and grown at 30°C in an incubator shaker to an OD_{600} of 0.8-1.0, which took 2-3 hr. The culture was transferred to a 50 ml tube, and spun down in a clinical centrifuge at full speed (International Equipment Company, Needham Heights, MA). The resulting pellet was washed twice, first with 25 ml of sterile water, then with 1 ml of 100 mM $LiCH_3COO$, and finally resuspended in 400 µl of 100 mM $LiCH_3COO$. 50 µl of this suspension was transferred to a sterile microcentrifuge tube, and pelleted (Sorvall Pico, Mandel Scientific, Guelph, ON). The supernatant was discarded and replaced with 360 µl of transformation mix, which contained 240 µl 50% PEG 3350, 36 µl of 1 M $LiCH_3COO$, 50 µl of 2 mg/ml sheared salmon sperm DNA, 200 ng of each of the three PCR fragments, and 100 ng of pRS416 digested with *Xba* I and *Xho* I. The reaction was incubated for 30 min at 30°C in an air incubator, and then at 42°C in a water bath. The cells were pelleted, rinsed with 1 ml of sterile water, and resuspended in 200 µl of sterile water. 100 µl of this mixture was then spread on each of two plates containing synthetic complete medium without uracil (SC-Ura), which allowed for the selection of cells harboring the URA3 gene present in pRS416. The plates were then incubated at 30°C for three days.

Figure 2.1. Generation of *N. crassa rtg-2* knockout strains. **(A)** Schematic of the plasmid used to knockout the *rtg-2* gene. PCR amplification produced three fragments containing sequences upstream and downstream of the *rtg-2* coding region, and a hygromycin resistance cassette (*hph*). These fragments were subsequently inserted into pRS416, which had been previously digested with *Xho* I and *Xba* I, by transforming all four fragments into yeast cells and allowing the formation of the desired plasmid through homologous recombination. Homologous terminal sequences that facilitated recombination are connected by dotted lines. The primers used in these experiments are indicated at the ends of each fragment. **(B)** Knockout scheme for *N. crassa rtg-2*. A DNA fragment containing the *hph* gene flanked by *rtg-2* upstream and downstream sequences was PCR amplified from the plasmid in panel A using MCHA15 and MCHA18 and then transformed into *N. crassa* strains that carry out highly efficient homologous recombination. The recombination event replaced the endogenous *rtg-2* coding sequence with a hygromycin resistance cassette, which was used to select for *rtg-2* knockout strains.

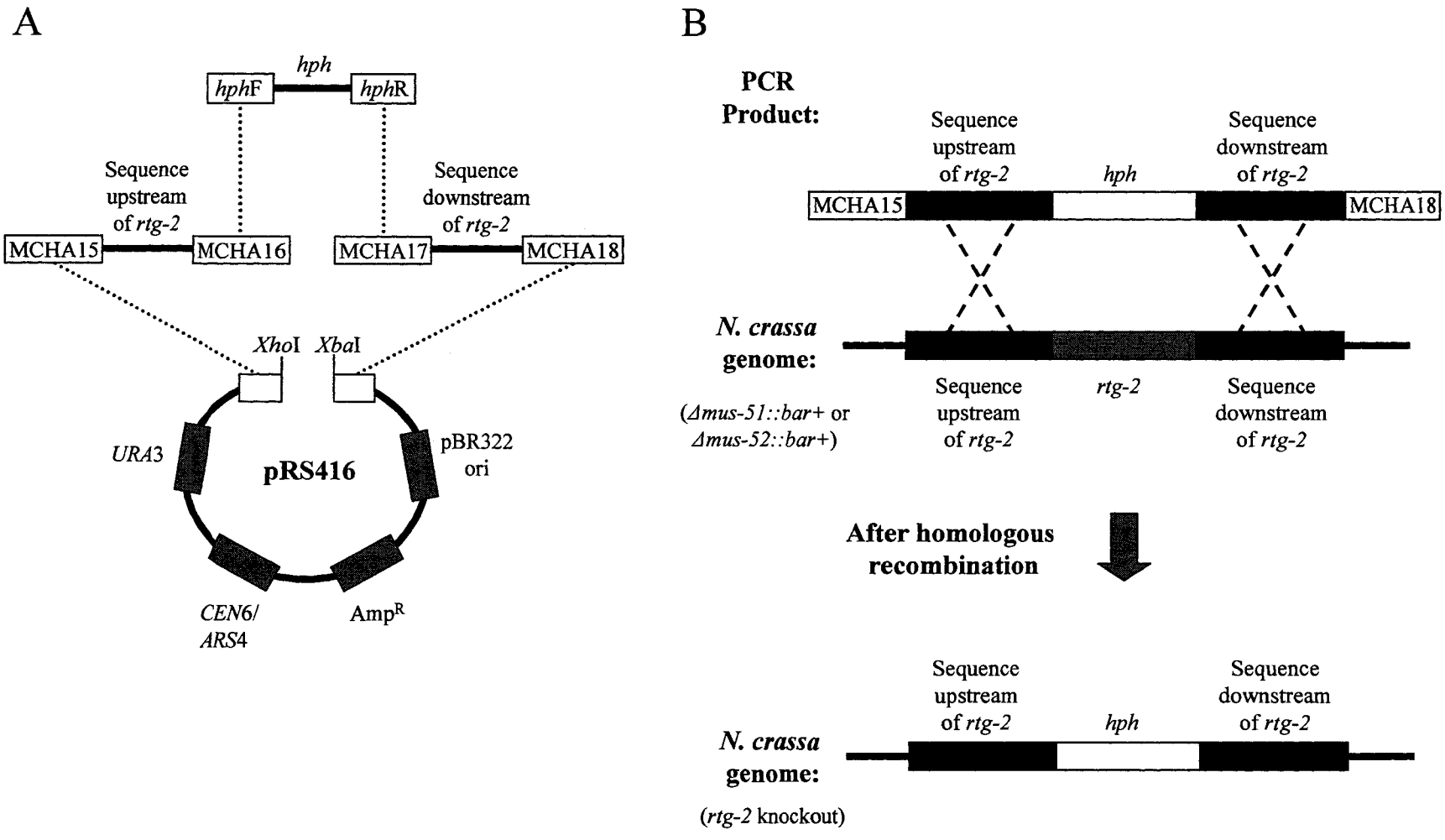
A
hph
hphF
hphR
Sequence upstream of rtg-2
Sequence downstream of rtg-2
MCHA15
MCHA16
MCHA17
MCHA18
XhoI
XbaI
URA3
pRS416
pBR322 ori
CEN6/ ARS4
AmpR
B
PCR Product:
Sequence upstream of rtg-2
hph
Sequence downstream of rtg-2
MCHA15
MCHA18
N. crassa genome:
(Δmus-51::bar+ or Δmus-52::bar+)
Sequence upstream of rtg-2
rtg-2
Sequence downstream of rtg-2
After homologous recombination
Sequence upstream of rtg-2
hph
Sequence downstream of rtg-2
N. crassa genome:
(rtg-2 knockout)

2.2.3.3. DNA preparation from yeast

Once colonies were visible on the SC-Ura plates (2.2.3.2), 2 ml of YPAD were placed on the surface of the solid media, and a sterile loop was used to suspend all of the colonies on the plate. The cells were pelleted at 13000 rpm in a microcentrifuge tube (Sorvall Pico, Mandel Scientific, Guelph, ON), then resuspended in 200 µl of yeast lysis buffer (2% triton X-100; 1% SDS; 100 mM NaCl; 10 mM Tris-Cl; 1 mM EDTA), 200 µl of phenol:chloroform (1:1), and 0.3 g of 0.45 mm glass beads. The mixture was vortexed for 2 min, followed by a 10 min spin in a microcentrifuge. 100 µl of the aqueous phase was transferred to a new microcentrifuge tube containing 10 µl of 3 M sodium acetate and 250 µl of chilled 95% ethanol. The nucleic acids were precipitated, washed with 70% ethanol, and then resuspended in 20 µl of sterile water.

2.2.3.4. *E. coli* transformation and plasmid isolation

The DNA isolated in 2.2.3.3 was added to 200 µl of *E. coli* XL-2 competent cells and placed on ice for 15 min. The cells were then transferred to a 42°C water bath for 90 sec. After the heat shock, 1 ml of sterile Luria-Bertani (LB) was added, and the mixture was incubated for 30 min in a 37°C water bath. The mixture was then spread over LB plates containing ampicillin (0.1 mg/ml) which were then placed in a 37°C air incubator overnight. Plasmid DNA was isolated from resulting colonies using a QIAprep Spin Miniprep Kit as per the manufacturer's instructions (Qiagen, Mississauga, ON). Identification of the desired plasmid, pRTG2KO-1, was performed through restriction digest with *Eco*R I, which generated 6.7 kb and 1.3 kb fragments. Subsequent DNA sequencing confirmed the identity of the desired plasmid. This was accomplished using a BigDye® Terminator v3.1 cycle sequencing kit (Applied Biosystems, Streetsville, ON), as per the manufacturer's instructions. The sequencing reactions were analyzed by the Molecular Biology Service Unit (MBSU; Department of Biological Sciences, University of Alberta) using an Applied Biosystems 3730 DNA Analyzer.

2.2.3.5. Preparation of knockout construct DNA for *N. crassa* transformation

MCHA15 and MCHA18 were employed to PCR amplify a 3.7 kb fragment from pRTG2KO-1 containing the *hph* gene flanked by *rtg-2* upstream and downstream

sequence. The PCR reaction contained 50 µl of 1.1X PCR mix, 1 µl of each primer (10 µM), 0.5 µl of pRTG2KO-1 (10 ng/µl), and 0.5 µl of *Taq*/*Pfu* (2.5U *Taq*/0.03U *Pfu*), and was subjected to the PCR program listed in 2.2.3.1. The products were resolved on an agarose gel and the desired fragment was purified through gel extraction (2.2.3.1). As described below, 5 µl of the purified DNA (0.5 µg) was transformed into two *N. crassa* strains, 9718 and 9719 (Table 2.1). These *N. crassa* strains virtually eliminate non-homologous recombination due to knockouts of either the *mus-51* or *mus-52* gene, respectively, both of which encode proteins involved in non-homologous end joining. This insures a high percentage of knockout events among the transformants (NINOMIYA *et al.* 2004). A diagram of the events leading to the knockout of *rtg-2* in *N. crassa* is shown in Figure 2.1, panel B.

2.2.3.6. *N. crassa* transformation

Conidia from the *N. crassa* strains 9718 and 9719 were harvested in 50 ml of sterile, distilled water, and then pelleted in a clinical centrifuge at full speed (International Equipment Company, Needham Heights, MA). The conidia were then washed three times with 40 ml of sterile, chilled 1 M sorbitol. Following the final wash, the concentration was adjusted to 2 x 10^9 conidia/ml using 1 M sorbitol. Electroporation conidia were then distributed into 40 µl aliquots, to which 0.5 µg of linear DNA (in a total volume of 5 µl) was added. This mixture was then placed in an electroporation cuvette (2 mm gap), followed by electroporation (2.1 kV, 475 Ω, 25 µF). 1 ml of chilled 1 M sorbitol was added immediately after electroporation and the transformation mixture was then incubated at 30°C for 30 to 60 min. Various amounts (10 to 100 µl) of conidia were mixed with 45°C molten top agar (Vogel's sorbose medium with 1.5% agar) supplemented with the appropriate nutritional requirements and hygromycin B (200 U/ml). To ensure isolation of homokaryotic colonies, the original transformants were first picked to a slant containing Vogel's sucrose containing hygromycin B (100 U/ml). To obtain single colonies, conidia from these slants were then streaked on hygromycin B (200 U/ml) containing sorbose plates, and one colony from each originally picked transformant was isolated to Vogel's medium without hygromycin B and used in further experimentation.

2.2.4. Preparation of crude mitochondrial and cytoplasmic protein

Vacuum filtration was used to harvest liquid cultures of *N. crassa* strains. The resulting mycelial pad was ground with an equal mass of sand (white quartz, -50-70 mesh, Sigma-Aldrich, Oakville, ON) and two volumes of SEM (0.25 M sucrose; 1 mM EDTA, pH 8.0; 10 mM MOPS, pH 7.2) containing 1 mM of freshly added phenylmethylsulphonyl fluoride (PMSF). The sand and cellular debris were pelleted in an SS-34 rotor by centrifugation at 5000 rpm for 10 min at 4°C (Sorvall RC 5C Plus; Sorvall, Mandel Scientific, Guelph, ON). The supernatant, which contained both cytosol and mitochondria, was transferred to a new tube and centrifuged at 12000 rpm for 30 min at 4°C. The supernatant (cytosolic protein) was placed directly into tubes for storage, while the mitochondrial pellet was resuspended in a small volume of SEMP buffer (SEM containing 1 mM PMSF) before being transferred to microcentrifuge tubes. Protein concentrations were obtained using the Bio-Rad Bradford protein assay as per the manufacturer's instructions (Bio-Rad, Mississauga, ON). Samples were used immediately or stored at -80°C.

2.2.5. SDS-polyacrylamide gel electrophoresis and Western blotting

SDS-polyacrylamide gel electrophoresis (SDS-PAGE) was performed using Laemmli's discontinuous buffer system (SAMBROOK and RUSSELL 2001). 25 µg of mitochondrial or 120 µg of cytosolic protein was resolved using a 12.5% polyacrylamide gel (29:1 acrylamide:bisacrylamide). The protein was then electroblotted (67 V for 84 min) to nitrocellulose membranes using a Bio-Rad transblot electrophoretic transfer cell (Bio-Rad, Mississauga, ON) filled with transfer buffer (25 mM Tris; 190 mM glycine; 20% methanol).

Following transfer, the nitrocellulose membrane was blocked for 30 min in either milk buffer (5% skim milk powder in TBS-Tween: 20 mM Tris-HCl, pH 7.5; 150 mM sodium chloride; 0.5% Tween) or BSA blocking buffer (3% BSA in TBS-Tween). After blocking, the membrane was incubated with the primary antibody for at least one hr (diluted 1/1000 – 1/100000 in milk or BSA blocking buffer, depending on the antibody used). The membrane was washed three times with TBS-Tween for five min each, prior

to a thirty min incubation with the appropriate secondary antibody coupled to horseradish peroxidase (diluted 1/3000 in milk buffer). Three ten min TBS-Tween washes were then performed followed by single washes with TBS and distilled water. Antibody detection was achieved using the LumiGLO chemiluminescent kit (Mandel, Guelph, ON) and exposure to Kodak XAR film. For these experiments, the following antibodies were used: α-yeast actin (A generous gift of Gary Eitzen, Department of Cell Biology, University of Alberta) at 1/100000; α-RTG2 (4-2-1; this study) at 1/1000; α-AOD1 (IE3; Nargang lab) at 1/10000 and α-Tom70 (Nargang lab) at 1/10000.

2.2.6. Spot test growth

Conidia from *N. crassa* strains were harvested in 50 ml of sterile, distilled water, and then pelleted in a clinical centrifuge at full speed (International Equipment Company, Needham Heights, MA). The conidia were washed three times before resuspension in 25 ml of sterile, distilled water. Conidia were counted by placing 10 µl on a hemacytometer, followed by visualization under a microscope. The concentration of each conidial solution was adjusted to 10^4 conidia per µl using sterile distilled water. Serial dilutions of the concentrated stock produced 10^3, 10^2, and 10^1 conidia per µl mixtures. For each strain examined, 10 µl of the four dilutions was sequentially spotted on plates containing the desired medium, which were then incubated at either 30°C or 37°C.

2.2.7. Measurement of oxygen consumption

Oxygen consumption was measured using freshly grown *N. crassa* cultures and an oxygen monitor (Model 53, YSI, Yellow Springs, OH) fitted with a Clark oxygen electrode. 3 ml of liquid culture were placed into a glass chamber into which air was bubbled for 1 min. The probe was then placed into the glass chamber to measure the oxygen concentration in the sample. After a constant rate of respiration was seen, 50 µl of potassium cyanide (0.2 M in 10 mM Tris-HCl, pH 7.2; 5 mM EDTA) was placed into to the chamber. If respiration continued after exposure to cyanide, 50 µl of SHAM (0.3 M in 95% ethanol) was then added. Oxygen consumption tracings were recorded on a chart recorder.

2.2.8. Antibody production

2.2.8.1. Creation of *E. coli* strains expressing DHFR-RTG2 fusion protein

PCR amplification of a 601 bp region of *rtg-2* was achieved using the primers MCH12 and MCH13 (Table 2.2), which include information for *Sal* I and *Hind* III sites, respectively, for cloning of the amplified product. Genomic DNA isolated from the wild-type *N. crassa* strain, 76-26, was used as the template DNA in PCR reactions. The resulting PCR product and the expression vector pQE-40 (Qiagen, Mississauga, ON), were digested with *Sal* I and *Hind* III and then ligated using T4 DNA ligase (Invitrogen, Burlington, ON). The desired plasmid would allow for expression of an estimated 40 kDa fusion protein consisting of a dihydrofolate reductase (DHFR) moiety and a hexahistidinyl tag fused upstream of a 192 amino acid region of RTG2. Plasmid DNA was transformed into *E. coli* XL-2 competent cells as previously described (2.2.3.4). Restriction digestion and sequence analysis of plasmid DNA isolated from the transformants confirmed the existence of the appropriate plasmid. The desired plasmid, pRtg2-Ab2-3 was then transformed into BL21 *E. coli* cells containing the plasmid pREP4 (Novagen, Mississauga, ON) for expression of the fusion protein. The BL21 strain is deficient for the proteases encoded by *ompT* and *lon*. The pREP4 plasmid contains the *lac* operon repressor, which prevents leaky protein expression. Restriction digestion was again used to confirm the correct plasmid and the strain carrying the plasmid was named RTG2-Ab2-3C.

2.2.8.2. DHFR-RTG2 fusion protein expression

A 500 ml culture of LB media supplemented with ampicillin (0.1 mg/ml; to select for pRtg2-Ab2-3) and kanamycin (25 μg/ml; to select for pREP4) was inoculated with RTG2-Ab2-3C and placed in a 37°C shaking incubator. Once the OD_{600} reached 0.6-0.8, 5 ml of 25 mg/ml isopropyl-beta-D-thiogalactopyranoside (IPTG) was added to the culture. After an additional 4-5 hrs of growth at 37°C, the culture was distributed into 2 centrifuge bottles and spun at 4000 rpm for 20 min at 4°C in a Sorvall SLC-1500 rotor (Sorvall, Mandel Scientific, Guelph, ON). The pellet was resuspended in five volumes of urea lysis buffer (8 M urea; 100 mM NaH_2PO_4; 10 mM Tris-Cl, pH 8.0) supplemented

with 1 mM PMSF and protease inhibitor cocktail (10 µl per ml of buffer; Sigma-Aldrich, Oakville, ON). After 1 hr of gentle shaking, the cellular debris was pelleted at 15000 rpm for 15 min at 4°C in a Sorvall SS-34 rotor (Sorvall, Mandel Scientific, Guelph, ON). The supernatant was transferred to a new tube, and Ni-NTA agarose (Qiagen, Mississauga, ON) was added (4 volumes of supernatant to 1 volume of Ni-NTA agarose). The mixture was shaken gently for 1 hr at 4°C prior to loading into an empty 20 ml Bio-rad Econo-Pac Column (Bio-Rad, Mississauga, ON). The beads were washed twice with 8 ml of urea wash buffer (8 M urea; 100 mM NaH_2PO_4; 10 mM Tris-Cl, pH 6.3). Bound proteins were eluted from the column with 5 ml of SDS elution buffer (0.1% SDS; 10 mM Tris-Cl, pH 7.5). The eluate was transferred to microcentrifuge tubes, heated to 100°C for 3 min to denature the proteins, and then stored at -20°C.

2.2.8.3. Antibody production in mice

Five mice were injected with a mixture containing 160 µl of the eluate isolated in 2.2.8.2 combined with 140 µl of Freund's complete adjuvant (Difco, Kansas, MO). Two booster injections were carried out four and twelve weeks after the initial injection. These injections were performed using a solution similar to that used in the initial injection except that Freund's incomplete adjuvant (Difco, Kansas, MO) was used in place of the complete form. Antibody production was monitored through two test bleeds, which were performed four weeks after each booster injection. The blood was allowed to coagulate at room temperature for 3 hours, and after centrifugation in a clinical centrifuge at full speed (International Equipment Company, Needham Heights, MA), the blood serum was transferred to a new tube. The presence of an α-RTG2 antibody was observed in the second test bleed in four of the five mice (4-2-1 to 4-2-4). A final bleed was immediately collected from each of the four mice and the resulting serum was stored at -80°C.

2.3. Results

2.3.1. Identification of *N. crassa* RTG homologues

One of the major projects in the Nargang lab is focused on the regulation of alternative oxidase production. This enzyme is regulated through retrograde signaling as it is absent under normal growth conditions but appears when mitochondrial oxidative phosphorylation is inhibited by mutations or inhibitors (LI *et al.* 1996). Thus, it was of interest to determine if components of the well-characterized yeast *RTG* pathway existed in *N. crassa*, and if so, whether or not they were involved in induction of alternative oxidase. Protein sequences of the *RTG* genes from *S. cerevisiae* were used as queries in BLAST searches of the *N. crassa* database of the Broad Institute. Of the three *RTG* genes in yeast, only Rtg2p was found to have an obvious *N. crassa* homologue. This homologue has a 27% identity and a 52% similarity with yeast Rtg2p (Figure 2.2). The greatest similarity occurs in the N-terminal half of the protein, which displays homology to ATP binding serine/threonine phosphatases (KOONIN 1994). Because of its similarity to yeast Rtg2p, the gene encoding the *N. crassa* protein was named *rtg-2*. The *N. crassa* *rtg-2* gene contains three exons (579 amino acids) and is predicted to encode a protein with a molecular weight of 62 kDa (Figure 2.3).

2.3.2. Creation of a *N. crassa rtg-2* knockout

N. crassa deficient for *rtg-2* were generated using strains constructed for efficient homologous recombination (NINOMIYA *et al.* 2004). These strains, Fungal Genetics Stock Center (FGSC) numbers 9718 and 9719, were transformed with a linear DNA fragment containing a hygromycin resistance cassette flanked by *rtg-2* upstream and downstream sequences (Figure 2.1, panel B). Selection of transformants was achieved by plating on medium containing hygromycin. Strains Rtg2-KO18-2 and Rtg2-KO19-5 were chosen for further work after purification as described in the materials and methods (2.2.3.6). Cytosolic protein extracts were isolated from strains Rtg2-KO18-2 and Rtg2-KO19-5 as well as control strains following growth in either standard medium or medium containing chloramphenicol. Chloramphenicol inhibits mitochondrial translation and severely reduces synthesis of the mitochondrial encoded components of the respiratory complexes leading to induction of alternative oxidase. Western-blot analysis of cytosolic proteins revealed that the two parental strains, 9718 and 9719, contained similar amounts

Figure 2.2. Alignment of RTG2 protein sequences from *S. cerevisiae* (*S.c.*) and *N. crassa* (*N.c.*). The protein sequence of *S. cerevisiae* Rtg2p was used as a query in BLAST searches of the *N. crassa* database of the Broad Institute. This search identified a *N. crassa* homologue, with 27% identity (black boxes) and 52% similarity (grey boxes) to *S. cerevisiae*. Forward and reverse arrows located above the protein sequence indicate the residues involved in phosphate and adenine binding, respectively.

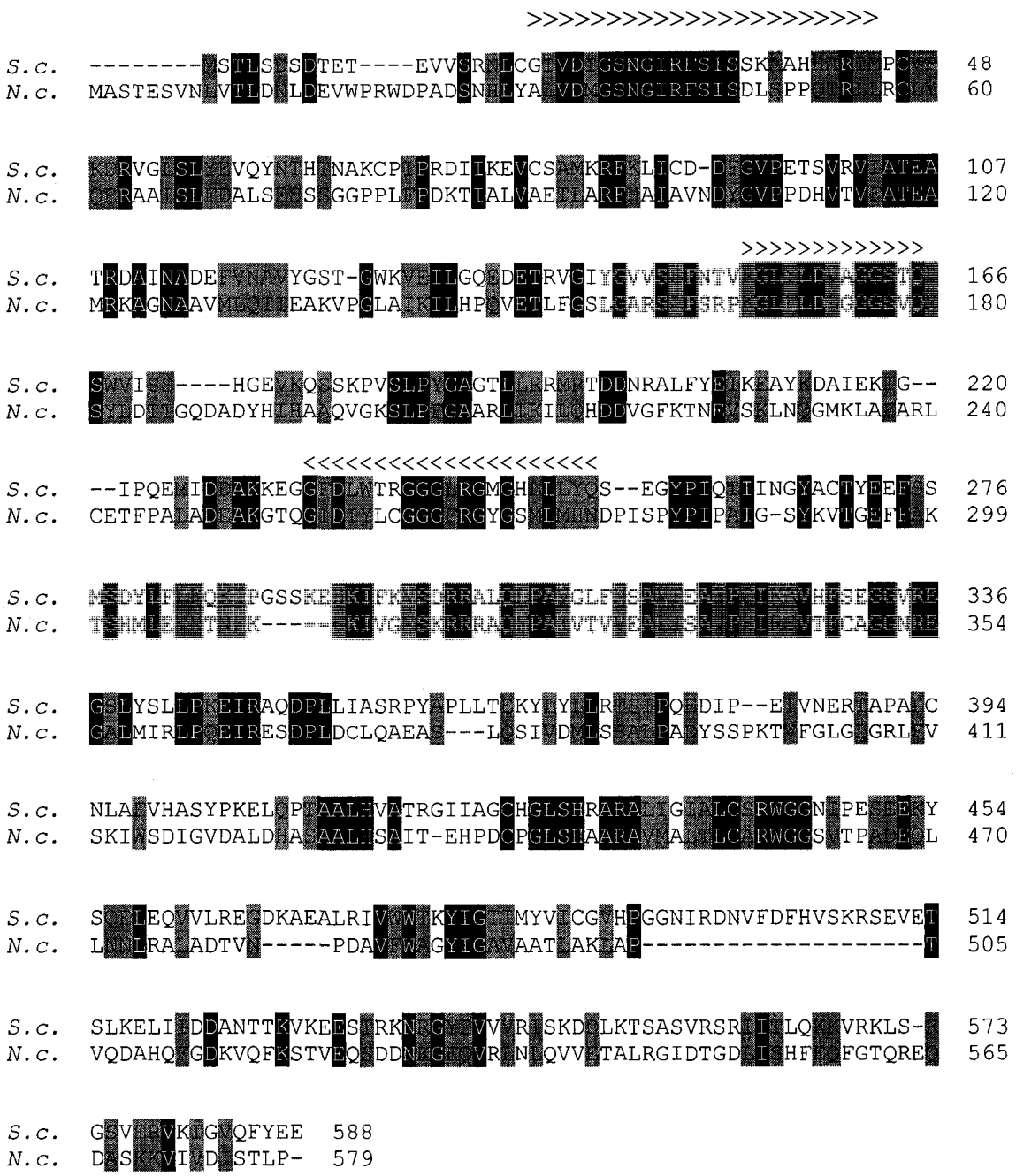

Figure 2.3. The predicted *N. crassa rtg-2* genomic sequence. The *N. crassa rtg-2* gene (NCU08611.3) consists of three exons and two introns with a total length of 1881 bp (579 amino acids). Nucleotides located in coding regions are in uppercase. Amino acid residues are indicated beneath the corresponding codons. The *rtg-2* gene is predicted to encode a 62 kDa protein. The transcription start site is unknown so the first position of the ATG start codon was arbitrarily chosen as the +1 site of the sequence.

```
tcccactttcggcagtcagtgcttctacccaaggtactactttgtacaccagttgagctg      -245

ggcaggaacagccagtgtagctccaggtccttcccactctgggtgaactacacaatccag      -185

cagctgtgatgattggctgaatcacagctgtgtggagctcccggccgtcttgctggccga      -125

cattgggcatcatcggcgtcagttccttcgcatgatctttgaactttgctttcttttctt      -65

cctttggctttcgatttcaagttcctcctggagtgatatttcagctgctcagtttaccca      -5

aaag ATG GCA TCA ACA GAA TCA GTC AAC TTG GTC ACG TTG GAC AAT       42
     M   A   S   T   E   S   V   N   L   V   T   L   D   N       14

CTC GAC GAG GTA TGG CCT CGC TGG GAC CCC GCC GAC TCG AAC CAC       87
L   D   E   V   W   P   R   W   D   P   A   D   S   N   H       29

CTC TAT GCC TTG GTT GAT ATG GGC AGgtaagctggctacagtaccgtattt      138
L   Y   A   L   V   D   M   G   S                                38

gcacttttccccctcgtggtgctcatatcctgattaatttctttatttgtttcacagT      196

AAT GGC ATC CGG TTC TCC ATT TCC GAC CTC TCC CCG CCA CAG ACT       241
N   G   I   R   F   S   I   S   D   L   S   P   P   Q   T       53

CGC CTG CTC AGG TGT CTT TAC CAG GAG CGA GCC GCC ATC TCC CTC       286
R   L   L   R   C   L   Y   Q   E   R   A   A   I   S   L       68

TTC GAT GCC CTG AGC GAG TCT TCA TCT GGT GGC CCC CCG CTT TTC       331
F   D   A   L   S   E   S   S   S   G   G   P   P   L   F       83

CCC GAC AAA ACC ATC GCC CTT GTG GCC GAG ACA CTG GCC CGG TTC       376
P   D   K   T   I   A   L   V   A   E   T   L   A   R   F       98

CAT GCC ATT GCT GTC AAC GAC TAC GGC GTA CCC CCC GAC CAT GTC       421
H   A   I   A   V   N   D   Y   G   V   P   P   D   H   V       113

ACC GTC TTT GCT ACA GAG GCC ATG CGG AAA GCG GGC AAC GCT GCT       466
T   V   F   A   T   E   A   M   R   K   A   G   N   A   A       128

GTC ATG CTA CAG ACC ATC GAG GCC AAG GTC CCT GGA CTT GCT ATC       511
V   M   L   Q   T   I   E   A   K   V   P   G   L   A   I       143

AAG ATT CTG CAC CCC CAA GTT GAG ACC TTG TTC GGC TCA CTG GGA       556
K   I   L   H   P   Q   V   E   T   L   F   G   S   L   G       158

GCC AGA TCG GCC TTT TCT CGT CCC AAG GGT CTC TTC CTT GAC CTT       601
A   R   S   A   F   S   R   P   K   G   L   F   L   D   L       173

GGC GGT GGC AGT GTC CAG ATG TCT TAT CTG GAC ACC ACC GGT CAA       646
G   G   G   S   V   Q   M   S   Y   L   D   T   T   G   Q       188

GAT GCC GAC TAT CAC ATC CAC GCA GCA CAG GTC GGC AAG AGT TTG       691
D   A   D   Y   H   I   H   A   A   Q   V   G   K   S   L       203

CCT TTT GGT GCT GCT CGC TTG ATC AAA ATC CTT CAA CAC GAC GAT       736
P   F   G   A   A   R   L   I   K   I   L   Q   H   D   D       218
```

```
GTT GGC TTC AAG ACC AAC GAG GTT TCG AAG CTC AAC CAA GGT ATG        781
V   G   F   K   T   N   E   V   S   K   L   N   Q   G   M        233

AAG CTG GCT TTT GCT AGG CTT TGC GAG ACC TTC CCT GCC CTT GCG        826
K   L   A   F   A   R   L   C   E   T   F   P   A   L   A        248

GAC GAA GCC AAG GGC ACA CAA GGC ATC GAT ATT TAT CTC TGC GGA        871
D   E   A   K   G   T   Q   G   I   D   I   Y   L   C   G        263

GGA GGG TTC CGA GGC TAC GGC AGC ATG CTG ATG CAC AAC GAT CCA        916
G   G   F   R   G   Y   G   S   M   L   M   H   N   D   P        278

ATC TCC CCG TAT CCC ATA CCA GCA ATA GGC TCC TAC AAA GTC ACG        961
I   S   P   Y   P   I   P   A   I   G   S   Y   K   V   T        293

GGC GAA TTC TTT GCC AAG ACC AGT CAT ATG CTC GAA GTG AAC ACC       1006
G   E   F   F   A   K   T   S   H   M   L   E   V   N   T        308

AAT TTC AAG AAG AAG ATC GTT GGA ATG TCC AAG CGC CGC CGA GCC       1051
N   F   K   K   K   I   V   G   M   S   K   R   R   R   A        323

CAG TTT CCT GCC ATC GTC ACG GTC GTT GAG GCT CTC ATC TCG GCC       1096
Q   F   P   A   I   V   T   V   V   E   A   L   I   S   A        338

GTT CCA CAC ATA CGA TCG GTC ACG TTT TGT GCC GGA GGA AAC AGA       1141
V   P   H   I   R   S   V   T   F   C   A   G   G   N   R        353

GAG GGT GCG CTC ATG ATC AGG CTG CCC CAG GAG ATT CGC GAG AGC       1186
E   G   A   L   M   I   R   L   P   Q   E   I   R   E   S        368

GAT CCG TTG GAT TGT CTC CAA GCC GAG GCA TCA CTC CAA AGT ATC       1231
D   P   L   D   C   L   Q   A   E   A   S   L   Q   S   I        383

GTT GAT ATG CTG TCA TCG GCG CTT CCA GCT GAC TAC AGC AGC CCA       1276
V   D   M   L   S   S   A   L   P   A   D   Y   S   S   P        398

AAA ACG GTA TTT GGT CTT GGT CTT GGC CGC CTG TTC GTG AGC AAG       1321
K   T   V   F   G   L   G   L   G   R   L   F   V   S   K        413

ATT TGG TCT GAC ATC GGC GTT GAT GCC CTT GAT CAT GCC TCT GCC       1366
I   W   S   D   I   G   V   D   A   L   D   H   A   S   A        428

GCA TTG CAC AGC GCC ATC ACG GAG CAT CCG GAT TGT CCT GGT CTA       1411
A   L   H   S   A   I   T   E   H   P   D   C   P   G   L        443

TCG CAC GCG GCC CGG GCT GTA ATG GCT CTG ACA CTT TGT GCG AGA       1456
S   H   A   A   R   A   V   M   A   L   T   L   C   A   R        458

TGG GGC GGT AGC GTC ACT CCG GCG GAT GAA CAG CTG TTG AAC AAC       1501
W   G   G   S   V   T   P   A   D   E   Q   L   L   N   N        473

TTG CGG GCA TTG GCC GAC ACT GTC AAC CCT GAC GCT GTG TTC TGG       1546
L   R   A   L   A   D   T   V   N   P   D   A   V   F   W        488

GCG GGC TAC ATT GGA GCT GTA GCT GCC ACA CTT GCG AAA CTG GCA       1591
A   G   Y   I   G   A   V   A   A   T   L   A   K   L   A        503
```

```
CCA ACG GTC CAG GAT GCT CAT CAA TTT GGA GAC AAG GTT CAgtaagt      1638
P   T   V   Q   D   A   H   Q   F   G   D   K   V   Q          517

tgattgatggactaaacagctgtttgatagtgtactgatcatgctggcgccagG TTT      1695
                                                        F      518

AAA TCG ACC GTG GAA CAG TCC GAT GAT AAC AAA GGG TTT CAA GTT      1740
K   S   T   V   E   Q   S   D   D   N   K   G   F   Q   V      533

CGC CTC AAC CTC CAG GTT GTC GAA ACA GCT CTT CGC GGC ATT GAC      1785
R   L   N   L   Q   V   V   E   T   A   L   R   G   I   D      548

ACC GGA GAC CTG ATA TCC CAT TTC GAA CAA TTC GGC ACG CAG AGA      1830
T   G   D   L   I   S   H   F   E   Q   F   G   T   Q   R      563

GAG CAA GAT GCC AGC AAA AAG GTC ATT GTG GAC ATA AGC ACG CTT      1875
E   Q   D   A   S   K   K   V   I   V   D   I   S   T   L      578

CCT TGA tgtggcaagttgttatgatgctgtcgacagtgattattctatctctacgtcc      1933
P                                                               579

atggacattatgtcaatatgccattacgatattgttctacttctgtaagccgttcgcagt

ctctcataccttcctctagtaccaaacgcctgtatagtcggacctatgtactagtatct

ctttgtcttctgcttggggactcaagcttgcttcttctcgcacactttccctttccttc

gttactccgccggttcaagaccaactcttcccaggttacg
```

of RTG2 protein when grown in the presence and absence of chloramphenicol (Figure 2.4). Constitutive expression of *rtg-2* was also observed in a standard laboratory wild-type control strain, NCN251-5, as well as a strain (7207) carrying a frameshift mutation in the *aod-1* gene (Li *et al.* 1996), which encodes alternative oxidase (Figure 2.4). Conversely, no RTG2 protein was observed in either of the *rtg-2* knockout strains, Rtg2-KO18-2 and Rtg2-KO19-5 under either growth condition (Figure 2.4). Actin levels were similar in all strains regardless of growth conditions.

2.3.3. *N. crassa rtg-2* mutant phenotypes

2.3.3.1. Alternative oxidase expression

The *rtg-2* knockout strains were tested for alternative oxidase activity by examining their respiratory characteristics following growth in standard medium or medium containing chloramphenicol. In standard medium, oxygen consumption of both knockout and control strains was completely inhibited in the presence of cyanide (Figure 2.5). Similarly, no differences from controls were observed when *rtg-2* knockout strains were grown in the presence of chloramphenicol as all strains displayed the cyanide-insensitive respiration that is characteristic of alternative oxidase activity (Figure 2.5). The cyanide-insensitive respiration of all strains was inhibited by SHAM, a known inhibitor of alternative oxidase (Figure 2.5). These results were confirmed by Western-blot analysis performed on mitochondrial proteins isolated from cultures grown in the presence and absence of chloramphenicol. Despite lacking the *rtg-2* gene, the knockout strains displayed no alteration in the expression of *aod-1* as the protein was only present when cultures were grown in the presence of chloramphenicol (Figure 2.4). Taken together, these data suggest that *rtg-2* is not required for alternative oxidase expression.

2.3.3.2. Growth requirements

In *S. cerevisiae*, *RTG* mutants display growth phenotypes that are characteristic of strains that carry mutations affecting steps in both the TCA and glyoxylate cycles. For instance, when grown in media where ammonium sulfate is the only source of nitrogen,

Figure 2.4. Characterization of proteins in *rtg-2* mutant strains. Cytosolic and mitochondrial protein fractions were prepared from two *rtg-2* mutant strains (Rtg-2KO18-2 and Rtg-2KO19-5), their parental strains (9718 and 9719), a standard laboratory wild-type strain (NCN251-5), and an *aod-1* mutant strain (7207). Cultures were grown in the presence and absence of chloramphenicol (Cm), which inhibits synthesis of mitochondrial-encoded proteins. Proteins were separated by SDS-PAGE, blotted to nitrocellulose membrane and probed with antibodies as indicated on the left. Cytosolic fractions (120 μg per lane) were examined for the presence of RTG2 protein and actin (loading control). Mitochondrial fractions (25 μg per lane) were analyzed for AOD1 and Tom70 (loading control).

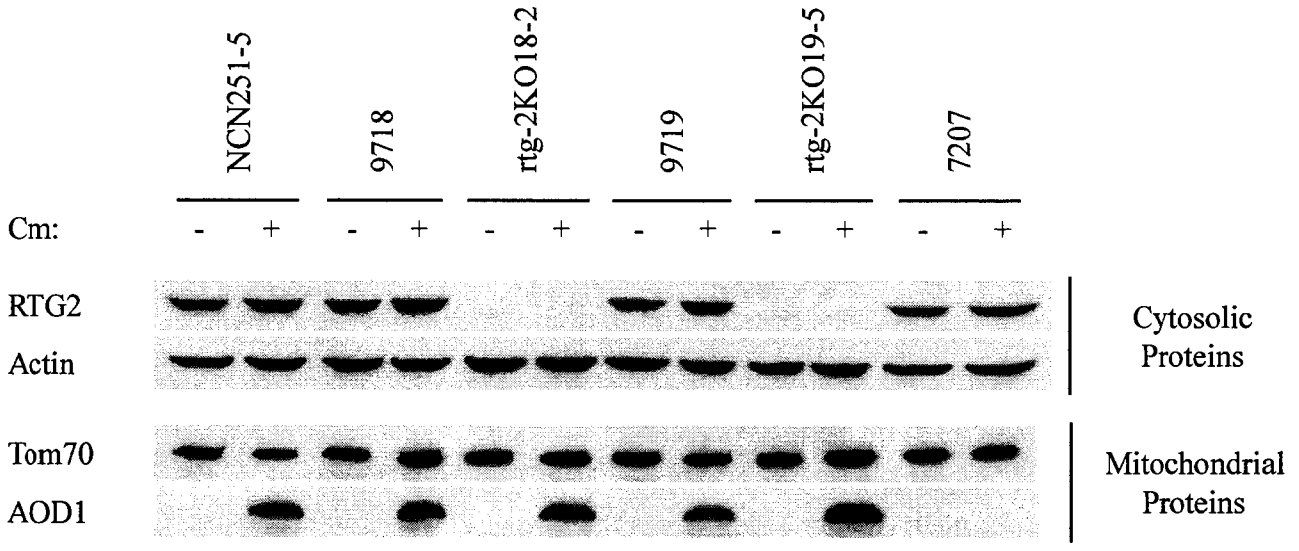
NCN251-5
9718
rtg-2KO18-2
9719
rtg-2KO19-5
7207
Cm:
- + - + - + - + - + - +
RTG2
Actin
Tom70
AOD1
Cytosolic Proteins
Mitochondrial Proteins

Figure 2.5. Measurement of oxygen consumption. Respiration was examined in the *rtg-2* mutant strains (Rtg-2KO18-2 and Rtg-2KO19-5) and control strains (described in Figure 2.4 legend) following growth in the presence or absence of chloramphenicol (Cm). Normal respiration causes oxygen concentration (y-axis) to decrease steadily over time (x-axis). Respiratory inhibitors potassium cyanide (KCN) and salicylhydroxamic acid (SHAM) were added as indicated and their effects on respiration were observed. Complete inhibition of respiration prevented cells from consuming oxygen and thus a further decrease in oxygen concentration was no longer observed.

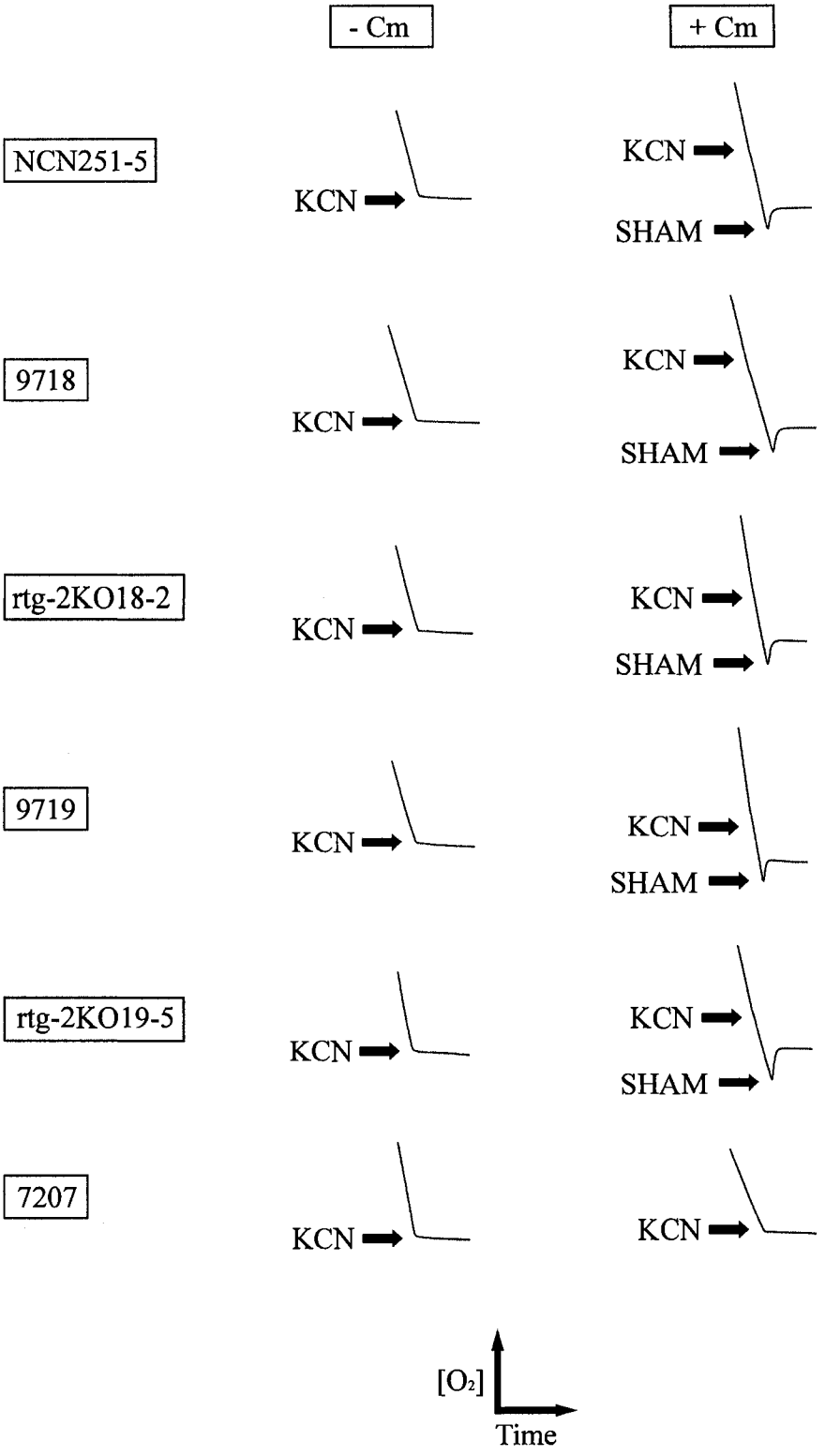
- Cm
+ Cm
NCN251-5
KCN
KCN
SHAM
9718
KCN
KCN
SHAM
rtg-2KO18-2
KCN
KCN
SHAM
9719
KCN
KCN
SHAM
rtg-2KO19-5
KCN
KCN
SHAM
7207
KCN
KCN
[O2]
Time

yeast *RTG* mutants are auxotrophic for glutamic and aspartic acid (LIAO and BUTOW 1993). To assess whether *N. crassa rtg-2* mutants displayed a similar phenotype, conidia from control and knockout strains were tested for nitrogen requirements. The wild-type strain, NCN251-5, the two parental strains, and both *rtg-2* mutant strains displayed similar rates of growth on minimal medium (Figure 2.6). However, unlike what is observed in yeast *RTG* mutants, the *N. crassa rtg-2* knockout strains did not display growth defects on nitrogen-limiting plates, even when the mutants were grown at elevated temperatures (37°C) (Figure 2.6).

2.4. Discussion

2.4.1. RTG homologues in *N. crassa*

Of the three *RTG* genes identified in *S. cerevisiae*, only RTG2 was identified in *N. crassa* by BLAST searches. The inability to identify RTG1 and RTG3 homologues could be due to poor conservation of the proteins in *N. crassa* or may imply that these genes are specific to *S. cerevisiae*. It is also possible that the functions of Rtg1p and Rtg3p may be performed by different proteins or are not required in *N. crassa*. Rtg2p is thought to be the key regulator protein of the *RTG*-mediated retrograde pathway and its amino acid sequence is well conserved among fungal species, whereas other members of the yeast *RTG*-mediated retrograde pathway are not (LIU and BUTOW 2006; LIU *et al.* 2003; LIU *et al.* 2005). The wide-spread conservation of Rtg2p suggests that it performs a broader and perhaps more important function, though clearly no obvious phenotype is apparent in *N. crassa* cells lacking the gene.

2.4.2. Phenotypes of the *rtg-2* knockout strains

Although mitochondrial dysfunction appears to increase expression of *CIT2* in yeast, Northern-blot analysis of RNA isolated from cultures of *N. crassa rtg-2* mutant strains grown in the absence and presence of the respiratory inhibitor antimycin A suggests that there are extremely low transcript levels of the *N. crassa* peroxisomal isoform of citrate synthase under either condition (data not shown). In addition, the *N.*

Figure 2.6. Growth of *N. crassa* strains. Conidia from the *rtg-2* knockouts (Rtg-2KO18-2 and Rtg-2KO19-5) and control strains (described in Figure 2.4 legend) were harvested and adjusted to a concentration of 10^4 conidia per μl. The conidial stocks were then subjected to three 1/10 serial dilutions. 10 μl of each conidial suspension was placed on plates containing minimal medium or a low nitrogen medium in which ammonium sulfate (0.25%) was the sole nitrogen source. Plates were incubated at 30°C or 37 °C (as indicated). Photographs were taken after 24 hours of growth.

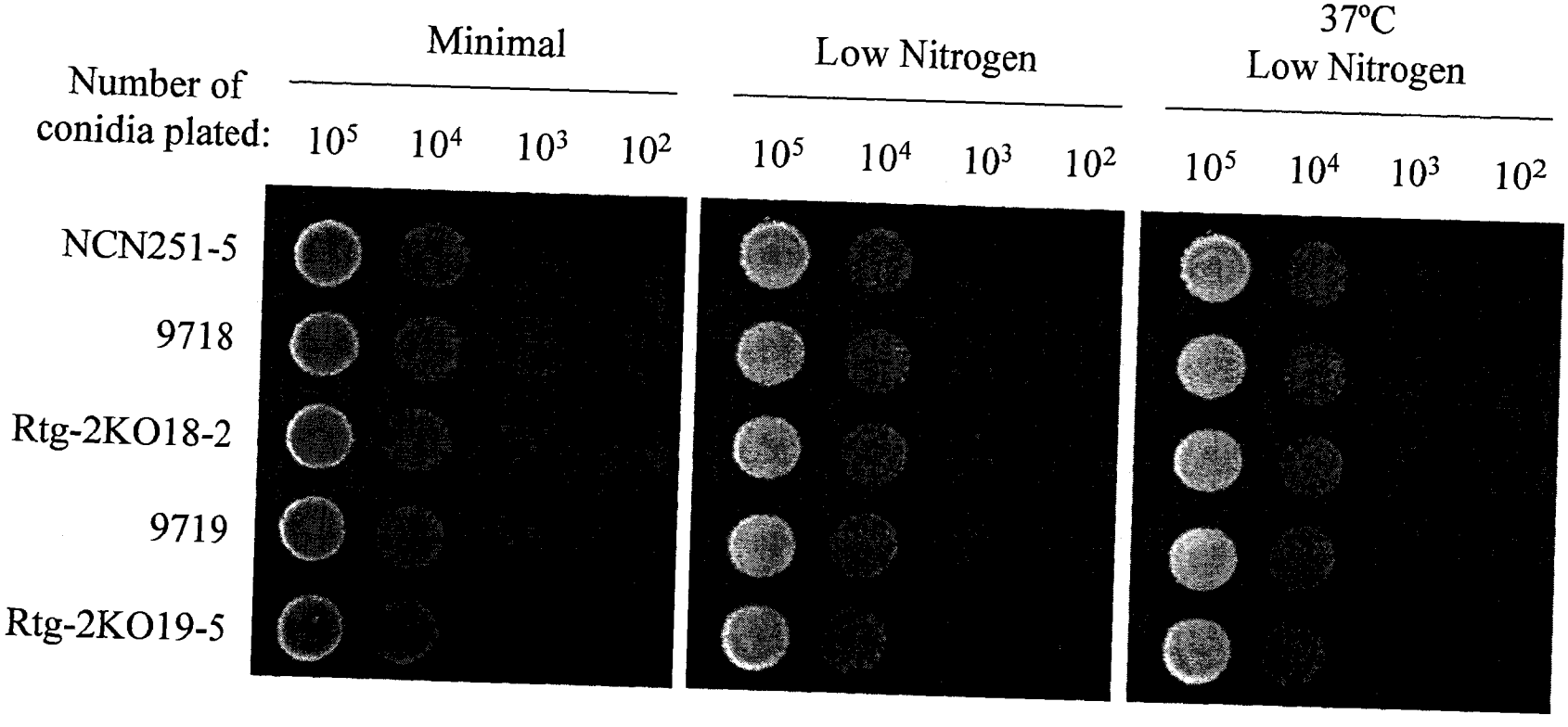
Minimal
Low Nitrogen
37°C
Low Nitrogen
Number of conidia plated:
10^5 10^4 10^3 10^2
10^5 10^4 10^3 10^2
10^5 10^4 10^3 10^2
NCN251-5
9718
Rtg-2KO18-2
9719
Rtg-2KO19-5

crassa rtg-2 mutants did not display any of the growth phenotypes that are observed in *RTG* mutants of yeast, such as glutamate or aspartate auxotrophy. However, it should be noted that even in yeast there is evidence that dependence on an *RTG*-mediated retrograde response varies depending on the type of carbon source present in the growth medium and the genetic background of the strain (BUTOW and AVADHANI 2004; KIRCHMAN *et al.* 1999). For example, yeast ρ^0 cells grown in the presence of raffinose display much greater increases in *CIT2* mRNA production compared to cells cultured in medium where glucose is the sole carbon source (KIRCHMAN *et al.* 1999). Additionally, when grown in the presence of glucose, some yeast strains actually demonstrate greater levels of *CIT2* mRNA in grande cells compared to isochromosomal petites (W303-1A and A364A) (KIRCHMAN *et al.* 1999). Thus, it is possible that unexamined factors in the growth media used in our experiments result in bypass of the requirement for an *RTG*-mediated retrograde response, or that our *rtg-2* mutants possess a genetic background which renders them less reliant on the activation of this retrograde pathway.

2.4.3. *rtg-2* and alternative oxidase

Both *rtg-2* knockout strains produced in this study displayed wild-type alternative oxidase expression, characterized by the accumulation of alternative oxidase protein and activity only when grown in the presence of chloramphenicol, which results in inhibition of the respiratory chain due to inefficient translation of mitochondrial gene products. These data demonstrate that an *RTG*-mediated retrograde response pathway is not required for alternative oxidase induction or function.

Although we were initially interested in determining if *rtg-2* was involved in the expression of alternative oxidase, it is possible that the capacity for inducing alternative oxidase in *N. crassa* may actually circumvent the need for an *RTG*-controlled retrograde pathway as it exists in yeast. The major purpose of this retrograde response in yeast is thought to be the maintenance of Krebs cycle intermediates which become limiting when the respiratory chain is disrupted (BUTOW and AVADHANI 2004; LIAO *et al.* 1991). However, in *N. crassa*, blockage of the electron transport chain results in the production of alternative oxidase, which allows for the continuation of both energy production and the Krebs cycle. Thus, in *N. crassa*, inhibition of the cytochrome-mediated respiratory

chain alone is not likely to require activation of the classic *RTG*-mediated retrograde response.

2.5. Conclusions

This research has shown that in *N. crassa*, *rtg-2* is not required for the induction or function of alternative oxidase, at least in the strains examined. Numerous genes in yeast display *RTG*-independent retrograde regulation, suggesting that there are likely several mitochondrial-to-nucleus signaling pathways (EPSTEIN *et al.* 2001). Since alternative oxidase and RTG2 are likely both involved in the maintenance of Krebs cycle intermediates, it is of interest to determine if there is any interaction between the two pathways. To test this hypothesis, we have obtained *aod-1 rtg-2* double mutants by crossing an *aod-1* mutant strain (7207) with our *rtg-2* knockout strains. Our preliminary results suggested that the *aod-1 rtg-2* double mutants are more sensitive to low doses of respiratory inhibitors than the *aod-1* mutant strain, which suggests that the RTG2 protein of *N. crassa* may help maintain Krebs cycle intermediates when respiration is hindered. Unfortunately, further experimentation revealed that the *aod-1* mutant strain used to generate the *aod-1 rtg-2* double mutants may have sustained an additional mutation that hindered its growth on minimal medium and this unknown mutation was believed to have emerged in this strain prior to it use in the sexual cross from which the double mutants were obtained. Thus, the increased sensitivity to low concentrations of antimycin A observed in the double mutants may have resulted from the unknown mutation present in 7207. This concern may be addressed by using gene replacement methodologies to knockout the *aod-1* gene in the existing *rtg-2* mutant strains. This *aod-1 rtg-2* double mutant may be able to confirm that both AOD1 and RTG2 are involved in ensuring that the Krebs cycle can function despite perturbations in respiration. Uncovering a relationship between an *RTG*-mediated retrograde response and the induction of alternative oxidase may enhance our understanding of the individual pathways and would also provide insight into retrograde regulation as a whole.

Chapter 3: Identification of an alternative oxidase binding motif (AIM) which is bound by the DNA-binding domains of AOD2 and AOD5 *

3.1. Introduction

3.1.1. The alternative oxidase promoter

The inducible form of alternative oxidase is normally observed only under stressful conditions, which can be achieved through exposure to several chemicals or through exposure to harsh environments. Numerous studies have shown that the appearance of the alternative oxidase protein correlates with increased rates of transcription and the accumulation of mRNA (DOJCINOVIC *et al.* 2005; LI *et al.* 1996; TANTON *et al.* 2003; VANLERBERGHE and MCINTOSH 1997; YUKIOKA *et al.* 1998). Thus,

---

* Portions of the work presented in this chapter have appeared in:

1. CHAE, M.S., C.C. LIN, K.E. KESSLER, C.E. NARGANG, L.L. TANTON, L.B. HAHN and F.E. NARGANG, 2007a Identification of an alternative oxidase induction motif in the promoter region of the *aod-1* gene in *Neurospora crassa.* Genetics **175**: 1597-1606.

2. CHAE, M.S., C.E. NARGANG, I.A. CLEARY, C.C. LIN, A.T. TODD and F.E. NARGANG, 2007b Two zinc cluster transcription factors control induction of alternative oxidase in *Neurospora crassa.* Genetics **177**: 1997-2006.

Although these papers have multiple authors, only data that I collected is presented in this thesis. In some cases, I was assisted by undergraduate students (C.C. Lin and L.B. Hahn) who worked under my supervision. Plasmids pMMAX and pMCMAX were generated by L.L. Tanton and were used as controls in my work. The deletion constructs were made by K.E. Kessler.

it is likely that the alternative oxidase promoter contains a sequence element(s) that is integral to inducible expression of the protein.

Analysis of the alternative oxidase gene promoter has been performed in several different plants, including *S. guttatum*, *G. max* and *A. thaliana* (DOJCINOVIC *et al.* 2005; RHOADS and MCINTOSH 1993b; THIRKETTLE-WATTS *et al.* 2003). Although several putative promoter elements have been uncovered through comparative analysis, there is currently very little experimental evidence to support the function of these elements. Systematic deletions within the *AOX1a* promoter of *A. thaliana* identified a 93 bp region necessary for induction of alternative oxidase (DOJCINOVIC *et al.* 2005). This sequence, termed the mitochondrial retrograde regulation (MRR) region, contains two G (for G-rich) box-like motifs (CACGTG) that are known to bind members of a basic leucine zipper (bZIP) family of transcription factors. Mutation of either G-box-like motif of the MRR reduced the ability of the *AOX1a* promoter to increase rates of transcription of a reporter gene when exposed to antimycin A or the TCA cycle inhibitor, monofluoroacetate (DOJCINOVIC *et al.* 2005).

The sequence elements within the *aod-1* gene promoter that are required for wild-type expression of alternative oxidase in *N. crassa* were shown to be contained in a construct (pMMAX) containing the *aod-1* coding sequence, along with 255 bp of sequence upstream of the transcription start site, and 374 bp of downstream sequence (TANTON *et al.* 2003). Conversely, when the upstream sequence was shortened to 10 bp (pMCMAX), the resulting construct could not restore wild-type alternative oxidase expression to an *aod-1* mutant strain. This suggested that in *N. crassa*, expression of alternative oxidase may require an important regulatory element(s) that resides within the 245 bp that occurs in pMMAX but is absent in pMCMAX.

3.1.2. Zn(II)2Cys6 binuclear cluster transcription factors

In *N. crassa*, expression of alternative oxidase was shown to require the *aod-2*, *aod-4*, *aod-5* and *aod-7* genes (BERTRAND *et al.* 1983; DESCHENEAU *et al.* 2005). Recently, *aod-2* and *aod-5* were cloned in our lab by Cheryl Nargang (CHAE *et al.* 2007b). Analysis of their amino acid sequence suggested that these proteins may belong

to the Zn(II)2Cys6 binuclear cluster (zinc cluster) family (Figure 3.1), which comprise the largest fungal specific class of transcription factors (MACPHERSON *et al.* 2006; TODD and ANDRIANOPOULOS 1997). For example, genome analysis has suggested that *N. crassa* and *S. cerevisiae* encode 77 and 58 putative zinc cluster proteins, respectively (BORKOVICH *et al.* 2004; MACPHERSON *et al.* 2006; SCHJERLING and HOLMBERG 1996). In addition to their DNA-binding domains, zinc cluster proteins may also contain a variety of other domains that can regulate protein function. For example, many zinc cluster proteins contain motifs that mediate cellular localization, and/or interaction with other proteins and cofactors. The "typical" protein of this family is characterized by a modular structure of several important domains as described below.

3.1.2.1. The DNA-binding domain

Zinc cluster family members are defined by the presence of a highly conserved Cys-X_2-Cys-X_6-Cys-X_{5-12}-Cys-X_2-Cys-X_{6-8}-Cys motif, which is normally observed in the N-terminus of the protein. The six conserved cysteine residues of the DNA-binding domain coordinate the binding of two zinc atoms and are thus essential to protein assembly and function (BAI and KOHLHAW 1991; CHAE *et al.* 2007b; DEFRANOUX *et al.* 1994; JOHNSTON and DOVER 1987; MACPHERSON *et al.* 2006). Zinc cluster proteins usually bind as homo- or heterodimers with each subunit interacting with specific nucleotides of its target DNA sequence. Typically, zinc cluster proteins bind to trinucleotide repeats arranged in either a direct, inverted or everted orientation and are separated by a spacer region of variable length (MARMORSTEIN *et al.* 1992; SCHJERLING and HOLMBERG 1996). Each subunit of the dimer is thought to bind to one of the triplet repeats. One of the best known proteins of this class is Gal4p of *S. cerevisiae*. This protein was shown to bind two inverted CGG triplets separated by 11 nucleotides. Another well studied *S. cerevisiae* protein, Hap1p interacts with a CGG-N_6-CGG motif (MARMORSTEIN *et al.* 1992; ZHANG and GUARENTE 1994). CGG repeats are a common triplet sequence bound by this class of protein, but there is a wide variety of DNA sequences that have been shown to be bound by this family (MACPHERSON *et al.* 2006). The nature of the spacer region has also been shown to regulate binding. Although the sequence of the spacer region can influence binding efficiencies, maintenance of proper

Figure 3.1. Domain organization of AOD2 and AOD5 proteins. The putative nuclear localization signal (NLS), zinc cluster, and PAS domain are indicated by white boxes and are drawn to scale. The codons that comprise each of these potential motifs are shown in parentheses. The regions representing the predicted DNA-binding domains of AOD2 and AOD5 are indicated by a solid line below each protein.

aod-2:

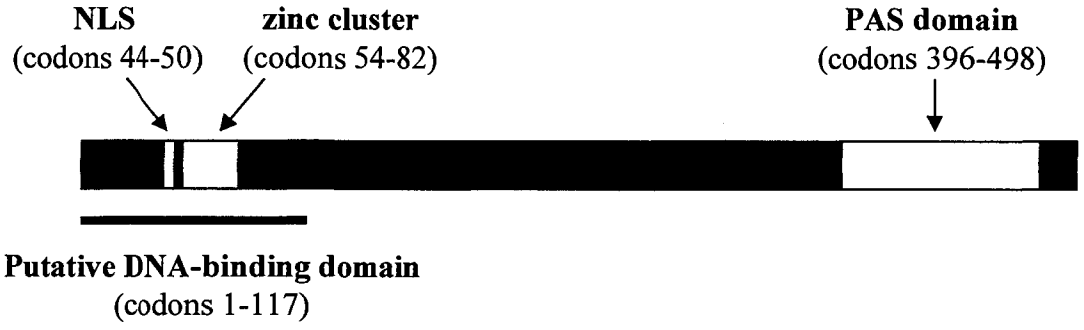
NLS
(codons 44-50)
zinc cluster
(codons 54-82)
PAS domain
(codons 396-498)
Putative DNA-binding domain
(codons 1-117)

aod-5:


NLS
(codons 55-70)
zinc cluster
(codons 75-103)
PAS domain
(codons 477-590)
Putative DNA-binding domain
(codons 1-142)

spacing between the trinucleotide repeats appears to be of greater importance (LIANG *et al.* 1996; VASHEE *et al.* 1993).

The DNA-binding domain of zinc cluster proteins contains a linker region and a dimerization motif. The linker region, which does not possess a conserved sequence or structure, is thought to ensure binding of zinc cluster proteins to the proper target sequence. This hypothesis is based on the observation that switching the linker domains of zinc cluster proteins alters DNA-binding specificity (MAMANE *et al.* 1998; REECE and PTASHNE 1993). Additionally, mutations in the linker region can eliminate protein function by preventing proper interaction with the sequence elements (JOHNSTON and DOVER 1987). The dimerization motif of zinc cluster proteins typically contains heptad repeats that form a coiled-coiled element, a structure which promotes protein-protein interactions (SCHJERLING and HOLMBERG 1996).

3.1.2.2. The middle homology region

The majority of zinc cluster proteins possess a regulatory region known as the middle homology region. This domain is not well conserved at the primary sequence level, but is predicted to form a highly-conserved three dimensional structure (SCHJERLING and HOLMBERG 1996). The precise function of the middle homology region is not known, although it is thought to be involved in the regulation of protein function. For example, removal of the middle homology region in Hap1p of *S. cerevisiae* resulted in its constitutive activation (PFEIFER *et al.* 1989). Similarly, deletion of the middle homology region in Gal4p rendered the protein insensitive to glucose repression (STONE and SADOWSKI 1993). In contrast, transcriptional activation is completely abolished when the middle homology region is removed from the *fluffy* protein, which functions as the primary regulator of conidiation in *N. crassa* (RERNGSAMRAN *et al.* 2005).

3.1.2.3. Activation domains

The nature of the activation domain present in zinc cluster proteins is not well-characterized. This domain, which is generally located at the C-terminus of the protein, is highly variable and can display a wide variety of structures and/or functions (MACPHERSON *et al.* 2006). One of the most common activation domains of zinc cluster

proteins consists of a stretch of acidic amino acids, which produces a region of negative charge (SCHJERLING and HOLMBERG 1996). Removal of the 32 residue acidic region from the C-terminus of Leu3p abolishes transcriptional activity of the protein (SCHJERLING and HOLMBERG 1996; ZHOU and KOHLHAW 1990). Furthermore, domain swapping experiments demonstrated that the acidic regions of Leu3p and Cha4p are interchangeable, although the association with a foreign activation domain resulted in constitutive function of both proteins (WANG *et al.* 1999). Proper regulation was restored when each activation domain was combined with its appropriate middle homology region, regardless of which DNA-binding domain is present. These data suggest that the functions performed by the activation domain and the middle homology region are intimately linked.

3.1.3. PAS domains

The AOD2 and AOD5 proteins were also shown to contain a PAS domain (Figure 3.1). The PAS domain is a protein module that was named after the first three proteins in which it was observed: period (PER), aryl hydrocarbon receptor nuclear translocator protein (ARNT) and single-minded (SIM) (GILLES-GONZALEZ and GONZALEZ 2004; HEFTI *et al.* 2004; LINDEBRO *et al.* 1995; PONGRATZ *et al.* 1998). This motif, which has been observed in proteins from all kingdoms of life can participate in a wide range of functions, but is generally involved in signal transduction (GILLES-GONZALEZ and GONZALEZ 2004). The PAS domain forms a highly conserved tertiary structure despite having very little conservation at the amino acid level. The conserved PAS fold consists of two apparently inseparable subdivisions, PAS and PAC, which together form a five-stranded β-sheet in close proximity to four α-helices (HEFTI *et al.* 2004).

The involvement of PAS domains in signal transduction is often manifested through their interaction with specific cofactors, such as heme, flavin adenine dinucleotide (FAD) and flavin mononucleotide (FMN). For instance, the bacterial FixL protein contains a PAS domain that associates with heme, allowing it to function in a two-component system that responds to changes in intracellular oxygen concentrations (RODGERS and LUKAT-RODGERS 2005; TUCKERMAN *et al.* 2001). The dissociation of oxygen from heme causes a conformational change in FixL, which initiates the signal

transduction pathway and activates transcription of downstream targets. In *N. crassa*, the PAS domain of the circadian clock protein WC-1 interacts with a chromophore FAD molecule (HE *et al.* 2005; VITALINI *et al.* 2006). Exposure to blue-light stimulates WC-1, which leads to dimerization with WC-2 and subsequent activation of light-inducible genes.

The PAS domain has also been implicated in protein dimerization. Gel filtration chromatography demonstrated that removal of a single α-helix in the PAS domain of the *Drosophila* clock protein PERIOD prevented homodimer formation (YILDIZ *et al.* 2005). Similarly, immunoprecipitation experiments in *N. crassa* have shown that the PAS domains of WC-1 and WC-2 are essential for their dimerization (BALLARIO *et al.* 1998). Conversely, the PAS domain of the mouse dioxin receptor was not necessary for dimerization, although its presence was required for specific interaction with Arnt (PONGRATZ *et al.* 1998).

3.1.4. Objectives of this research

The main goal of the research presented in this chapter was to uncover the mechanisms through which alternative oxidase is induced in response to blocks in the cytochrome-mediated respiratory chain. Our first approach was to create specific mutations within the sequence upstream of the *aod-1* structural gene in an attempt to identify a sequence element(s) that is required for efficient expression of the alternative oxidase protein. In addition, since the AOD2 and AOD5 proteins were previously identified as putative zinc cluster transcription factors, it was of interest to determine whether either or both of these proteins interacted directly with the *aod-1* promoter sequence. Uncovering such information would help characterize the pathway that regulates alternative oxidase expression and may provide insight into how mitochondria-to-nucleus signaling in achieved.

3.2. Materials and Methods

3.2.1. *N. crassa* strains and growth conditions

The *N. crassa* strain used in this study, 7207, harbors a frameshift mutation in the coding sequence of *aod-1* (LI *et al.* 1996). This mutation produces a premature stop codon that prevents accumulation of *aod-1* transcript and protein. Growth and handling of this *N. crassa* strain was performed as previously described (DAVIS and DE SERRES 1970). To determine if transformants produced alternative oxidase, cells were grown in the presence of 0.25 to 0.50 μg/ml antimycin A, depending on the lot used. When required, bleomycin was used at a concentration of 1.0 μg/ml.

3.2.2. Deletion analysis

3.2.2.1. Plasmid construction strategy

Plasmids pMMAX and pMCMAX were constructed by a former student in the lab (Lesley Tanton) and have been previously described (TANTON *et al.* 2003). To generate pΔP-1 to pΔP-4, pMMAX was first subjected to site-directed mutagenesis using single-stranded template DNA (as described in section 3.2.2.2) and the primer FNA410 (Table 3.1), which restored a *Bgl* II site at position -255. The repaired version of pMMAX was named rpMMAX. In a similar manner, a second *Bgl* II site was introduced at various locations within the *aod-1* promoter using one of four additional primers, FNA395 to FNA 398 (Table 3.1). The resulting plasmids were digested with *Bgl* II, and then re-ligated, thereby removing small regions of *aod-1* promoter sequence located between the *Bgl* II sites.

3.2.2.2. Site-directed mutagenesis using single-stranded DNA

Site-directed mutagenesis was carried out as described in Sambrook and Russell (2001) with modification. This protocol was performed using *E. coli* cells (CJ236) deficient for dUTPase and uracil-*N*-glycosylase, which results in the occasional incorporation of dUTP instead of dTTP. The F' episome pCJ105 is carried in CJ236 cells and harbors genes enabling the formation of pili, which facilitate phage infection. To obtain single-stranded template DNA, *E. coli* cells carrying pMMAX or rpMMAX were grown at 37°C in 50 ml of 2XYT broth (1.6% tryptone; 1.0% yeast extract; 80 mM NaCl) supplemented with ampicillin (0.1 mg/ml) to maintain the MMAX plasmid and

Table 3.1. Primers used in deletion analysis

Primer Name	Sequence (5' → 3')	Comments
FNA410	GAACCCGGAAAGCTCCAGATCTGCTTGGC GTAATCATGG	Used in site-directed mutagenesis to create rpMMAX; restores the original *Bgl* II site in pMMAX; *Bgl* II site is underlined
FNA395	GGTCTCAAAGGAGCAATAGATCTCCGACA CTGCCC	Used in site-directed mutagenesis to create pΔP-1; *Bgl* II site is underlined
FNA396	GGGAAAAATTTGGAATACGAGATCTGACT GAAAACACCG	Used in site-directed mutagenesis to create pΔP-2; *Bgl* II site is underlined
FNA397	CGGGACCTTTATATCGTCCAGATCTGCCC CCAGTTGC	Used in site-directed mutagenesis to create pΔP-3; *Bgl* II site is underlined
FNA398	CGGACAGCACATGAGATCTGACGTTTATA TCGTCC	Used in site-directed mutagenesis to create pΔP-4; *Bgl* II site is underlined

chloramphenicol (10 μg/ml) to select for pCJ105. Once the culture reached an OD_{600} of 0.7 to 1.0, M13 helper phage was added, which was maintained through kanamycin (70 μg/ml) supplementation. The cultures were then allowed to grow overnight at 37°C. The saturated cultures were spun at 15000 rpm for 20 min (4°C) in an SS34 rotor (Sorvall, Mandel Scientific, Guelph, ON), after which the supernatant was transferred to a clean tube. The centrifugation was repeated, and the twice-cleared supernatant was incubated at room temperature with 3 μg/ml DNase-free RNaseA for 30 min. An equal amount of filter sterilized 3.5 M NH_4CH_3COO, 20% PEG 6000 was added, and then the mixture was incubated on ice for 30 min. The pellet formed after centrifugation at 15000 rpm for 15 min (4°C) was dried, and then resuspended in high-salt buffer (300 mM NaCl; 1 mM EDTA; 100 mM Tris-Cl, pH 8.0). Phenol/chloroform extraction was then performed, followed by ethanol precipitation of the single-stranded DNA, and subsequent dissolving in sterile distilled water.

Mutagenic primers were then mixed with the single-stranded template DNA and 10X annealing buffer (100 mM Tris-Cl, pH 7.4; 20 mM $MgCl_2$; 500 mM NaCl). This mixture was incubated at 70°C for two min, and then slowly cooled to 30°C to allow hybridization of the primer to the template. The reactions were placed on ice for 3 min, after which synthesis buffer (4 mM each dNTP; 7.5 mM ATP; 175 mM Tris-Cl, pH 7.4; 37.5 mM $MgCl_2$; 15 mM DTT), 5U T4 DNA ligase and 0.5U T7 DNA polymerase were added. After successive 5 min incubations first on ice, and then at room temperature, the mixture was placed at 37°C for 90 min. The total reaction was then used to transform *E. coli* (XL-2) competent cells, which were then spread on LB plates containing ampicillin (0.1 mg/ml) as described in 2.2.3.4. Once taken up in the XL-2 cells, the template DNA strand which contains uracil should be degraded, leaving the mutant, *in vitro* synthesized strand intact.

3.2.3. PCR mutagenesis

3.2.3.1. Primer phosphorylation

Phosphorylation of primers was carried out in a reaction mixture containing 1 μl of each primer (1 μg/μl), 5 μl of 5X forward reaction buffer (Invitrogen, Burlington, ON),

2.5 µl of 10 mM ATP, 15.5 µl of sterile distilled water and 1 µl (10 U) of T4 polynucleotide kinase. After 45 min at 37°C, an additional 300 µl of sterile distilled water was added. The mixture was extracted twice with an equal volume of phenol:chloroform (1:1), followed by a single chloroform extraction. The nucleic acids were then precipitated through the addition of 30 µl of 3 M sodium acetate and 900 µl of 95% ethanol. Following 15 min at -20°C, the mixture was spun for 15 min at 4°C in a microcentrifuge (Biofuge Fresco, Mandel Scientific, Guelph, ON). The pellet was then washed with 500 µl of 70% ethanol, air-dried, and dissolved in 10 µl of sterile distilled water.

3.2.3.2. PCR mutagenesis protocol

PCR mutagenesis was performed using primers listed in Table 3.2 and Table 3.3. 200 ng of phosphorylated primer was added to 17 µl of 1.1X PCR reaction mix, 1 µl of 10 mM NAD, 2 µl of rpMMAX (0.5 µg), 0.5 µl of DMSO, 0.3 µl (12 U) of *Taq* ligase and 1 µl (2.5U) of *Pfu* polymerase. The reaction was placed in a thermocycler where it was heated to 95°C for 5 min, followed by 30 cycles of 95°C for 1 min, 55°C for 1 min, and 65°C for 10 min. After PCR amplification, 0.5 µl (10U) of *Dpn* I was added to the reaction mixture, which was then left at 37°C overnight. *Dpn* I can only digest methylated DNA strands and therefore, the template strand will be destroyed while the newly synthesized strand will be unharmed. The entire solution was then used to transform *E. coli* (XL-2) competent cells, which were subsequently spread over three LB plates supplemented with ampicillin. Identification of desired plasmids was achieved through sequence analysis performed on plasmid DNA isolated from resulting colonies as described in 2.2.3.4. For linker scanning mutagenesis, eight 14 bp regions were replaced with the sequence ACGAGGATCCTAGC, which introduced a *Bam*H I site (GGATCC) that assisted in the identification of the desired plasmids.

3.2.4. *N. crassa* transformation

The plasmids generated through site-directed or PCR mutagenesis were linearized using *Sca* I, and then transformed into the *aod-1* mutant strain, 7207 as described in

Table 3.2. Primers used in linker scanning mutagenesis

Primer Name	Sequence (5' → 3')	Comments
KK-LSM-1	CCCAGTTGCAACTCCTTTCAGGGACGAGGA TCCTAGCCGAGAGCTGACTGAAAACACCGA	Used in PCR mutagenesis to create pLSM1; *Bam*H I site is underlined
KK-LSM-2	GTGTCGGACAGCACTAGACACGGACGAGGA TCCTAGCCCTTTCCTGCCCCCAGTTGCAAC	Used in PCR mutagenesis to create pLSM2; *Bam*H I site is underlined
KK-LSM-3	GGAACTCGCTTGAGGTTTGTGATACGAGGA TCCTAGCGTCGGACAGCACTAGACACGGGA	Used in PCR mutagenesis to create pLSM3; *Bam*H I site is underlined
KK-LSM-4	AGGTCTCAAAGGAGCAATACGAGGATCCTA GCGCCCAAGCAATCTCCATTTTTTAACATC	Used in PCR mutagenesis to create pLSM4; *Bam*H I site is underlined
KK-LSM-5	CACCGAGTTTGTCCGTGCCTGGTACGAGGA TCCTAGCAGAGTTCCGACACTGCCCAAGCA	Used in PCR mutagenesis to create pLSM5; *Bam*H I site is underlined

Table 3.2. Continued

Primer Name	Sequence (5' → 3')	Comments
KK-LSM-6	GACTGAAAACACCGAGTTACGAGGATCCTA GCCTCAAAGGAGCAATAGAG	Used in PCR mutagenesis to create pLSM6; *Bam*H I site is underlined
KK-LSM-7	AATTTGGAATACGAGAGCTGACTACGAGGA TCCTAGCTGTCCGTGCCTGGTCTCAAAGGA	Used in PCR mutagenesis to create pLSM7; *Bam*H I site is underlined
KK-LSM-8	TCAGGGAAAAATTTGGAAACGAGGATCCTA GCGAAAACACCGAGTTTGTC	Used in PCR mutagenesis to create pLSM8; *Bam*H I site is underlined

Table 3.3. Primers used in the identification of the AIM sequence

Primer Name	Sequence (5' → 3')	Comments
MCHA8b	CTTTGAGACCAGGCAGGGACAAACTCGGTG TTT	Used in PCR mutagenesis to create pMCHA8b
MCHA9b	AGGCACGGACAAACTGGGTGTTTTCAGTCA GCT	Used in PCR mutagenesis to create pMCHA9b
MCHA27	CTCCTTTGAGACCAGAGACGGACAAACTCG	Used in PCR mutagenesis to create pMCHA27
MCHA28b	TTGAGACCAGGCACGAACAAACTCGGTGTT	Used in PCR mutagenesis to create pMCHA28b
MCHA29	CCAGGCACGGACAAGCTCGGTGTTTTCAGT	Used in PCR mutagenesis to create pMCHA29
MCHA30	CACGGACAAACTCGATGTTTTCAGTCAGCT	Used in PCR mutagenesis to create pMCHA30
MCHA31	ACAAACTCGGTGTTCTCAGTCAGCTCTCGT	Used in PCR mutagenesis to create pMCHA31

Table 3.3. Continued

Primer Name	Sequence (5' → 3')	Comments
MCHA66	TGAGACCAGGCACAGACAAACTCGGTGTTT	Used in PCR mutagenesis to create pMCHA66
MCHA67	ACGGACAAACTCAGTGTTTTCAGTCAGCTC	Used in PCR mutagenesis to create pMCHA67

2.2.3.6. Following electroporation and subsequent incubation of the ~1 ml transformation reaction at 30°C, 600 µl was mixed with 30 ml of top agar containing antimycin A and spread evenly over three plates containing sorbose medium and antimycin A. All constructs used in these experiments possess a bleomycin resistance cassette, which was used to ensure that each DNA fragment demonstrated relatively similar transformation efficiencies. This was achieved by adding 90 µl of the transformation reaction to 30 ml of top agar containing bleomycin, and spreading an equal volume of the resulting mixture over three bleomycin-containing plates. Transformation plates containing bleomycin or antimycin A were photographed after incubation at 30°C for four or five days, respectively.

3.2.5. Generation of AOD2 and AOD5 protein lysates

3.2.5.1. Creation of *E. coli* strains expressing his-tagged DNA-binding domains of AOD2 or AOD5

Truncated forms of the AOD2 and AOD5 proteins were generated in *E. coli* Rosetta (DE3) cells (Novagen, Mississauga, ON) harboring the plasmid p55-4a or p58-1 (see below), respectively. These cells are advantageous for expressing proteins because the T7 RNA polymerase that is used to express the fusion proteins is contained within the lambda DE3 lysogen and is induced by IPTG. This facilitates control of its expression and the timing of foreign protein production. The Rosetta cells also contain the plasmid pRARE, which encodes 10 tRNAs that are underrepresented in *E. coli* and helps overcome any expression problems caused by codon bias.

To generate p55-4a, the primers MCHA53 and MCHA55 (Table 3.4) were used to PCR amplify the first 351 bp (117 codons) of *aod-2* coding sequence, which contains the putative DNA binding domain (Figure 3.1 and Figure 3.2). 100 ng of each primer was added to 20 µl of 1.1X PCR mix, 0.5 µl of template pGEX2c-7 (0.5 ng) and 1 µl (2.5 U) of *Pfu* polymerase. pGEX2c-7 contains the coding sequence of *aod-2* and was obtained by cloning a full-length cDNA (start to stop codon) into the vector pGEX-2T (GE Healthcare Life Sciences, Baie d'Urfe, QC). The reaction mixture was incubated at 95°C for 5 min in a thermocycler, followed by 30 cycles of 65°C for 1 min, 72°C for 45 sec,

Table 3.4. Primers used to generate *E. coli* expression constructs

Primer Name	Sequence (5' → 3')	Comments
MCHA53	GTAGCATCCATATGACGGGAACAGAAGCCA CGGAAAAGCCC	AOD2 DNA-binding domain cloning primer; top strand; *Nde* I site is underlined
MCHA55	GTAGCATCGTCGACTGTAGCGTTGCGCCCA ATGTCCGG	AOD2 DNA-binding domain cloning primer; bottom strand; *Sal* I site is underlined
MCHA56	GTAGCACTCATATGCCGGACGACGTTGGAC CCGCC	AOD5 DNA-binding domain cloning primer; top strand; *Nde* I site is underlined
MCHA58	GTAGCACTCTCGAGATGGCCATTCCGGACA GATACAGCG	AOD5 DNA-binding domain cloning primer; bottom strand; *Xho* I site is underlined
MCHA105	ACGTGAATTCTCA**CTTGTCGTCGTCGTCCT TGTAGTC**TGTAGCGTTGCGCCCAATGTCCG	AOD2 DNA-binding domain cloning primer; bottom strand; inserts a FLAG- tag (in boldface); *Eco*R I site is underlined

Table 3.4. Continued

Primer Name	Sequence (5' → 3')	Comments
MCHA106	ACGTGAATTCTCA**CTTGTCGTCGTCGTCCT** **TGTAGTC**ATGGCCATTCCGGACAGATACAG	AOD5 DNA-binding domain cloning primer; bottom strand; inserts a FLAG-tag (in boldface); *Eco*R I site is underlined

Figure 3.2. The DNA-binding domains of AOD2 and AOD5. N-terminal fragments of AOD2 and AOD5 were expressed in *E. coli* and used in EMSA, pull-down and size exclusion chromatography experiments. Amino acid residues that comprise the DNA-binding domains of AOD2 and AOD5 are shown. The zinc cluster domain is indicated in boldface. Cysteine residues believed to coordinate binding of zinc atoms are indicated using boxes. A hexahistidinyl tag (underlined) was added to the C-terminus of each fragment. The double underlined residues were introduced during the cloning procedure. For FLAG-tagged versions of the DNA-binding domains, both the single and double underlined residues were replaced with DYKDDDDK.

AOD2 DNA-binding Domain:

1 MTGTEATEKP NGKEAGTKDI TKSGSDTKPK DHHPTPADDV

41 QKAPKKRRKV NHACLYCRRS HMTCDLERPC TRCIKRNIGH

81 LCHDEPRDTE SRKAKSVLGT STLHDSESQP DIGRNATVEH

121 HHHHH

AOD5 DNA-binding Domain:

1 MPDDVGPAEA EVSGAVSESD NEYDETEVTT KDDDDEKMAE

41 RSVASEGVET NGDQKKKYDP KDPLRPRRKK ARRACYACQR

81 AHLTCGDERP CQRCIKRGLA EACQDGVRKK AKYLHDAPPE

121 ALRPVLGPNY NPAAAVSVRN GHLEHHHHHH

and 98°C for 1 min, and then a final cycle of 65°C for 1 min, followed by 5 min at 72°C. MCHA53 introduced an *Nde* I restriction site at the 5' end of the fragment that included the start codon, and MCHA55 inserted a *Sal* I restriction site immediately following the 351 bp of *aod-2* coding sequence. These restriction sites were used to clone the *aod-2* fragment into the *Nde* I and *Xho* I restriction sites of the expression vector pET-26b (Novagen, Mississauga, ON). This cloning procedure inserted a hexahistidinyl tag at the C-terminus of the DNA-binding domain of AOD2 (Figure 3.2). Sequence analysis was performed to ensure the integrity of the resulting plasmid, before transformation into Rosetta (DE3) cells. The desired transformant was named RSA2-DB-1.

Construction of p58-1 was achieved in a similar fashion, but with the following deviations: PCR amplification of the first 426 bp (142 codons) of *aod-5* coding sequence, which contained the putative DNA binding domain (Figure 3.1 and Figure 3.2), was performed using the primers MCHA56 and MCHA58 (Table 3.4) and the template pGEX5cF-17. This plasmid contains the coding sequence of *aod-5* and was generated by insertion of a full-length cDNA (start to stop codon) into pGEX-2T. The resulting DNA product was digested with *Nde* I and *Xho* I, which facilitated cloning into the corresponding sites of pET-26b. This cloning procedure resulted in a hexahistidinyl tag at the C-terminus of the AOD5 DNA binding domain (Figure 3.2). Rosetta (DE3) cells harboring p58-1 were named RSA5-DB-1.

pET-26b was also transformed into Rosetta (DE3) cells to produce the "empty vector" control strain, RSpET-26b-1.

3.2.5.2. Creation of *E. coli* strains expressing FLAG-tagged DNA-binding domains of AOD2 or AOD5

To generate DNA fragments encoding the DNA-binding domains of AOD2 or AOD5 with a C-terminal FLAG-tag (DYKDDDDK), PCR amplifications were executed as described in 3.2.5.1, but were performed using different reverse primers. The sequence encoding the first 351 bp (117 codons) of *aod-2* was amplified with MCHA53 and MCHA105, while MCHA56 and MCHA106 were used to generate a 426 bp (142 codons) fragment of *aod-5* (Table 3.4). In both reactions, the forward primer generated an *Nde* I site at the 5' end of the gene that included the start codon, while the reverse

primer inserted an *Eco*R I site and a FLAG-tag at the 3' end of the protein. The PCR products were electrophoresed through an agarose gel and then purified from the gel, as described in 2.2.3.1. The fragments were digested with *Nde* I and *Eco*R I, and cloned into the identical sites of pET-26b (Novagen, Mississauga, ON). DNA sequencing confirmed that two constructs, pA2DB-FLAG-125 and pA5DB-FLAG-16, contained the DNA-binding domains of *aod-2* and *aod-5*, respectively, each with a C-terminal FLAG-tag (Figure 3.2). These plasmids were transformed into Rosetta (DE3) cells to generate strains RSA2-FLAG-125 and RSA5-FLAG-16, which were used to produce FLAG-tagged DNA-binding domains of AOD2 and AOD5, respectively.

3.2.5.3. Production and isolation of bacterial cell lysate supernatants

The five transformed Rosetta (DE3) strains described in 3.2.5.1 and 3.2.5.2. were used to inoculate 5 ml of LB medium (1% tryptone; 0.5% yeast extract; 0.5% NaCl) containing 1 mM $ZnCl_2$, 25 μg/ml chloramphenicol and 25 μg/ml kanamycin. Addition of chloramphenicol selects for cells harboring pRARE, while the presence of kanamycin selects for pET-26b based plasmids. The 5 ml cultures were allowed to grow at 37°C overnight in an incubator shaker. 4.5 ml of the saturated culture was then transferred to 100 ml of pre-warmed (37°C) LB medium supplemented with 1 mM $ZnCl_2$, 25 μg/ml chloramphenicol and 25 μg/ml kanamycin. The cultures were grown at 37°C with shaking to an OD_{600} of about 0.8, which required roughly 2.5 hr, after which IPTG was added to a final concentration of 125 μM. After an additional 5 hr of growth at 37°C, cells were harvested at 5000 rpm for 10 min at 4°C (Sorvall RC 5C Plus; SLC-1500 rotor). The supernatant was discarded and the pellet was stored at -20°C overnight.

To isolate soluble protein from the Rosetta (DE3) cells, the pellets were thawed on ice, and then re-suspended in 5 ml of lysis buffer (50 mM Tris-Cl; 300 mM NaCl; 10 μM $ZnCl_2$; 10 mM imidazole, pH 8.0). 4.5 ml of the suspension was transferred to a 13 ml polypropylene tube containing 500 μl of 10 mg/ml lysozyme dissolved in chilled lysis buffer. The mixture was placed on a rotating orbital shaker for 1 hr at 4°C (Model 260200, Boekel Scientific, Feasterville, PA). Sonication was then performed on ice using 10-20 fifteen sec bursts with a micro-tip set at 35% (Fisher Sonic Dismembrator Model 300, Ottawa, ON). The sonicated lysate was transferred to three 2 ml microcentrifuge

tubes and spun at 13000 rpm for 15 min at 4°C (Biofuge Fresco, Mandel Scientific, Guelph, ON). The supernatants from the 3 tubes were then combined into a new microcentrifuge tube. The protein concentration of each lysate was determined using the Bio-Rad Bradford protein assay (Bio-Rad, Mississauga, ON). The lysates were adjusted to concentrations of 1 μg/μl using chilled lysis buffer and stored at 4°C. It was found that storage at 4°C for several weeks did not reduce activity as seen in mobility shift assays. For simplicity, the bacterial cell lysate supernatant fractions containing his-tagged DNA-binding domains will be referred to as AOD2-his or AOD5-his, while those containing the FLAG-tagged DNA-binding domains will be called AOD2-FLAG or AOD5-FLAG. Soluble protein lysate obtained from the *E. coli* strain carrying pET-26b ("empty vector") will be named VECTOR. It should be noted that although the affinity tags occurring on these proteins were used in pull down (3.2.7) and size exclusion (3.2.8) experiments, purification of proteins from *E. coli* cell extracts was not required for their use in mobility shift assays (3.2.6).

3.2.6. Electrophoretic mobility shift assays (EMSAs)

3.2.6.1. Generation of radiolabeled probes

A series of single-stranded oligonucleotides were used to generate labeled double-stranded probes for use in EMSAs (Table 3.5). Briefly, single-stranded oligonucleotides were re-suspended in sterile milli-Q water to a final concentration of 100 μM. Complementary oligonucleotides were annealed to create 40 μM stocks of double-stranded molecules with 7 nucleotide 5' overhangs at each end. This was achieved by placing 200 μl of each 100 μM oligonucleotide into a microcentrifuge tube containing 50 μl of 10X NEBuffer 2 (500 mM NaCl; 100 mM Tris-HCl; 100 mM $MgCl_2$; 10 mM DTT; pH 7.9: New England Biolabs, Pickering, Ontario) and 50 μl of sterile milli-Q water. The mixture was incubated at 95°C for 10 min in a heated aluminum block, which was then turned off and allowed to cool to room temperature.

The labeling reaction was assembled using 3 μl of 10X React 2 (500 mM Tris-HCl, pH 8.0; 100 mM $MgCl_2$; 500 mM NaCl: Invitrogen, Burlington, Ontario), 3 μl of 10 mM dNTPs (no dCTP), 2 μl of [α-^{32}P] dCTP (3000 Ci/mmol), 10 μl of sterile milli-Q

Table 3.5. Primers used in EMSAs

Primer Name	Sequence (5' → 3')	Comments
MCHA79	CTTTGAGACCAGGCACGGACAAACTCGGTG TTTTC	Wild-type (WT) probe; top strand. CGG trinucleotides that are often binding sites of zinc cluster transcription factors are underlined
MCHA80	GCTGACTGAAAACACCGAGTTTGTCCGTGC CTGGT	Wild-type (WT) probe; bottom strand
MCHA81	CTTTGAGACCAGGCATTTACAAACTCGGTG TTTTC	Mutant probe 1 (M1); replacement of first CGG trinucleotide; top strand
MCHA82	GCTGACTGAAAACACCGAGTTTGTAAATGC CTGGT	Mutant probe 1 (M1); replacement of first CGG trinucleotide; bottom strand
MCHA83	CTTTGAGACCAGGCACGGACAAACTTTTTG TTTTC	Mutant probe 2 (M2); replacement of second CGG trinucleotide; top strand

Table 3.5. Continued

Primer Name	Sequence (5' → 3')	Comments
MCHA84	GCTGACTGAAAACAAAAAGTTTGTCCGTGC CTGGT	Mutant probe 2 (M2); replacement of second CGG trinucleotide; bottom strand
MCHA85	CTTTGAGACCAGGCATTTACAAACTTTTTG TTTTC	Mutant probe 3 (M3); replacement of both CGG trinucleotides; top strand
MCHA86	GCTGACTGAAAACAAAAAGTTTGTAAATGC CTGGT	Mutant probe 3 (M3); replacement of both CGG trinucleotides; bottom strand
MCHA89	CTTTGAGACCAGGCACGGACAAGCTCGGTG TTTTC	Mutant probe 4 (M4); point mutation within the spacer region; top strand
MCHA90	GCTGACTGAAAACACCGAGCTTGTCCGTGC CTGGT	Mutant probe 4 (M4); point mutation within the spacer region; bottom strand

Table 3.5. Continued

Primer Name	Sequence (5' → 3')	Comments
MCHA91	CTTTGAGACCAGGCACGGACAAΔCTCGGTG TTTTC	Mutant probe 5 (M5); deletion within the spacer region; top strand
MCHA92	GCTGACTGAAAACACCGAGΔTTGTCCGTGC CTGGT	Mutant probe 5 (M5); deletion within the spacer region; bottom strand
MCHA93	CTTTGAGACCAGGCACGGAGTTACTCGGTG TTTTC	Mutant probe 9 (M9); trinucleotide substitution in the spacer region; top strand
MCHA94	GCTGACTGAAAACACCGAGTAACTCCGTGC CTGGT	Mutant probe 9 (M9); trinucleotide substitution in the spacer region; bottom strand
MCHA95	CTTTGAGACCAGGCACGGACAATACTCGGT GTTTTC	Mutant probe 6 (M6); insertion within the spacer region; top strand

Table 3.5. Continued

Primer Name	Sequence (5' → 3')	Comments
MCHA96	GCTGACTGAAAACACCGAGTATTGTCCGTG CCTGGT	Mutant probe 6 (M6); insertion within the spacer region; bottom strand
MCHA101	CTTTGAGACCAGGCACGGACAAACTCGGTG TATTC	Mutant probe 7 (M7); point mutation downstream of the CGG repeats; top strand
MCHA102	GCTGACTGAATACACCGAGTTTGTCCGTGC CTGGT	Mutant probe 7 (M7); point mutation downstream of the CGG repeats; bottom strand
MCHA103	CTTTGAGACCAGGCACGGACAAACTCGGTG TΔTTC	Mutant probe 8 (M8); deletion downstream of the CGG repeats; top strand
MCHA104	GCTGACTGAAΔACACCGAGTTTGTCCGTGC CTGGT	Mutant probe 8 (M8); deletion downstream of the CGG repeats; bottom strand

water, 10 µl of 40 µM annealed oligonucleotides and 2 µl of Klenow enzyme (0.5 U/µl). The labeling reaction was placed at 37°C for 1 hr. For each probe, two labeling reactions were assembled. Following the 37°C incubation, the two samples were combined and 290 µl of sterile milli-Q water, 35 µl of 3 M sodium acetate (pH 5.2) and 1 ml of 95% ethanol were added. After an overnight incubation at -20°C, the tubes were spun in a microcentrifuge at 13000 rpm for 30 min at 4°C (Biofuge Fresco, Mandel Scientific, Guelph, ON). The supernatant was discarded and the precipitated DNA was rinsed with 1 ml of 70% ethanol. The pellet was air-dried, then re-suspended in 100 µl of 1X NEBuffer 2 (50 mM NaCl, 10 mM Tris-HCl, 10 mM $MgCl_2$, 1 mM DTT, pH 7.9). 1 µl of the labeled probe was placed in 1 ml of sterile water and subjected to Cerenkov counting using a Packard Liquid Scintillation Analyzer (Model 1500 TR). The concentration of the probe was adjusted to 10000 cpm/µl using 1X NEBuffer 2 and stored at 4°C. Probes were used within 7 days of labeling. Generally, the labeling reaction required a 1 in 30 dilution to produce the desired probe concentration.

3.2.6.2. EMSA protocol

The binding reaction was assembled at room temperature as follows: 3 µl of 5X EMSA buffer (50 mM HEPES, pH 8.0; 5 mM EDTA, pH 8.0; 50 mM KCl; 50% glycerol; 50 µM $ZnCl_2$, and 5 mM DTT), 1 µl of sonicated salmon sperm DNA (1 µg/µl), and 5 µl of 1X NEBuffer 2. It was found that the DTT in the EMSA buffer was critical since binding was dramatically reduced in older buffers where the DTT had presumably been oxidized. For competition assays, only 2 µl of 1X NEBuffer 2 was used, followed by the addition of 3 µl of annealed unlabeled oligonucleotides (produced as described in 3.2.6.1) of various concentrations. 1 µl of labeled probe (10000 cpm) and 5 µl of protein lysate (1 µg/µl) were then sequentially placed in the microcentrifuge tube. The mixture was spun in a microcentrifuge at 2000 rpm for 5 sec (Biofuge Fresco, Mandel Scientific, Guelph, ON), followed by a 30 min incubation at room temperature. 1 µl of bromophenol blue (dissolved in 1X EMSA buffer) was added immediately before loading of the samples into the well of a 6% polyacrylamide (79:1 acrylamide:bis-acrylamide) gel made in 0.5X TBE (90 mM Tris base; 90 mM boric acid; 2 mM EDTA, brought to pH 8.2 using solid boric acid immediately before use). Prior to loading, the polyacrylamide

gel was pre-run at 100V for 2 hr at 4°C. The samples were run for 3 hr under the same conditions. The gels were dried under vacuum onto Whatman 3MM chromatography paper using a Bio-Rad Slab Gel Dryer (1 hour at 80°C) then exposed to XAR film for various amounts of time to achieve the desired intensity (usually between 4 and 24 hours).

3.2.7. Pull-down assay

To determine whether the DNA-binding domains of AOD2 and AOD5 physically interacted, a pull-down assay was performed. 500 µl of AOD5-FLAG (1 µg/µl) was combined with an equal amount of 1 µg/µl VECTOR, AOD2-his or AOD5-his, and the resulting mixtures were placed at 4°C overnight. 325 µl of each protein mixture was transferred to a microcentrifuge tube and combined with 75 µl of Ni-NTA agarose slurry (Qiagen, Mississauga, ON), 100 µl of 5X EMSA buffer containing 100 mM imidazole (final concentration of 20 mM), and 2.5 µl of Tween 20. The mixture was placed at 4°C on an orbital rocker for 1h (Model 260200, Boekel Scientific, Feasterville, PA). The microcentrifuge tubes were spun at 2000 rpm for 15 seconds (Biofuge Fresco, Mandel Scientific, Guelph, ON), and the supernatant (or "flow-through") was transferred to a new tube. The pelleted Ni-NTA agarose was washed twice with 250 µl of 1X EMSA buffer. Proteins that were retained by the Ni-NTA were then eluted with 40 µl of elution buffer (50 mM Tris-Cl, pH 8.0; 300 mM NaCl; 10 µM $ZnCl_2$; 250 mM imidazole). 10 µl of 5X Laemmli cracking buffer (0.3125 M Tris-HCl pH 6.7; 12.5% SDS; 25% β-mercaptoethanol; 25% sucrose) was added to 50 µl of each eluate and the samples were analyzed using SDS-PAGE and Western-blot analysis as described in 2.2.5. Detection of his-tagged proteins was achieved using a commercial mouse anti-penta-his antibody (at 1/1000; Cat. No 34660, Qiagen, Mississauga, ON). FLAG-tagged proteins were visualized using a mouse anti-FLAG antibody (at 1/1500; Cat. No F3040, Sigma-Aldrich, Oakville, ON).

In the reciprocal experiments, protein mixtures were created by mixing 200 µl (1 µg/µl) of AOD2-FLAG with 800 µl (1 µg/µl) of VECTOR, AOD2-his or AOD5-his. Pull-down experiments were performed as above with the following modifications: each reaction tube contained 5 µl of Tween 20 instead of 2.5 µl, the Ni-NTA agarose was

washed seven times instead of twice, the wash buffer contained 1% Tween 20, and elution was performed with 200 µl of elution buffer. These changes were made to counteract non-specific interactions that appeared to occur between non-his-tagged AOD2 and the Ni-NTA agarose.

3.2.8. Size-exclusion chromatography

Interaction between the DNA-binding domains of AOD2 and AOD5 was also examined using size-exclusion chromatography. His-tagged DNA-binding domains of AOD2 and AOD5 were purified using Ni-NTA agarose (Qiagen, Mississauga, ON), as described in 2.2.8.2 except that the columns were washed with lysis buffer (50 mM Tris-Cl; 300 mM NaCl; 10 µM $ZnCl_2$; pH 8.0) containing 20 mM imidazole, and bound proteins were eluted using lysis buffer containing 250 mM imidazole. The protein concentrations of the two eluates were determined using the Bio-Rad Bradford protein assay, and adjusted to 0.25 µg/µl using lysis buffer. Equal amounts (500 µl) of each eluate were combined and then stored at 4°C overnight. Two control mixtures were generated by mixing 500 µl of each eluate with an equal amount of lysis buffer. Size-exclusion chromatography was then performed using 1 ml of the experimental and control protein samples. This was achieved using an AKTA-explorer 100A FPLC (Amersham Pharmacia Biotech, Piscataway, NJ) and a prepacked Superdex 75 column, and was performed at the Molecular Biology Service Unit (MBSU; Department of Biological Sciences, University of Alberta). Fifty 0.5 ml fractions were collected from each chromatography experiment. 64 µl of every second fraction was mixed with 16 µl of 5X cracking buffer, and then subjected to SDS-PAGE and Western-blot analysis using an anti-his antibody (1/250; Qiagen, Mississauga, ON).

3.3. Results

3.3.1. Characterization of the *aod-1* gene promoter through deletion analysis

A previous study showed that the promoter element(s) required for inducible expression of *aod-1* are located between -255 and -10 (TANTON *et al.* 2003). To narrow

down the location of potential regulatory elements, we constructed a series of plasmids, designated as pΔP-1 to pΔP-4, each carrying the *aod-1* gene controlled by various lengths of promoter sequence (Figure 3.3, panel A). These plasmids, along with the control plasmids rpMMAX and pMCMAX, also contain a bleomycin resistance cassette, which was used to monitor the success of transformation experiments. All six constructs were independently transformed into conidia from the *aod-1* mutant strain, 7207. The resulting conidia were mixed with molten top agar supplemented with either bleomycin or antimycin A, then spread over a plate containing the corresponding antibiotic.

When conidia from 7207 were transformed with rpMMAX, pMCMAX or any of the four deletion constructs, a similar number of colonies appeared on plates containing bleomycin (Figure 3.3, panel B). When compared to the lack of growth on plates containing conidia transformed with sterile water, these data show that all six constructs transformed the conidia of the *aod-1* mutant strain at a similar efficiency. Alternatively, only conidia transformed with rpMMAX and pΔP-1 produced robust growth when grown in media supplemented with antimycin A (Figure 3.3, panel B). This suggested that only these plasmids contain sufficient promoter sequence to allow inducible expression of alternative oxidase. Consequently, the regulatory element(s) required for efficient expression of *aod-1* must be located within the 52 bp region that was present in pΔP-1, but absent in pΔP-2.

3.3.2. Linker scanning mutagenesis

To further define the region required for wild-type expression of alternative oxidase, a linker scanning mutagenesis was performed. PCR mutagenesis was employed to replace various 14 bp fragments encompassing the 52 bp region of interest, as well as some flanking region, with a sequence of equal size (Figure 3.4, panel A). This allowed the removal of specific sequences while maintaining the spacing of potential promoter elements. In addition, the putative TATA box and +1 transcriptional start site were removed (Figure 3.4, panel A). The resulting plasmids were transformed into strain 7207 and assayed for growth on plates containing bleomycin or antimycin A.

As anticipated, a similar amount of growth was observed on bleomycin plates containing conidia transformed with the two control plasmids or any of the eight linker

Figure 3.3. Deletion analysis. **(A)** Schematic representation of the *aod-1* gene and flanking sequences present in each of the six constructs used in deletion analysis. Each construct contains all exons and introns of the *aod-1* gene, as well as 374 base pairs downstream of the stop codon. The dotted line in the middle of the *aod-1* gene indicates that the gene is not drawn to scale, relative to the rest of the construct. +1 indicates the transcription start site originally determined for *aod-1* (LI *et al.* 1996). However subsequent analysis suggested multiple start sites extending 37 bp downstream of the original +1 (CHAE *et al.* 2007a). The number of base pairs upstream of the +1 transcription start site in each construct is indicated. **(B)** Induction of alternative oxidase requires a 52 base pair region upstream of the *aod-1* gene. Conidia from strain 7207 were transformed with the various deletion constructs indicated on the left (panel A), and a "No DNA" negative control. The resulting transformants were plated on medium containing either bleomycin or antimycin A. The results of the bleomycin plates confirmed that the transformation efficiencies of all six constructs were similar, as each plasmid contains a bleomycin resistance cassette. Antimycin A plates were used to determine if alternative oxidase was being produced, which would only occur from constructs containing sufficient promoter sequence.

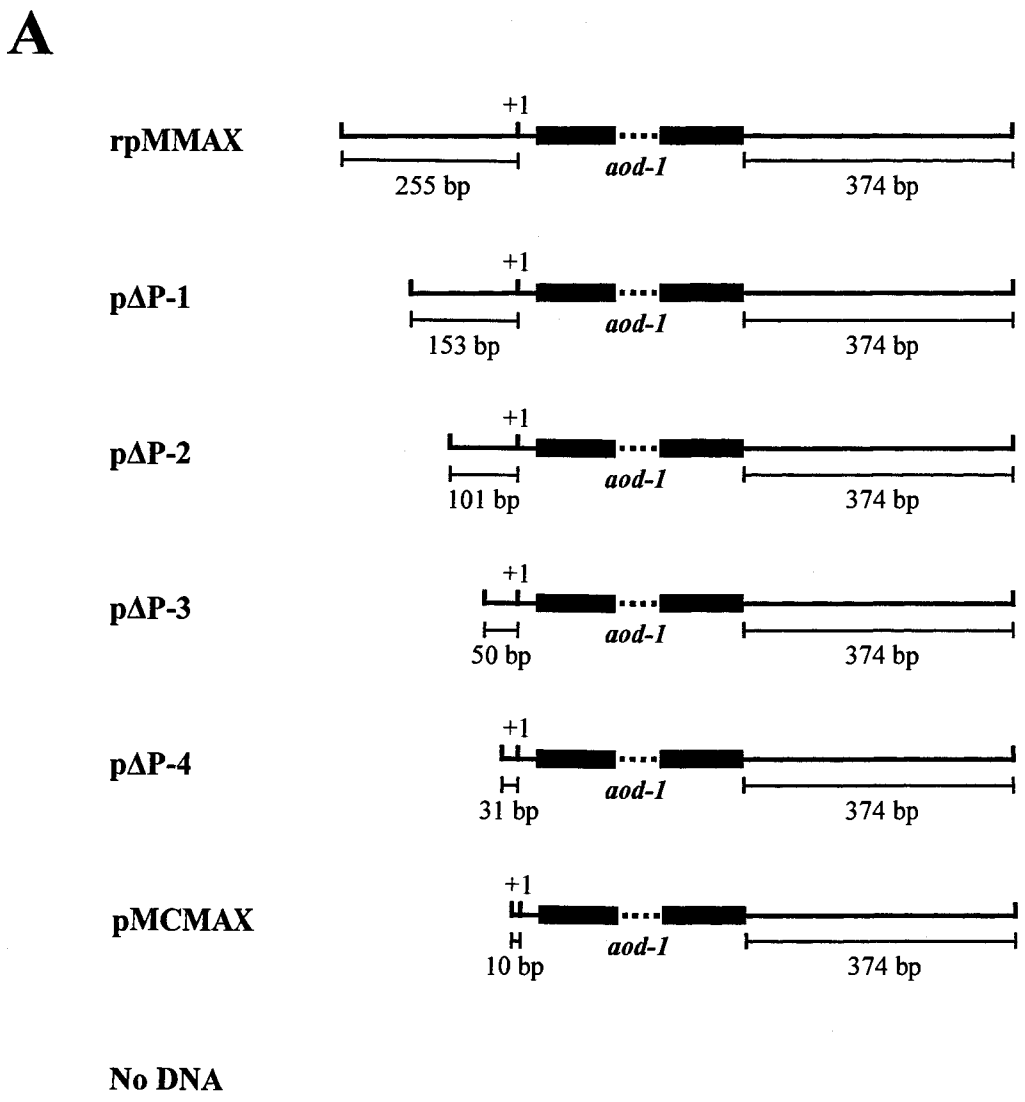
A
rpMMAX
+1
255 bp
aod-1
374 bp
pΔP-1
+1
153 bp
aod-1
374 bp
pΔP-2
+1
101 bp
aod-1
374 bp
pΔP-3
+1
50 bp
aod-1
374 bp
pΔP-4
+1
31 bp
aod-1
374 bp
pMCMAX
+1
H
10 bp
aod-1
374 bp
No DNA

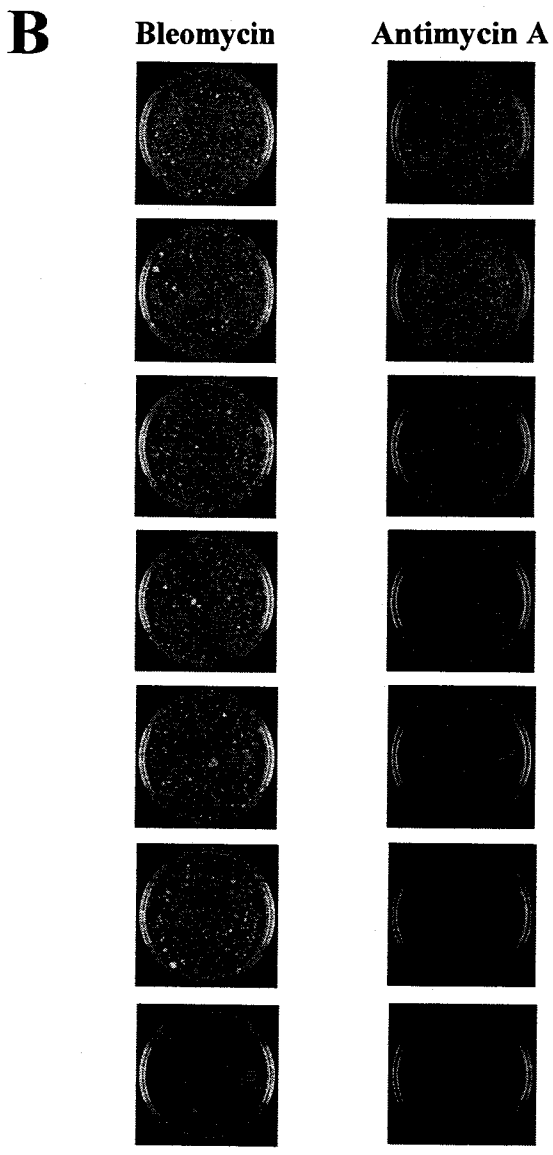
B
Bleomycin
Antimycin A

Figure 3.4. Linker scanning mutagenesis. **(A)** Mutations introduced into the *aod-1* gene promoter through linker scanning mutagenesis. The sequence present upstream of *aod-1* in the plasmid rpMMAX is shown. The 52 base pair sequence that was shown by deletion analysis to be required for efficient induction of alternative oxidase is underlined. rpMMAX was subjected to linker scanning mutagenesis to produce eight plasmids (pLSM 1 through pLSM 8). In each, a different 14 base pair region (as indicated above the sequence) was replaced with the sequence GCTAGGATCCTCGT. The bases shown in boldface represent the putative TATA box, the previously determined +1 transcription start site (C) and the *aod-1* start codon (ATG). **(B)** Growth of 7207 conidia transformed with the various control and linker scanning mutagenesis constructs. Plasmids used in the transformation procedure are indicated above each set of plates. Transformation and plating were as in the legend to Figure 3.3.

A

-255 GATCTGGAGCTTTCCGGGTTCCTTTCGCTAGCGCCCGCTATTTGCTTGTTCCTGGATTGT

pLSM 4 pLSM 5

-195 CTTGATGTTAAAAAATGGAGATTGCTTGGGCAGTGTCGGAACTCTATTGCTCCTTTGAGA

pLSM 6 pLSM 7 pLSM 8 pLSM 1

-135 CCAGGCACGGACAAACTCGGTGTTTTCAGTCAGCTCTCGTATTCCAAATTTTTCCCTGAA

pLSM 2

-75 AGGAGTTGCAACTGGGGGCAGGAAAGGACGA**TATA**AACGTCCCGTGTCTAGTGCTGTCCG

pLSM 3

-15 ACACATATGGACCAT**C**ATCACAAACCTCAAGCGAGTTCCATTACAACTTCACATCACTCC

+46 CTAAACTCTCG **ATG**

B

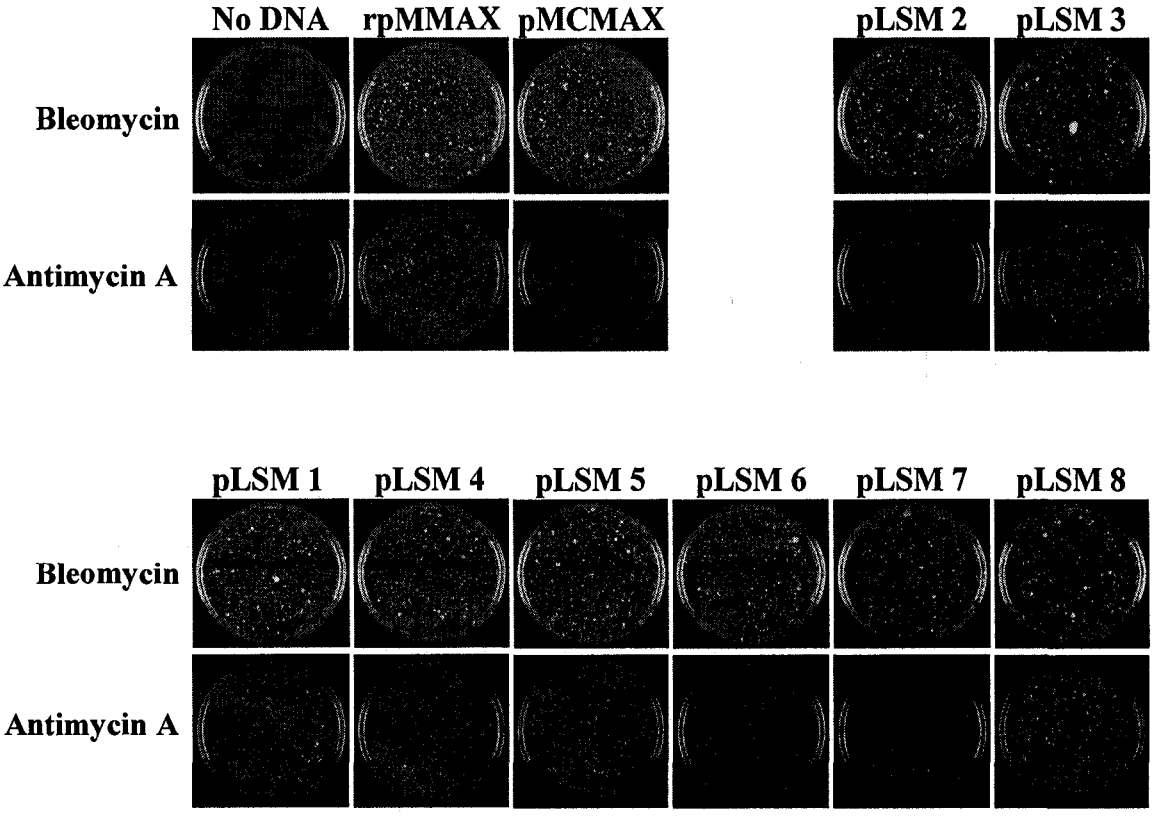

scanning mutagenesis constructs (Figure 3.4, panel B). The growth patterns observed on plates containing antimycin A were as expected for the control plasmids rpMMAX and pMCMAX (Figure 3.4, panel B). The construct lacking the putative +1 transcription start site, was able to rescue the *aod-1* mutant strain (Figure 3.4, panel B, pLSM 3). However, *aod-1* transcripts beginning at several different positions have been observed in *N. crassa* cDNA libraries, suggesting that numerous sequences are able to act as transcription start sites (CHAE *et al.* 2007a). Conversely, removal of the putative TATA box rendered the construct incapable of producing robust growth when transformed into an *aod-1* mutant strain, suggesting that we have identified the authentic TATA box (Figure 3.4, panel B, pLSM 2). The remaining constructs contained six distinct 14 bp mutations, which span the 52 bp region of interest, as well as some flanking sequence. When these constructs were transformed into 7207 and the resulting conidia spread over plates supplemented with antimycin A, abundant growth was observed on all plates, except for those containing conidia transformed with pLSM 6 or pLSM 7 (Figure 3.4, panel B). The lack of growth on these plates indicated an absence of alternative oxidase induction suggesting that a crucial regulatory element(s) is contained within a 28 bp sequence that extends from -109 to -136.

3.3.3. Identification of an alternative oxidase induction motif (AIM)

A preliminary scan of the sequence that constitutes the 28 bp promoter region of interest identified two CGG repeats, separated by 7 bp. This was significant as similar arrangements of trinucleotide pairs arranged as either direct, inverted or everted repeats were known to be bound by proteins belonging to a zinc cluster family of transcription factors that are very common in fungi (MACPHERSON *et al.* 2006; SCHJERLING and HOLMBERG 1996; TODD and ANDRIANOPOULOS 1997). Members of this family include HAP1 and GAL4, which have been shown to bind CGG repeats separated by 6 or 10-12 bp, respectively. To determine if these repeats were involved in the induction of alternative oxidase, PCR mutagenesis was employed to mutate each of the six nucleotides that comprise the CGG repeats, as well as four surrounding nucleotides (Figure 3.5, panel A). As previously described, these constructs were transformed into conidia of strain

Figure 3.5. Identification of an alternative oxidase induction motif (AIM). **(A)** Constructs used to analyze the importance of the CGG trinucleotide repeats. PCR mutagenesis was employed to introduce various mutations in the 28 base pair region required for *aod-1* induction, as determined by linker scanning mutagenesis. Mutations targeted the six nucleotides that form the two CGG trinucleotides (in bold), as well as four surrounding nucleotides. The names of the mutant plasmids are shown on the left and the mutations in each are indicated under the wild-type sequence. Boxes indicate the mutations affecting the CGG triplets. **(B)** Growth of conidia from 7207 transformed with various control and mutant constructs as indicated above each set of plates. Transformation and plating were performed as described in the legend of Figure 3.3.

A

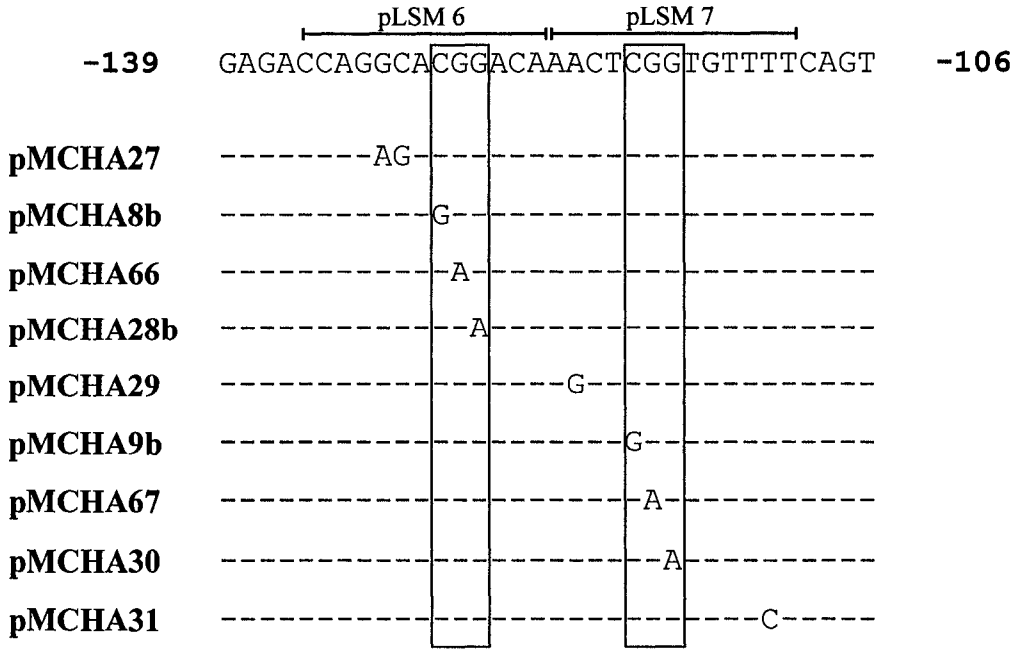
pLSM 6
pLSM 7
-139
GAGACCAGGCACGGACAAACTCGGTGTTTTCAGT
-106
pMCHA27 --------AG----------
pMCHA8b ----------G----------
pMCHA66 ----------A----------
pMCHA28b ----------A----------
pMCHA29 ----------G----------
pMCHA9b ----------G----------
pMCHA67 ----------A----------
pMCHA30 ----------A----------
pMCHA31 ----------C-----

B

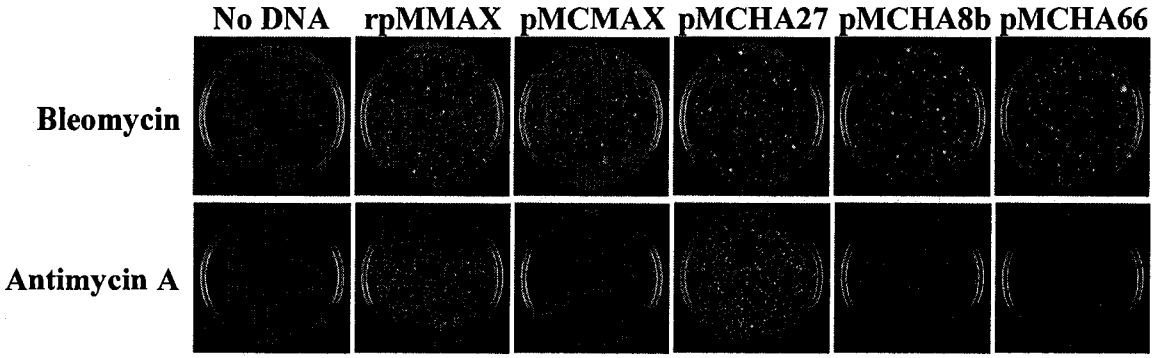
No DNA
rpMMAX
pMCMAX
pMCHA27
pMCHA8b
pMCHA66
Bleomycin
Antimycin A

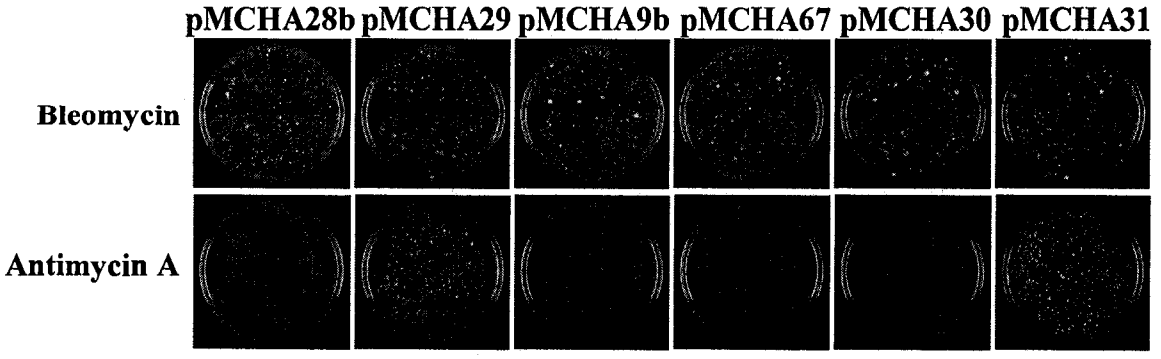
pMCHA28b
pMCHA29
pMCHA9b
pMCHA67
pMCHA30
pMCHA31
Bleomycin
Antimycin A

7207, which were then spread over plates supplemented with either bleomycin or antimycin A.

The set of bleomycin plates again demonstrate that all constructs are able to transform conidia with a similar efficiency (Figure 3.5, panel B). A mutation in any of four nucleotides which surround the CGG repeats did not affect the ability of that construct to promote expression of alternative oxidase, as indicated by the abundant growth on plates containing antimycin A (Figure 3.5, panel B). Conversely, conidia transformed with constructs containing mutations to any of the six nucleotides within either of the CGG trinucleotides are unable to grow when antimycin A is present (Figure 3.5, panel B). Altogether, these data suggest that we have identified an AIM, consisting of two CGGs separated by 7 bp, which is required for inducible expression of *aod-1*. Furthermore, analysis of the region upstream of the alternative oxidase coding sequence of several fungal species revealed that the AIM sequence and TATA box appear to be conserved among members of the Sordariales Order (Figure 3.6).

3.3.4. EMSAs

Recently, two genes required for the induction of alternative oxidase, *aod-2* and *aod-5*, were cloned in our lab (CHAE *et al.* 2007b; DESCHENEAU *et al.* 2005). These genes were found to encode putative transcription factors belonging to the zinc cluster family, whose members are known to bind elements similar to the AIM sequence. Thus, it was of interest for us to see if the AOD2 and/or AOD5 proteins were capable of binding the AIM found within the *aod-1* gene promoter. This hypothesis was examined though EMSAs.

The putative DNA-binding domains of AOD2 and AOD5 were individually cloned into an expression vector, which resulted in the addition of a hexahistidinyl tag at the C-terminus of each protein (Figure 3.2). Extracts of soluble protein were produced from *E. coli* cells harboring either of these expression plasmids or from a strain carry the empty expression vector (Figure 3.7, panel A). These extracts were used in EMSA experiments using a wild-type and nine different mutant radiolabeled DNA probes (Figure 3.7, panel B). EMSAs performed using the DNA-binding domains of either AOD2 or AOD5 showed that neither protein was able to bind to the wild-type probe

Figure 3.6. The AIM sequence is conserved in other fungal species. A comparison of the sequence upstream of the alternative oxidase gene in several fungal species revealed that the *N. crassa* AIM sequence element and TATA box are likely conserved in six other species of the Order Sordariales. The two CGG repeats that comprise the AIM sequence and the bases that are conserved in the TATA box region are indicated using boxes. Bases that differ from those observed in *N. crassa* are denoted using lower case letters. The underlined bases represent residues within the spacer region of the AIM that are completely conserved. The ATG start codon is indicated on the right. The spacing of the AIM, TATA box and the start codon is also shown.

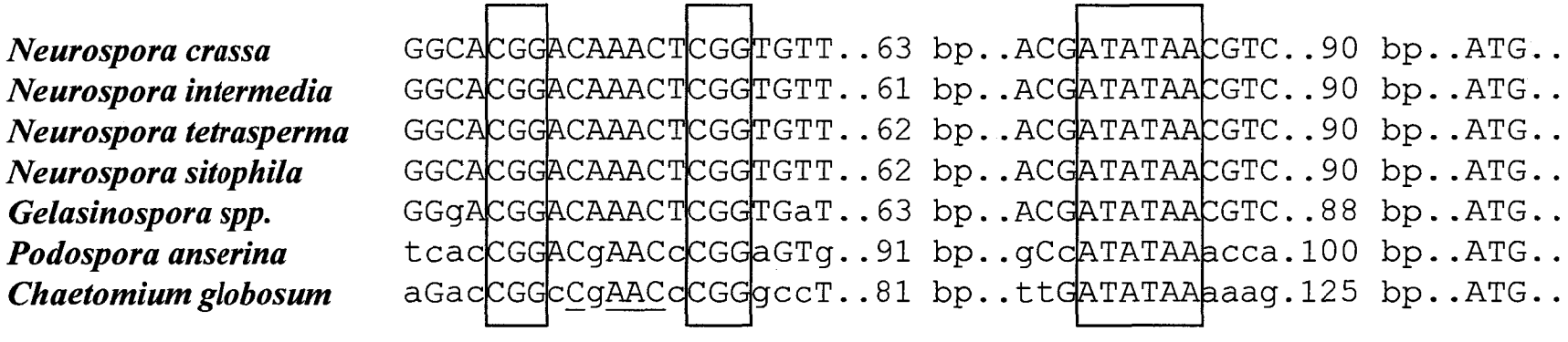
Neurospora crassa GGCACGGACAAACTCGGTGTT..63 bp..ACGATATAACGTC..90 bp..ATG..
Neurospora intermedia GGCACGGACAAACTCGGTGTT..61 bp..ACGATATAACGTC..90 bp..ATG..
Neurospora tetrasperma GGCACGGACAAACTCGGTGTT..62 bp..ACGATATAACGTC..90 bp..ATG..
Neurospora sitophila GGCACGGACAAACTCGGTGTT..62 bp..ACGATATAACGTC..90 bp..ATG..
Gelasinospora spp. GGgACGGACAAACTCGGTGaT..63 bp..ACGATATAACGTC..88 bp..ATG..
Podospora anserina tcacCGGACgAACcCGGaGTg..91 bp..gCcATATAAacca.100 bp..ATG..
Chaetomium globosum aGacCGGcCgAACcCGGgccT..81 bp..ttGATATAAaaag.125 bp..ATG..

Figure 3.7. Protein extracts and oligonucleotides used in EMSA experiments. **(A)** Coomassie blue-stained gel showing lysates prepared from *E. coli* cells expressing his-tagged N-terminal fragments of AOD2 (AOD2-his) and AOD5 (AOD5-his). The relevant bands are indicated by arrows. Lysate prepared from cells harboring the empty cloning vector (VECTOR) is shown as a control. Each lane contains 40 μg of protein. The position of molecular weight markers are indicated on the left. The apparent molecular weights of the AOD2 and AOD5 DNA-binding domain were higher than the calculated values of 13 and 16 kDa, respectively. **(B)** Sequence of radiolabeled probes used in EMSA experiments. The sequence of the probe containing the wild-type AIM sequence (WT) is shown. Bases indicated below the wild-type sequence show the replacements made in the individual mutant probes (M1 to M9). Boxes indicate the CGG repeats thought to represent the binding sites for zinc cluster transcriptional activators. The "Δ" sign present in M5 and M8 indicates a deletion of a single base (A or T, respectively), while the inverted caret in M6 shows the position of an inserted base (T).

A

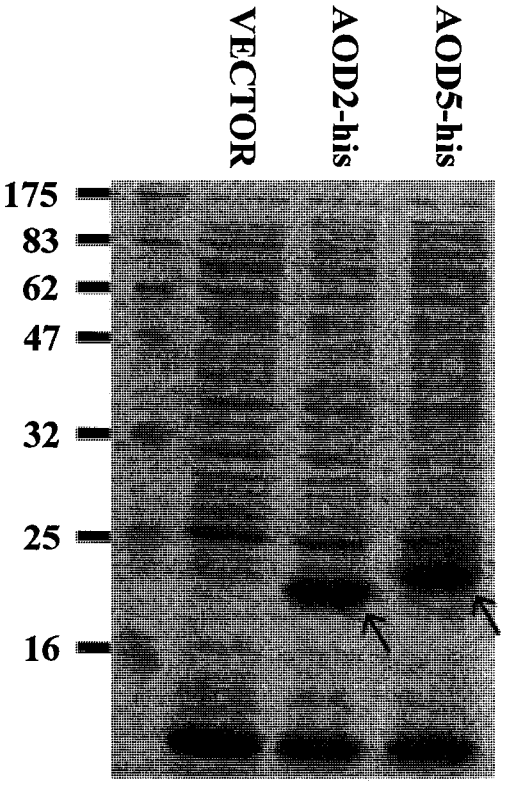
VECTOR
AOD2-his
AOD5-his
175
83
62
47
32
25
16

B

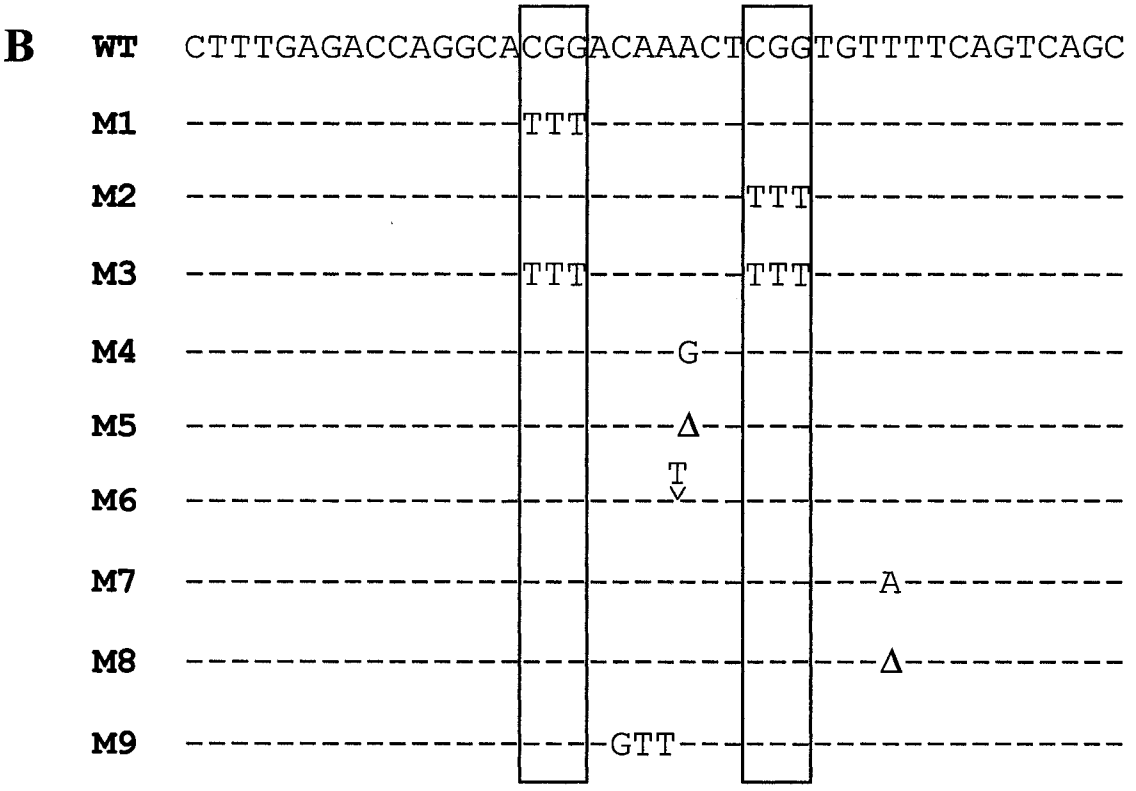
WT CTTTGAGACCAGGCACGGACAAACTCGGTGTTTTCAGTCAGC
M1 TTT
M2 TTT
M3 TTT TTT
M4 G
M5 Δ
M6 T
M7 A
M8 Δ
M9 GTT

individually, although some trailing was observed in each lane suggesting that both fragments can inefficiently bind to the AIM (Figure 3.8). However, a mobility shift was observed when the N-terminal fragments of AOD2 and AOD5 were both present, suggesting that formation of an AOD2/AOD5 heterodimeric complex is required for binding to the *aod-1* upstream sequence (Figure 3.8). The binding of the AOD2/AOD5 heterodimer to the AIM sequence was effectively competed using an excess of cold wild-type, but not cold mutant (M3), probe (Figure 3.9). To confirm that the CGG repeats which comprise the AIM are required for binding, EMSA experiments were performed using radiolabeled probes in which each CGG trinucleotide had been changed to TTT either individually or at the same time (Figure 3.7, panel B). Unlike the wild-type probe, these mutant probes were unable to produce a mobility shift when incubated with the DNA-binding domains of AOD2 and AOD5 (Figure 3.10).

To determine if the nucleotides between the CGG repeats influence binding, EMSA studies were carried out using additional mutant probes (Figure 3.7, panel B). A single base pair substitution of an "A" residue in the spacer region (M4) severely reduced, but did not eliminate binding of the proteins (Figure 3.11). Virtually no binding was observed when the length of the spacer region was changed to 6 (M5) or 8 bp (M6) (Figure 3.11). A point mutation (M7) or deletion (M8) downstream of the CGG repeats did not affect the ability of the probe to produce a mobility shift (Figure 3.11). Finally, a radiolabeled probe containing a trinucleotide substitution in the AIM spacer region (M9) still bound to the DNA-binding domains of AOD2 and AOD5 (Figure 3.11). These EMSA experiments suggest that an AOD2/AOD5 heterodimer is able to bind to the AIM sequence, and that this binding requires intact and properly spaced, CGG repeats.

3.3.5. Pull-down experiments

Although EMSA experiments suggested that the DNA-binding domains of AOD2 and AOD5 form a heterodimer that is capable of binding to the AIM, it was also possible that the two proteins bound to the AIM synergistically, but did not interact. The *S. cerevisiae* proteins Rds2p and Ybr239cp, which are thought to be homologues of *N. crassa* AOD2 and AOD5, were shown to interact in a yeast two-hybrid experiment, which suggested, but did not prove, that the two *Neurospora* proteins could physically

Figure 3.8. Synergistic binding of his-tagged N-terminal fragments of AOD2 and AOD5 to the AIM. Aliquots of the indicated lysates or lysis buffer ("No Protein") were incubated in binding reactions with a ^{32}P-labelled probe containing the wild-type AIM sequence (WT). The binding reactions were electrophoresed on polyacrylamide gels which were then dried and exposed to X-ray film. The arrow indicates probe bound by his-tagged N-terminal fragments of both AOD2 and AOD5.

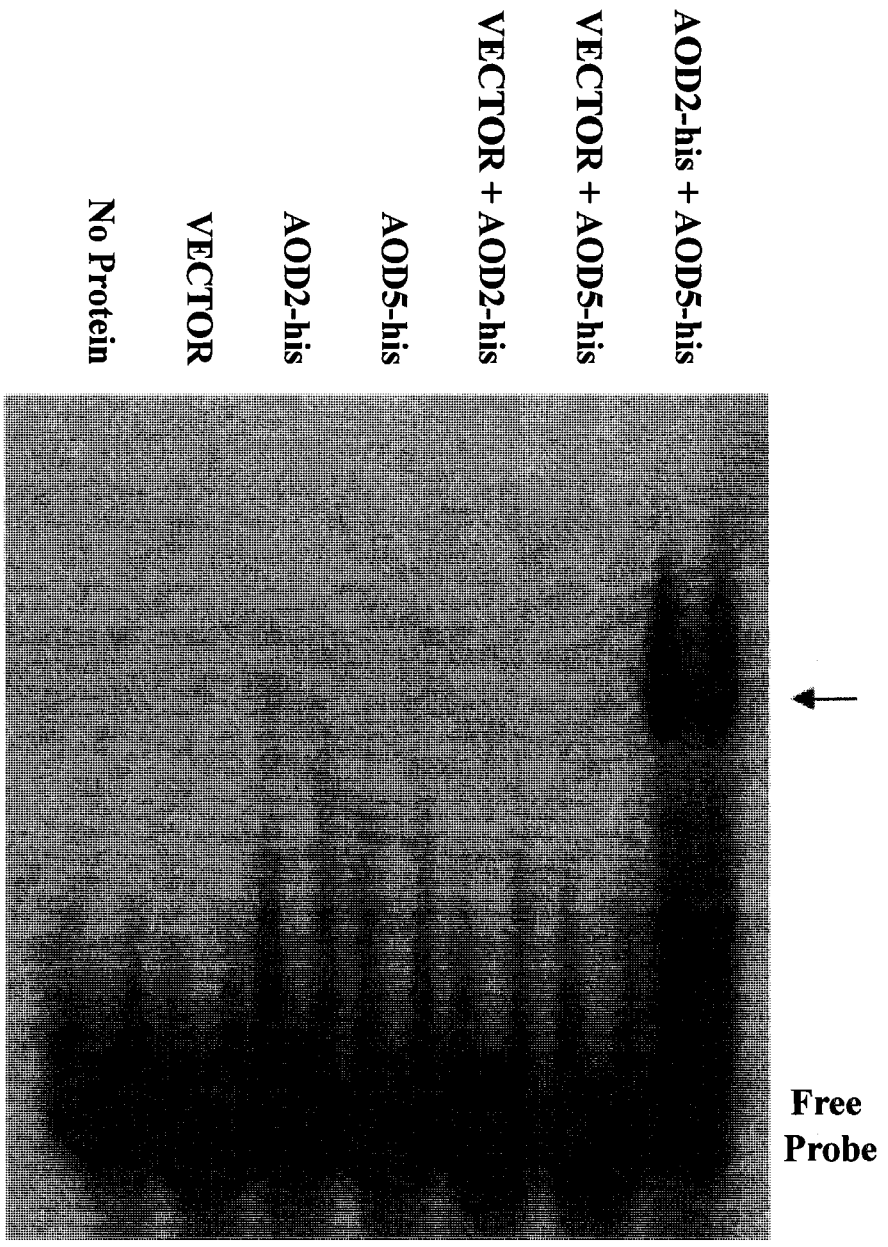

WT CTTTGAGACCAGGCACGGACAAACTCGGTGTTTTCAGTCAGC

Figure 3.9. Competition experiments. Binding reactions containing ^{32}P-labelled wild-type probe were incubated with aliquots of lysis buffer ("No Protein") or lysate containing his-tagged N-terminal fragments of AOD2 and AOD5. As indicated on the figure, aliquots of either unlabeled (cold) wild-type probe (WT), or unlabeled mutant M3 probe were added to the binding reaction at various concentrations. The arrow indicates probe bound by his-tagged N-terminal fragments of both AOD2 and AOD5. The reactions were processed as for Figure 3.8.

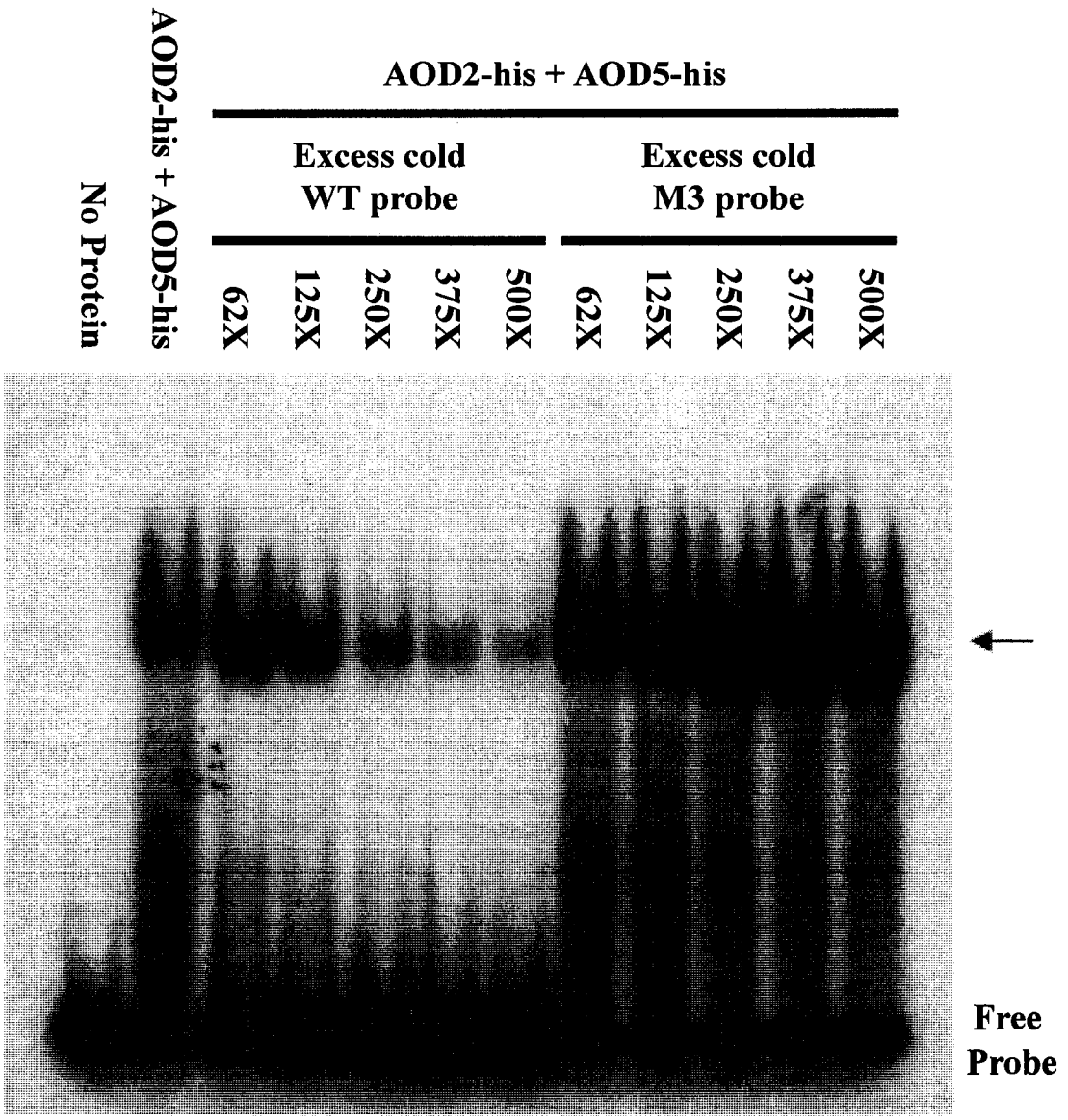


```
WT   CTTTGAGACCAGGCACGGACAAACTCGGTGTTTTCAGTCAGC
M3   ----------------TTT-------TTT--------------
```

Figure 3.10. EMSA experiments with mutant probes. Labeled probes of either wild-type (WT) sequence or containing specific mutations (M1 to M3) of the AIM sequence, were generated to determine the specificity of the binding sequence. Binding reactions containing lysis buffer (-) or his-tagged N-terminal fragments of AOD2 and AOD5 (+) were processed as described in Figure 3.8.

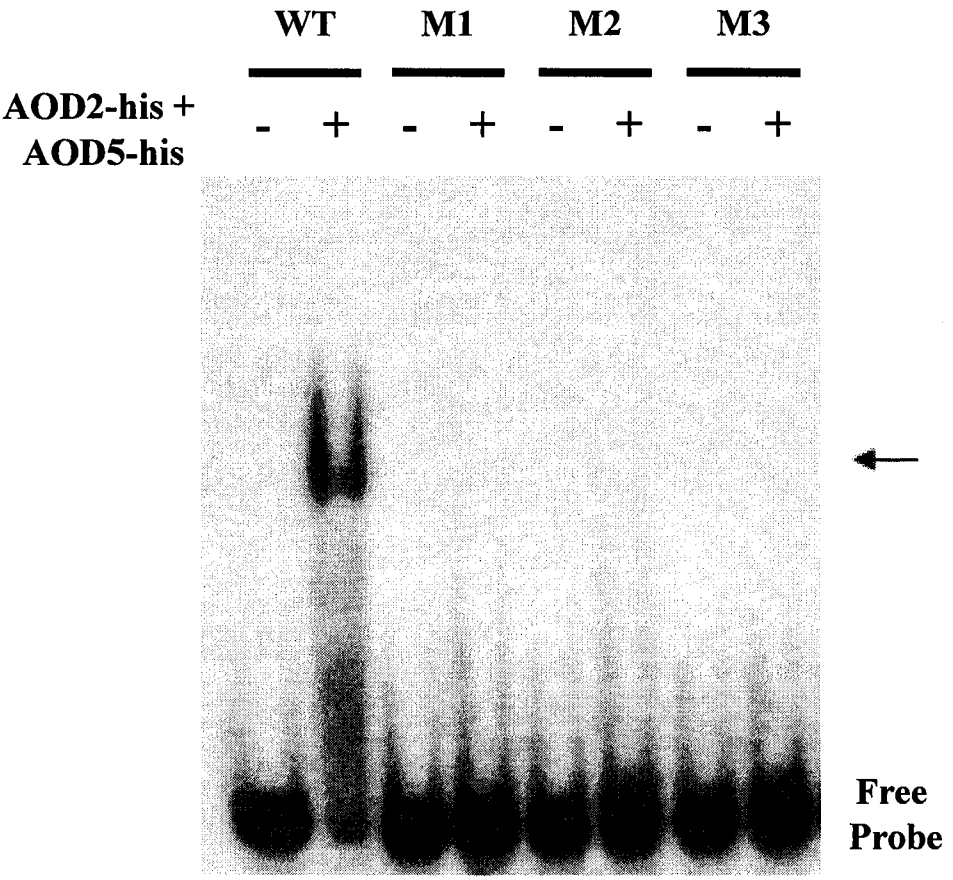


```
WT  CTTTGAGACCAGGCACGGACAAACTCGGTGTTTTCAGTCAGC
M1  ----------------TTT-----------------------
M2  ------------------------TTT---------------
M3  ----------------TTT-------TTT---------------
```

Figure 3.11. Examination of the spacer region between the CGG trinucleotide repeats. EMSA experiments were performed as described in Figure 3.10, except probes were either wild-type (WT) or mutants M4 to M9.

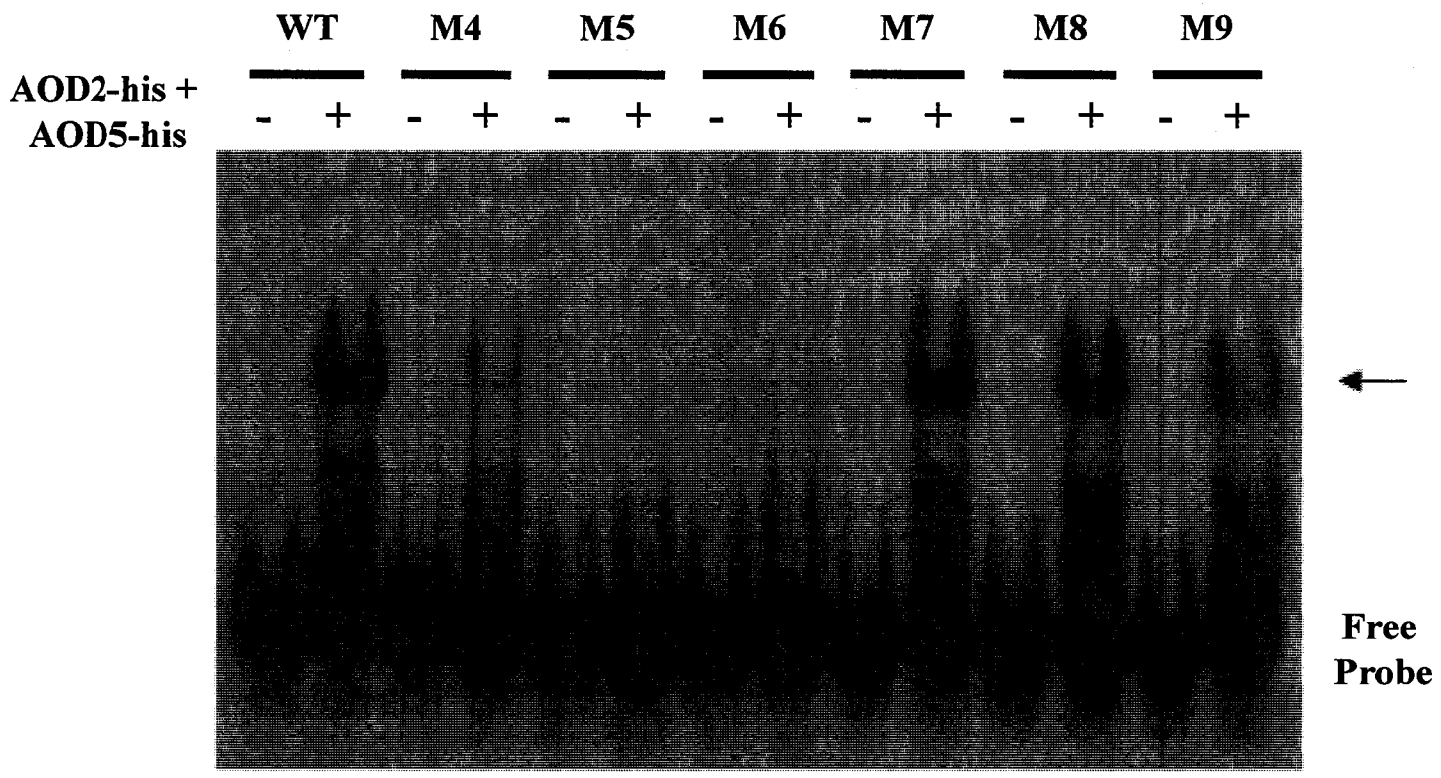


```
WT  CTTTGAGACCAGGCACGGACAAACTCGGTGTTTTCAGTCAGC
M4  ----------------------G-------------------
M5  ----------------------Δ-------------------
M6  ------------------------------------------
M7  ------------------------------A-----------
M8  ------------------------------Δ-----------
M9  --------------------GTT---------------------
```

interact (ITO *et al.* 2001). To address whether there was a physical interaction between the DNA-binding domains of AOD2 and AOD5, pull-down experiments were performed. Bacterial cell lysate supernatants were isolated from *E. coli* cells expressing the DNA-binding domains of AOD2 or AOD5 with either a hexahistidinyl or FLAG tag (Figure 3.12). A control soluble cell lysate was obtained from *E. coli* cells transformed with an empty vector (Figure 3.12). Various protein mixtures were subjected to batch purification using Ni-NTA agarose, which allowed for purification of his-tagged proteins and their interacting proteins. SDS-PAGE was performed on the resulting eluates, followed by Western-blot analysis using anti-penta-his and anti-FLAG antibodies. Use of the anti-penta-his antibody confirmed that his-tagged DNA-binding domains of AOD2 and AOD5 could be affinity purified using Ni-NTA agarose (Figure 3.13). Pull-down experiments demonstrated that AOD2-FLAG was not efficiently retained by the resin when mixed with VECTOR or AOD2-his, but was observed to co-elute with his-tagged AOD5 (Figure 3.13, panel A). This result was confirmed by the reciprocal experiment, which demonstrated that only his-tagged AOD2 could pull-down significant amounts of FLAG-tagged AOD5 (Figure 3.13, panel B). These data suggest that the DNA-binding domains of AOD2 and AOD5 can physically interact.

3.3.6. Size-exclusion chromatography

To confirm the results obtained from pull-down experiments, size-exclusion chromatography was performed using affinity purified his-tagged DNA-binding domains of AOD2 or AOD5, or an equal mixture of each. The protein samples were resolved using a Superdex 75 column, and eluted into fifty 0.5 ml fractions. Every second fraction was subjected to SDS-PAGE and Western-blot analysis using an anti-penta-his antibody. A low molecular weight protein was observed in the 45^{th} and 47^{th} fraction of each run, which was thought to represent monomers of AOD2 and/or AOD5 (Figure 3.14). However, when size-exclusion chromatography was performed on samples containing both AOD2 and AOD5, these proteins were also observed in fractions 11 through 19, as components of a higher molecular weight complex (Figure 3.14). Conversely, no protein was observed in these fractions when size-exclusion chromatography was performed on samples containing AOD2 or AOD5 individually (Figure 3.14). These data help confirm

Figure 3.12. Coomassie blue-stained gel showing lysates prepared from *E. coli* cells expressing N-terminal fragments of AOD2 or AOD5 with either a hexahistidinyl (AOD2-his or AOD5-his) or FLAG (AOD2-FLAG or AOD5-FLAG) tag. The relevant bands are indicated by arrows. Lysate prepared from cells harboring the empty cloning vector (VECTOR) is shown as a control. Each lane contains 40 μg of protein. The positions of molecular weight markers are indicated on the left.

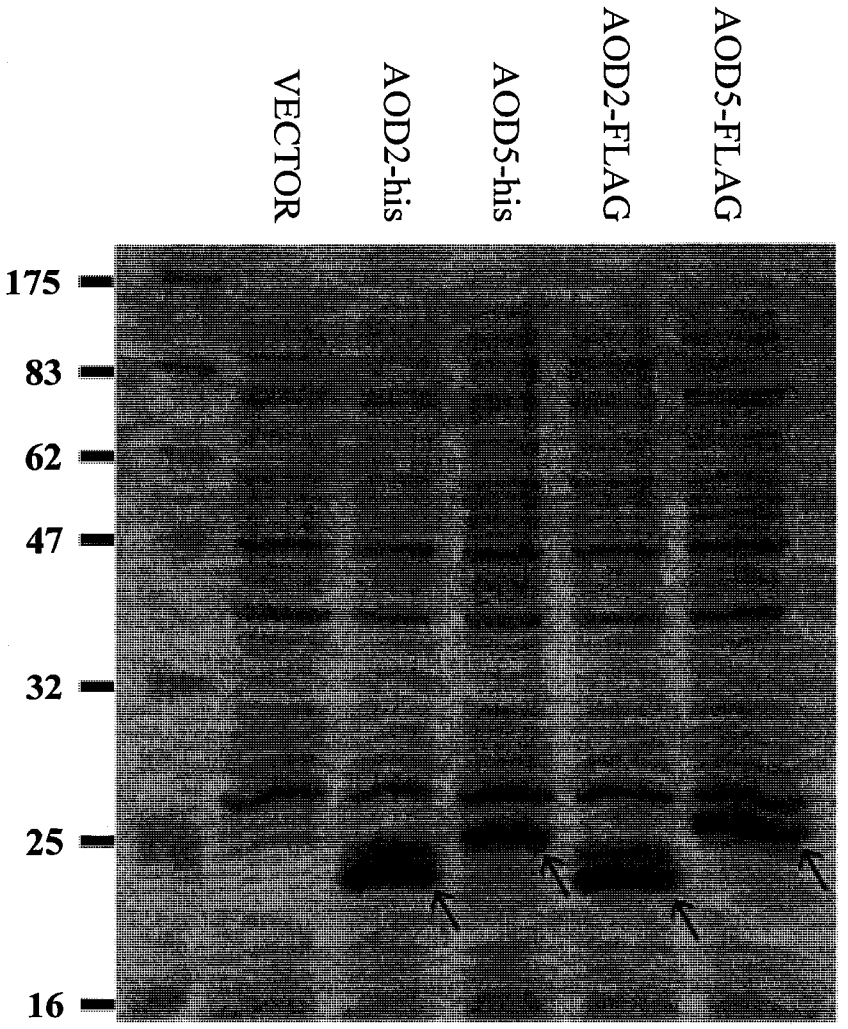
VECTOR
AOD2-his
AOD5-his
AOD2-FLAG
AOD5-FLAG
175
83
62
47
32
25
16

Figure 3.13. Pull-down experiments. **(A)** Bacterial lysate supernatants containing FLAG-tagged AOD2 DNA-binding domain (AOD2-FLAG) were mixed with those from *E. coli* cells expressing empty vector (VECTOR) or his-tagged DNA-binding domains of AOD2 (AOD2-his) or AOD5 (AOD5-his). Batch purification was performed using Ni-NTA agarose and the flow-through (FT) and eluate (E) were collected. These samples, as well as samples of all five bacterial lysate supernatants, were subjected to SDS-PAGE, electroblotted to nitrocellulose membrane and analyzed by Western-blot analysis using anti-his and anti-FLAG antibodies. **(B)** As in panel A, except FLAG-tagged AOD5 DNA-binding domain (AOD5-FLAG) was used instead of AOD2-FLAG. In this figure, the C-terminal his or FLAG tagged AOD2 runs as a doublet, suggesting that a small portion of the N-terminus has been proteolytically removed.

A

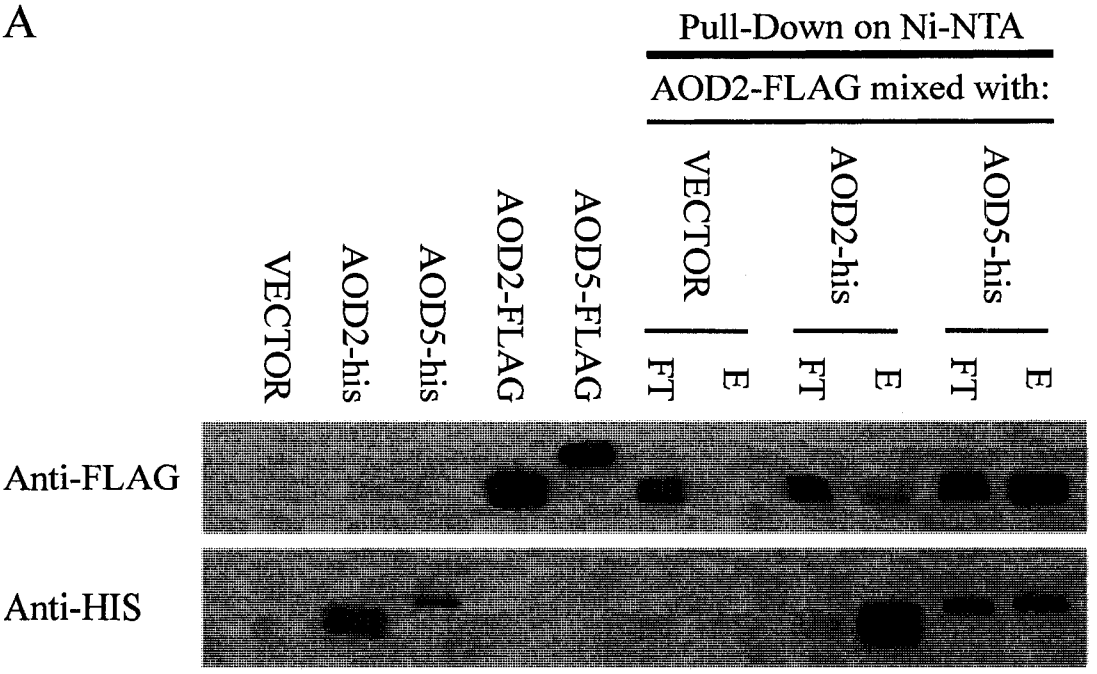
Pull-Down on Ni-NTA
AOD2-FLAG mixed with:
AOD5-his
AOD2-his
VECTOR
E
FT
E
FT
E
FT
VECTOR
AOD2-his
AOD5-his
AOD2-FLAG
AOD5-FLAG
Anti-FLAG
Anti-HIS

B

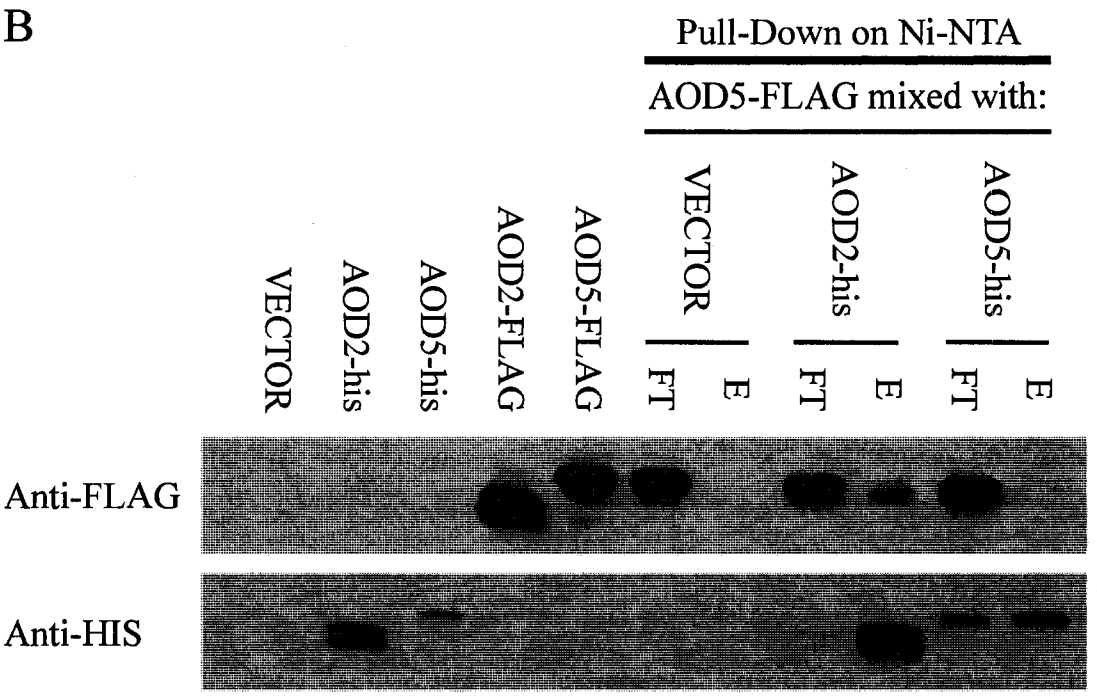
Pull-Down on Ni-NTA
AOD5-FLAG mixed with:
AOD5-his
AOD2-his
VECTOR
E
FT
E
FT
E
FT
VECTOR
AOD2-his
AOD5-his
AOD2-FLAG
AOD5-FLAG
Anti-FLAG
Anti-HIS

Figure 3.14. Size-exclusion chromatography. Three 1 ml samples were generated by adding 500 µl of lysis buffer to an equal amount of purified, his-tagged N-terminal fragments of AOD2 or AOD5 (0.25 µg/µl), or by mixing 500 µl aliquots of both proteins. Each of the three samples was then subjected to size-exclusion chromatography. Fifty 0.5 ml fractions were collected and every second fraction was analyzed though SDS-PAGE and subsequent Western-blot analysis using an anti-his antibody. The fractions containing the molecular weight markers bovine serum albumin (66 000 kDa), carbonic anhydrase (29 000 kDa) and cytochrome *c* (12 400 kDa) are also indicated. The calculated molecular weights of the N-terminal fragments of AOD2 and AOD5 were 13 and 16 kDa, respectively. However, in these experiments, the apparent molecular weight of both proteins was approximately 0.1 kDa. Similarly, the molecular weight of a heterodimer composed of the DNA-binding domains of AOD2 and AOD5 was predicted to be 29 kDa, while these proteins were observed to co-elute in fractions containing proteins with an apparent molecular weight of about 17.5 kDa. These findings suggest that both proteins may interact with the agarose beads that form the matrix of the size-exclusion chromatography column. For a more detailed discussion, see 3.4.4.

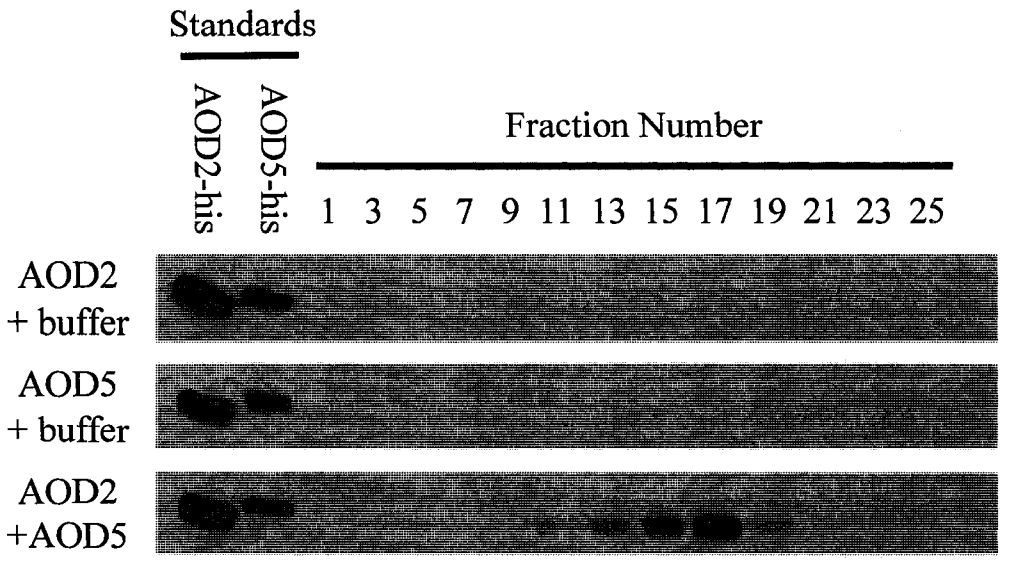

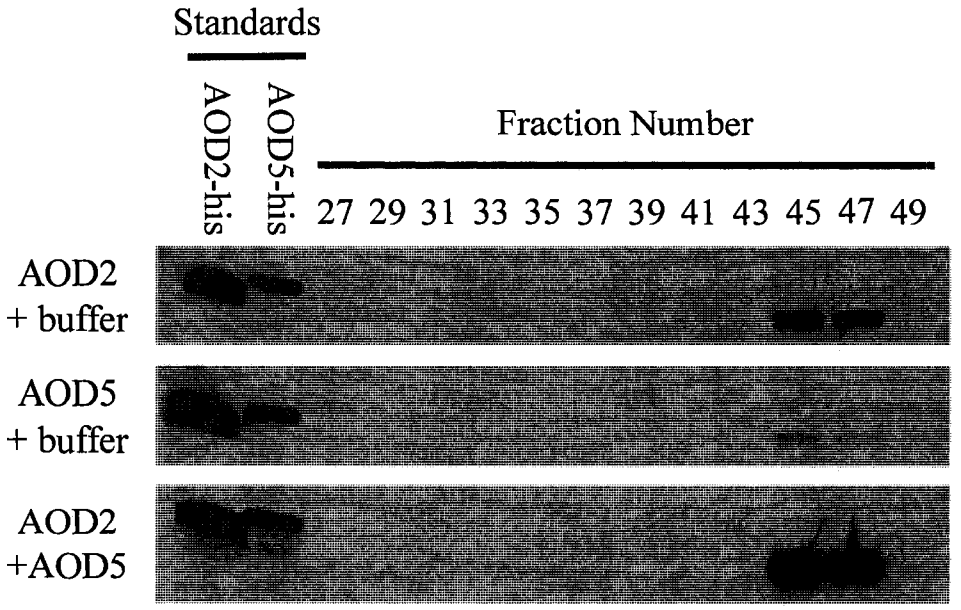

Molecular Weight Markers:

Fraction 9: Bovine serum albumin (66 000 kDa)
Fraction 14: Carbonic anhydrase (29 000 kDa)
Fraction 18: Cytochrome *c* (12 400 kDa)

the results of pull-down experiments suggesting that there is a physical interaction between the AOD2 and AOD5 N-terminal fragments used in these studies.

3.4. Discussion

3.4.1. Identification of the AIM sequence

We have used a qualitative *in vivo* assay to identify an alternative oxidase induction motif (AIM) that is required for efficient expression of the *aod-1* gene in *N. crassa*. The assay evaluates the ability of various *aod-1* constructs to restore efficient growth to *aod-1* mutant cells plated on antimycin A, which was judged by simple inspection of the number and size of colonies observed following transformation with the different plasmids. Transformants displaying little or no growth on medium containing antimycin A were deemed to harbor constructs carrying mutations that targeted sequence elements required for the induction of alternative oxidase. The AIM motif consists of two CGG trinucleotide direct repeats separated by 7 base pairs. Sequences resembling the AIM are known to be bound by members of the fungal-specific zinc cluster family of transcription factors. Although most proteins belonging to this family bind to inverted CGG repeats, others are known to bind triplet repeats in a direct or everted orientation (HON *et al.* 2005; MACPHERSON *et al.* 2006; SCHJERLING and HOLMBERG 1996). The importance of each base of the CGG triplet repeats of the AIM was demonstrated as *aod-1* mutant cells transformed with constructs bearing mutations at any of the six nucleotides grew extremely poorly in the presence of antimycin A. Furthermore, since disruption of the CGG trinucleotides reduced alternative oxidase expression, it is likely that the AIM binds an activator of *aod-1* transcription.

Comparison of the sequences upstream of the *aod-1* coding region in *Gelasinospora*, *Podospora anserina* and *Chaetomium globosum* suggests that the AIM sequence is functionally conserved within these three species, all of which are in the order Sordariales (Figure 3.6) (HUHNDORF *et al.* 2004). However, the AIM was not identified within a region 500 base pairs upstream of the alternative oxidase coding sequence in *Fusarium graminearum* or *M. grisea*, which are members of the orders

Hypocreales and Xylariales, respectively (CARLILE and WATKINSON 1997). Thus, the AIM sequence is apparently not a universal element for the induction of alternative oxidase transcription in fungi. Furthermore, since the AIM sequence is thought to be bound by fungal specific transcription factors, expression of alternative oxidase in other organisms will likely be regulated using different sequence element(s) and regulatory proteins. In support of this hypothesis, analysis of the alternative oxidase promoter of *A. thaliana* has identified two G-box like motifs that are thought to interact with basic leucine zipper transcription factors (DOJCINOVIC *et al.* 2005). Interestingly, members of this family of transcriptional regulators have been shown to function as sensors of environmental stress and can be activated by changes in redox state (AMOUTZIAS *et al.* 2006; MATHERS *et al.* 2004). This suggests that although the factors involved in the alternative oxidase induction pathway may differ between organisms, the general mechanism through which such regulation is achieved may be similar.

In addition to the discovery of the AIM sequence, our studies have provided evidence that a sequence in the promoter of *aod-1* previously suggested to function as a TATA box is necessary for efficient induction of the gene. Removal of the TATA box sequence through linker scanning mutagenesis dramatically reduced the ability of transformants to grow on antimycin A. A comparative analysis has shown that the sequence of the TATA box, as well as its position relative to the start codon is well conserved in other Sordariales species (Figure 3.6).

3.4.2. The appearance of antimycin A-resistant transformants carrying *aod-1* upstream sequences which lack the AIM sequence or TATA box

Transformation of the *aod-1* mutant strain with plasmids harboring mutations to the AIM sequence or the TATA box dramatically reduced the number and size of colonies formed after plating the transformants on antimycin A plates. However, a low number of small colonies were observed using these constructs. Data from nuclear run-on experiments in *N. crassa* have shown that there is a low level of constitutive transcription from the *aod-1* gene (TANTON *et al.* 2003), which may not be due to regulation by AOD2 and AOD5. In addition, it is thought that the presence of antimycin A and other inducers of alternative oxidase may inactivate systems that normally prevent

the accumulation and/or translation of *aod-1* transcript, thus defining a system of post-transcriptional regulation of alternative oxidase expression (CHAUDHURI *et al.* 2002; DESCHENEAU *et al.* 2005; TANTON *et al.* 2003; YUKIOKA *et al.* 1998). Therefore, the colonies that form with mutant constructs lacking the AIM sequence may arise because the presence of antimycin A promotes stability and/or translation of the small number of constitutive *aod-1* transcripts. Alternatively, ectopic integration of these constructs may occur near sites that promote constitutive transcription. However, the virtual absence of transformants with pMCMAX argues against this possibility. Another option is that additional elements contained within the upstream sequence of *aod-1* are able to stimulate low levels of transcription. A low number of small colonies were also observed in the presence of antimycin A in transformations involving the linker scanning mutagenesis construct which removed the TATA box. This suggests that some low level of transcription can be initiated from sequence lacking this site. Presumably, another sequence present in the construct is inefficiently fulfilling the role of the TATA box.

To determine if additional sequence elements are involved in the expression of alternative oxidase, a linker scanning mutagenesis could be performed to remove various regions of *aod-1* upstream sequence in the TATA-box deficient plasmid pLSM 2, or in plasmids harboring mutant AIM sequences, such as pLSM 6 or pLSM 7 (Figure 3.4, panel A). If additional mutations could eliminate the small amount of growth observed on antimycin A plates following transformation of the strain 7207 with the constructs mutant for the TATA box or AIM sequence alone, such mutations would define a secondary element capable of promoting inefficient expression of alternative oxidase. In this manner, it may be possible to identify other sequence elements that are present in the *aod-1* gene promoter.

3.4.3. EMSA analysis

The results of our EMSA data show that AOD2 and AOD5 act together to bind the AIM in a sequence specific fashion. Each of the CGG repeats in the AIM, and proper spacing between them, is required for binding. This agrees well with the promoter dissection observations showing that the CGG repeats are required for expression of alternative oxidase. The observations that neither *aod-2* nor *aod-5* mutants produce *aod-*

1 mRNA under inducing conditions (DESCHENEAU *et al.* 2005) and the fact that the AOD2 and AOD5 proteins cooperate to bind the AIM sequence, which is required for expression of alternative oxidase, strongly suggest that these proteins are directly required for inducing the *aod-1* gene.

Although binding of AOD2 and AOD5 may be reduced when substitutions are made to base pairs in the spacer region of the AIM sequence, insertion or deletion of a single base pair virtually eliminated binding. These data agree with previous work on zinc cluster transcription factors that demonstrated proper spacing between the trinucleotide repeats, but not necessarily sequence conservation, is required for binding (LIANG *et al.* 1996; VASHEE *et al.* 1993). Our data show that mutation of a conserved "A" residue in the AIM spacer region (M4 probe) dramatically reduced binding of AOD2 and AOD5 *in vitro* (Figure 3.11). However, this change does not appear to have a significant effect on alternative oxidase expression, as evidenced by the large number and size of colonies produced through transformation of an *aod-1* mutant with pMCHA29, which harbors the identical mutation observed in M4 (Figure 3.5). This suggests that the decreased binding observed in our *in vitro* experiments may not be so pronounced *in vivo*. Another possibility is that our transformation assay for alternative oxidase function is not sensitive enough to observe minor differences between binding of AOD2 and AOD5 to wild-type AIM sequences versus those carrying the single base pair substitution. That is, even somewhat reduced levels of alternative oxidase expression *in vivo* may still be enough to facilitate robust growth in the presence of antimycin A. A more precise measurement may be obtained by determining the amount of alternative oxidase mRNA and protein present in the transformants harboring pMCHA29 when grown in the presence or absence of antimycin A compared to wild-type strains.

3.4.4. A physical interaction between AOD2 and AOD5

Even though EMSA experiments suggested that N-terminal fragments of AOD2 and AOD5 bound to the AIM sequence as a heterodimer, there was no direct evidence confirming a physical interaction between the two proteins. The observation that the closest yeast homologues of these proteins, RDS2p and Ybr239cp, interacted in a yeast two-hybrid assay (ITO *et al.* 2001) supports the notion that AOD2 and AOD5 interact

with each other. Analysis of the protein sequence of the N-terminal AOD2 and AOD5 fragments used in the EMSA studies failed to reveal a coiled-coil motif that is commonly used as a dimerization domain in zinc cluster proteins. However, the coiled-coil motifs observed in some zinc cluster proteins have been difficult to detect by computer analysis (SCHJERLING and HOLMBERG 1996).

As a more direct measure of testing for an interaction between the AOD2 and AOD5 fragments, we performed a pull-down assay using hexahistidinyl and FLAG tagged versions of the fragments. Western-blot analysis of the eluates from Ni-NTA purification confirmed that the two proteins co-eluted even though only one contained a tag which bound to Ni-NTA agarose. Although both proteins were observed to bind Ni-NTA agarose non-specifically, especially AOD2, the amount of FLAG-tagged protein observed in the control eluates was always dramatically reduced compared to the levels detected in eluates where AOD2 and AOD5 were incubated together. Thus, the pull-down experiments strongly support the hypothesis that AOD2 and AOD5 interact.

The physical interaction between the N-terminal fragments of AOD2 and AOD5 was confirmed using size-exclusion chromatography, which showed that mixing of the two proteins caused a significant portion of each to elute at a higher molecular weight. Although the N-terminal fragments of AOD2 and AOD5 are predicted to have molecular weights of 13 and 16 kDa, respectively, the individual monomers eluted in fractions corresponding to roughly 0.1 kDa. Similarly, the AOD2/AOD5 heterodimer displayed an apparent molecular weight of 17.5 kDa, even though it is predicted to be 29 kDa. This discrepancy could result from non-specific binding of the proteins to the agarose matrix of the Superdex 75 column, as this would cause the proteins to remain in the column for longer than expected, based simply on their size. Pull-down experiments also suggested that the FLAG-tagged DNA-binding domains of AOD2 and AOD5 demonstrated some non-specific binding to Ni-NTA agarose beads. Although the apparent molecular weights do not agree with the predicted values, our data clearly shows that AOD2 and AOD5 can physically interact and thus generate a larger complex that elutes much earlier in size-exclusion chromatography experiments.

Even though the concentrations of purified protein samples were equalized before the size exclusion experiments were performed, Western-blot analysis of the eluates

revealed that very little AOD5 could be observed, relative to AOD2. One possibility is that the hexahistidinyl tag of AOD5 may be slightly sequestered so that the α-his antibody cannot efficiently bind. To test this hypothesis, identical amounts of the purified, his-tagged AOD2 or AOD5 N-terminal fragments could be compared by both coomassie blue staining and Western-blot analysis following SDS-PAGE.

3.4.5. The PAS domain

Analysis of *aod-2* and *aod-5* transcript levels using quantitative PCR suggested that both genes display similar or slightly lower levels of mRNA when cultures were grown in the presence of antimycin A, which is known to induce alternative oxidase (CHAE *et al.* 2007b). Thus, the activities of AOD2 and AOD5 in promoting expression of *aod-1* when the cytochrome-mediated respiratory chain is blocked do not appear to correlate with the level of transcript, suggesting that the regulation of these proteins likely occurs post-transcriptionally. Although there is currently no data on the level of the actual AOD2 and AOD5 proteins under the different conditions, it seems reasonable to assume that alterations in the pre-existing proteins control their activity. AOD2 and AOD5 both contain a PAS domain, which is a common motif found in transcriptional regulators that often functions in signal transduction. Mutagenesis of conserved amino acids within the PAS domain of AOD2 and AOD5 has been shown to decrease the ability of the proteins to rescue the null alleles and support growth of antimycin A, thereby confirming the importance of the PAS domain (CHAE *et al.* 2007b). It is possible that the PAS domains can respond to different conditions in the cell that are relevant to alternative oxidase induction. PAS domains are known to bind cofactors such as FAD, which enables detection of redox levels (TAYLOR and ZHULIN 1999). However, the putative PAS domains in AOD2 and AOD5 do not appear to be closely related to those known to bind FMN or FAD as cofactors (CROSSON and MOFFAT 2001; HUALA *et al.* 1997). Although our data demonstrate that the N-terminal fragments of AOD2 and AOD5 are capable of interacting with one another, the PAS domain may help regulate heterodimerization of the two proteins. Such a function could also affect activity and/or localization of the proteins and respond to different conditions in the cell.

3.4.6. Cysteine residues and protein regulation

Another mechanism for controlling the activity and/or localization of proteins relative to redox conditions in the cell is via changes in the oxidation state of cysteine residues (BUCHANAN and BALMER 2005; HANSEN *et al.* 2006). This can be achieved through a variety of mechanisms. For example, ROS induce intramolecular oxidation of cysteine residues in the C-terminus of the Yap1 transcription factor of *S. cerevisiae*, which results in a conformational change that masks a nuclear export signal (WOOD *et al.* 2004). Retention of Yap1p in the nucleus promotes the expression of several antioxidant defense genes. The MAP kinase ASK1 is also regulated by the oxidation state of cysteine residues present within the enzyme. Here, H_2O_2 promotes the formation of disulphide bonds between numerous ASK1 proteins, which produces a functional, multimeric enzyme (NADEAU *et al.* 2007). In addition, the binding of the transcription factors AP-1 and NF-κB to DNA appears to be dependent on the reduction of cysteine residues present within their DNA-binding domains (HANSEN *et al.* 2006). This process is thought to occur in the nucleus and is regulated by the antioxidant enzymes thioredoxin and redox factor-1 (GO *et al.* 2007). Both AOD2 and AOD5 contain five cysteine residues in addition to those associated with the zinc binding region of the protein. It is conceivable that the redox state of these residues could affect the function or localization of the proteins.

3.4.7. The alternative oxidase induction pathway

Our *in vitro* analyses suggest that AOD2 and AOD5 form a heterodimer that regulates alternative oxidase expression through interaction with the AIM present in the *aod-1* gene promoter. However, the precise mechanisms of alternative oxidase induction *in vivo* are currently unknown. As described in 3.4.6, one explanation is that AOD2 and/or AOD5 are capable of detecting the redox state of the cell through their cysteine residues and can regulate alternative oxidase expression accordingly (Figure 3.15, panel A). In this model, mitochondrial dysfunction would alter the oxidation state of cysteine residues in AOD2 and/or AOD5, resulting in the formation, activation or nuclear localization of the AOD2/AOD5 heterodimer and subsequent expression of alternative oxidase. However, a mutagenic screen in *N. crassa* has also identified several other

Figure 3.15. The expression of alternative oxidase. The data presented in this thesis suggest that the increased expression of alternative oxidase that is observed when mitochondria are dysfunctional requires the binding of an AOD2/AOD5 heterodimer to the AIM in the *aod-1* gene promoter. **(A)** It is possible that AOD2 and/or AOD5 are directly activated by mitochondrial dysfunction, which leads to elevated levels of *aod-1* mRNA and functional alternative oxidase protein. In this model, alternative oxidase expression is only regulated at the level of transcription. **(B)** The identification of other genes involved in the induction of alternative oxidase (DESCHENEAU *et al.* 2005) argues that the model presented in panel A may be incomplete. For example, additional protein factors may be responsible for recognizing mitochondrial dysfunction and/or activation of the AOD2/AOD5 heterodimer (X_1). In addition, the expression of alternative oxidase may also be regulated through additional mechanisms that may include transcript stability (X_2), initiation of translation (X_3) and post-translational modification (X_4).

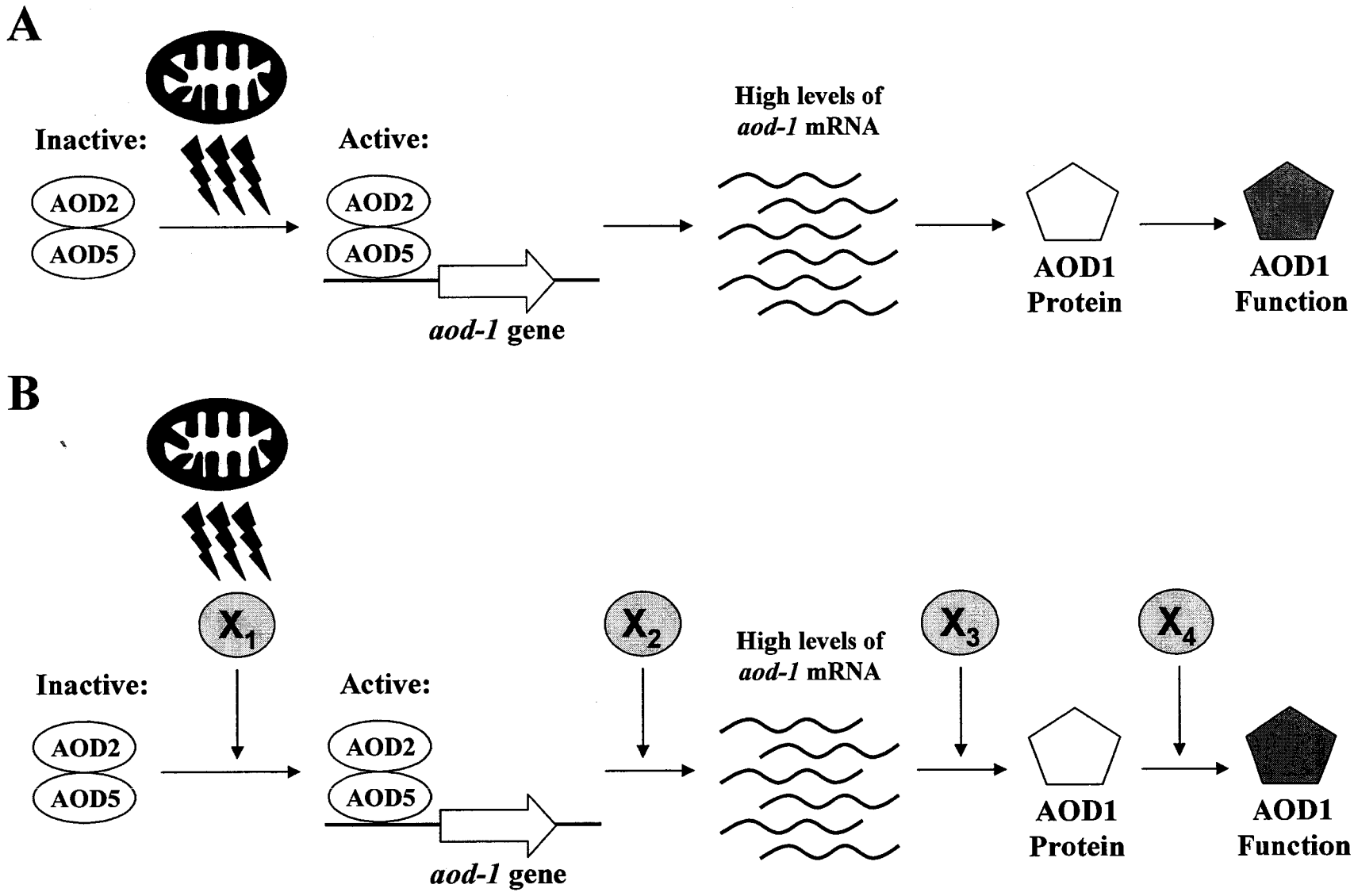
A
Inactive:
AOD2
AOD5
Active:
AOD2
AOD5
aod-1 gene
High levels of
aod-1 mRNA
AOD1
Protein
AOD1
Function
B
X1
Inactive:
AOD2
AOD5
Active:
AOD2
AOD5
aod-1 gene
X2
High levels of
aod-1 mRNA
X3
X4
AOD1
Protein
AOD1
Function

genes that are required for alternative oxidase expression and thus argues for a more complicated pathway of induction (Figure 3.15, panel B) (DESCHENEAU *et al.* 2005). It is possible that additional proteins or cofactors are involved in detection of mitochondrial dysfunction and/or the transmission of this signal to AOD2 or AOD5. Additionally, expression of alternative oxidase in *N. crassa* may also be regulated by transcript stability, as such mechanisms have been observed in *T. brucei* and *M. grisea* (CHAUDHURI *et al.* 2002; YUKIOKA *et al.* 1998). However, the identification of certain *N. crassa* strains that accumulate considerable amounts of *aod-1* mRNA but no protein suggests that stabilization of transcripts is not sufficient for protein expression and indicates that the initiation of alternative oxidase translation may also be regulated by additional factors (DESCHENEAU *et al.* 2005; TANTON *et al.* 2003).

3.5. Future Work

The data presented in this chapter suggest that induction of alternative oxidase is dependent on the binding of an AOD2/AOD5 heterodimer to the AIM sequence, which is found in the *aod-1* promoter region and consists of two directly-oriented CGG triplet repeats separated by 7 base pairs. However, the mechanisms that regulate this interaction are currently unknown. To approach this problem, it may be useful to examine these transcription factors *in vivo*. Western-blot analysis performed on proteins isolated from an *N. crassa* strain expressing his-tagged AOD2 or AOD5 has suggested that these proteins may not be expressed at high levels *in vivo* (Ian Cleary, personal communication). Thus, it may be useful to generate *N. crassa* strains in which the his-tagged *aod-2* or *aod-5* genes are being expressed from a strong, constitutive promoter, such as the glyceraldehyde-3-phosphate dehydrogenase promoter (WANG and KEASLING 2002). Western-blot analysis performed on cytosolic and nuclear protein fractions isolated from cultures grown in the presence or absence of antimycin A may reveal the intracellular localization of these transcription factors under inducing and non-inducing conditions, respectively.

One of the major goals of the *Neurospora* genome project is the generation of a library containing mutants in which virtually all genes have been individually knocked

out (COLOT *et al.* 2006). The knockout library could be screened for mutants that are not able to grow on medium containing antimycin A, which may indicate a defective alternative oxidase induction pathway. This simple procedure may allow for the identification of additional factors that are required for alternative oxidase expression. In addition, the gene rescue approach that was used to identify the *aod-2* and *aod-5* genes could be used to clone *aod-4* and *aod-7*, which have also been shown to be required for the induction of alternative oxidase (DESCHENEAU *et al.* 2005). Uncovering and characterizing additional genes that regulate alternative oxidase is likely to contribute to our understanding of the retrograde pathway that facilitates respiration through the alternative pathway.

Since the PAS domains of AOD2 and AOD5 are likely involved in the transduction of signals that lead to alternative oxidase induction, future work will be aimed at their characterization. One approach would be to mutate the cysteine residues in the PAS domains of each protein to determine if they are involved in the regulation of alternative oxidase. It is possible that these cysteine residues are able to respond to the redox state of the cell and regulate the expression of *aod-1* accordingly. Alternatively, the PAS domain may interact with protein cofactors that regulate AOD2 and/or AOD5 protein function. Mutation of conserved residues in the PAS domain may help us identify residues that are required for protein function and may reveal which amino acids are involved in cofactor binding. Further characterization of the PAS domain of AOD2 and/or AOD5 may provide great insight with regards to the nature of the signaling pathway which leads to their activation.

Although the data presented in this thesis have enhanced our knowledge of how alternative oxidase is induced in *N. crassa*, there are still many unanswered questions. For example, the nature and origin of the signals which trigger alternative oxidase expression are still unknown, although there is speculation that ROS is involved. In addition, the relationship between these signals and the activation of the AOD2/AOD5 heterodimer is not understood. It is likely that the activity of AOD2 and AOD5 is regulated by their PAS domains, but there is currently very little evidence to support this hypothesis. Full characterization of the alternative oxidase induction pathway may provide valuable information concerning how the functional status of mitochondria can

regulate gene expression, and may assist in the development of treatments aimed at overcoming mitochondrial dysfunction.

REFERENCES:

ABE, Y., T. SHODAI, T. MUTO, K. MIHARA, H. TORII *et al.*, 2000 Structural basis of presequence recognition by the mitochondrial protein import receptor Tom20. Cell **100:** 551-560.

ADAMS, K. L., K. SONG, P. G. ROESSLER, J. M. NUGENT, J. L. DOYLE *et al.*, 1999 Intracellular gene transfer in action: dual transcription and multiple silencings of nuclear and mitochondrial cox2 genes in legumes. Proc Natl Acad Sci U S A **96:** 13863-13868.

ADLER, V., Z. YIN, S. Y. FUCHS, M. BENEZRA, L. ROSARIO *et al.*, 1999 Regulation of JNK signaling by GSTp. Embo J **18:** 1321-1334.

AFFOURTIT, C., M. S. ALBURY, K. KRAB and A. L. MOORE, 1999 Functional expression of the plant alternative oxidase affects growth of the yeast Schizosaccharomyces pombe. J Biol Chem **274:** 6212-6218.

AFFOURTIT, C., K. KRAB and A. L. MOORE, 2001 Control of plant mitochondrial respiration. Biochim Biophys Acta **1504:** 58-69.

AGUILERA, P., T. BARRY and J. TOVAR, 2007 Entamoeba histolytica mitosomes: Organelles in search of a function. Exp Parasitol.

AHTING, U., C. THUN, R. HEGERL, D. TYPKE, F. E. NARGANG *et al.*, 1999 The TOM core complex: the general protein import pore of the outer membrane of mitochondria. J Cell Biol **147:** 959-968.

AJAYI, W. U., M. CHAUDHURI and G. C. HILL, 2002 Site-directed mutagenesis reveals the essentiality of the conserved residues in the putative diiron active site of the trypanosome alternative oxidase. J Biol Chem **277:** 8187-8193.

ALBURY, M. S., C. AFFOURTIT, P. G. CRICHTON and A. L. MOORE, 2002 Structure of the plant alternative oxidase. Site-directed mutagenesis provides new information on the active site and membrane topology. J Biol Chem **277:** 1190-1194.

ALCONADA, A., M. KUBRICH, M. MOCZKO, A. HONLINGER and N. PFANNER, 1995 The mitochondrial receptor complex: the small subunit Mom8b/Isp6 supports association of receptors with the general insertion pore and transfer of preproteins. Mol Cell Biol **15:** 6196-6205.

ALLEN, J. F., 2003 The function of genomes in bioenergetic organelles. Philos Trans R Soc Lond B Biol Sci **358:** 19-37; discussion 37-18.

ALLEN, S., V. BALABANIDOU, D. P. SIDERIS, T. LISOWSKY and K. TOKATLIDIS, 2005 Erv1 mediates the Mia40-dependent protein import pathway and provides a functional

link to the respiratory chain by shuttling electrons to cytochrome c. J Mol Biol **353:** 937-944.

AMIRSADEGHI, S., C. A. ROBSON, A. E. MCDONALD and G. C. VANLERBERGHE, 2006 Changes in plant mitochondrial electron transport alter cellular levels of reactive oxygen species and susceptibility to cell death signaling molecules. Plant Cell Physiol **47:** 1509-1519.

AMOUTZIAS, G. D., E. BORNBERG-BAUER, S. G. OLIVER and D. L. ROBERTSON, 2006 Reduction/oxidation-phosphorylation control of DNA binding in the bZIP dimerization network. BMC Genomics **7:** 107.

ANDERSSON, M. E., and P. NORDLUND, 1999 A revised model of the active site of alternative oxidase. FEBS Lett **449:** 17-22.

ANDERSSON, S. G., O. KARLBERG, B. CANBACK and C. G. KURLAND, 2003 On the origin of mitochondria: a genomics perspective. Philos Trans R Soc Lond B Biol Sci **358:** 165-177; discussion 177-169.

ANDERSSON, S. G., and C. G. KURLAND, 1999 Origins of mitochondria and hydrogenosomes. Curr Opin Microbiol **2:** 535-541.

ANDERSSON, S. G., A. ZOMORODIPOUR, J. O. ANDERSSON, T. SICHERITZ-PONTEN, U. C. ALSMARK *et al.*, 1998 The genome sequence of Rickettsia prowazekii and the origin of mitochondria. Nature **396:** 133-140.

ANTIGNANI, A., and R. J. YOULE, 2006 How do Bax and Bak lead to permeabilization of the outer mitochondrial membrane? Curr Opin Cell Biol **18:** 685-689.

AOSHIMA, M., 2007 Novel enzyme reactions related to the tricarboxylic acid cycle: phylogenetic/functional implications and biotechnological applications. Appl Microbiol Biotechnol **75:** 249-255.

ARANHA, M. M., A. R. MATOS, A. TERESA MENDES, V. VAZ PINTO, C. M. RODRIGUES *et al.*, 2007 Dinitro-o-cresol induces apoptosis-like cell death but not alternative oxidase expression in soybean cells. J Plant Physiol **164:** 675-684.

ATAMNA, H., P. B. WALTER and B. N. AMES, 2002 The role of heme and iron-sulfur clusters in mitochondrial biogenesis, maintenance, and decay with age. Arch Biochem Biophys **397:** 345-353.

ATTEIA, A., R. VAN LIS, J. J. VAN HELLEMOND, A. G. TIELENS, W. MARTIN *et al.*, 2004 Identification of prokaryotic homologues indicates an endosymbiotic origin for the alternative oxidases of mitochondria (AOX) and chloroplasts (PTOX). Gene **330:** 143-148.

BAE, Y. S., S. W. KANG, M. S. SEO, I. C. BAINES, E. TEKLE *et al.*, 1997 Epidermal growth factor (EGF)-induced generation of hydrogen peroxide. Role in EGF receptor-mediated tyrosine phosphorylation. J Biol Chem **272:** 217-221.

BAI, Y. L., and G. B. KOHLHAW, 1991 Manipulation of the 'zinc cluster' region of transcriptional activator LEU3 by site-directed mutagenesis. Nucleic Acids Res **19:** 5991-5997.

BALABAN, R. S., S. NEMOTO and T. FINKEL, 2005 Mitochondria, oxidants, and aging. Cell **120:** 483-495.

BALLARIO, P., C. TALORA, D. GALLI, H. LINDEN and G. MACINO, 1998 Roles in dimerization and blue light photoresponse of the PAS and LOV domains of Neurospora crassa white collar proteins. Mol Microbiol **29:** 719-729.

BARJA, G., 2004 Free radicals and aging. Trends Neurosci **27:** 595-600.

BARROS, M. H., F. G. NOBREGA and A. TZAGOLOFF, 2002 Mitochondrial ferredoxin is required for heme A synthesis in Saccharomyces cerevisiae. J Biol Chem **277:** 9997-10002.

BARTLETT, K., and S. EATON, 2004 Mitochondrial beta-oxidation. Eur J Biochem **271:** 462-469.

BAUD, C., C. DE MARCOS-LOUSA and K. TOKATLIDIS, 2007 Molecular interactions of the mitochondrial Tim12 translocase subunit. Protein Pept Lett **14:** 597-600.

BAUER, M. F., C. SIRRENBERG, W. NEUPERT and M. BRUNNER, 1996 Role of Tim23 as voltage sensor and presequence receptor in protein import into mitochondria. Cell **87:** 33-41.

BERTHOLD, D. A., 1998 Isolation of mutants of the Arabidopsis thaliana alternative oxidase (ubiquinol:oxygen oxidoreductase) resistant to salicylhydroxamic acid. Biochim Biophys Acta **1364:** 73-83.

BERTHOLD, D. A., M. E. ANDERSSON and P. NORDLUND, 2000 New insight into the structure and function of the alternative oxidase. Biochim Biophys Acta **1460:** 241-254.

BERTRAND, H., A. ARGAN and N. A. SZAKACS, 1983 Genetic control of the biogenesis of cyanide insensitive respiration in *Neurospora crassa*, pp. 495-507 in *Mitochondria*, edited by R. J. SCHWEYEN, K. WOLF and F. KAUDEWITZ. Walter de Gruyter Co., Berlin.

BIHLMAIER, K., N. MESECKE, N. TERZIYSKA, M. BIEN, K. HELL *et al.*, 2007 The disulfide relay system of mitochondria is connected to the respiratory chain. J Cell Biol **179:** 389-395.

BISWAS, G., M. GUHA and N. G. AVADHANI, 2005 Mitochondria-to-nucleus stress signaling in mammalian cells: nature of nuclear gene targets, transcription regulation, and induced resistance to apoptosis. Gene **354:** 132-139.

BLANCHARD, J. L., and M. LYNCH, 2000 Organellar genes: why do they end up in the nucleus? Trends Genet **16:** 315-320.

BONNET, S., S. L. ARCHER, J. ALLALUNIS-TURNER, A. HAROMY, C. BEAULIEU *et al.*, 2007 A mitochondria-K+ channel axis is suppressed in cancer and its normalization promotes apoptosis and inhibits cancer growth. Cancer Cell **11:** 37-51.

BORECKY, J., F. T. NOGUEIRA, K. A. DE OLIVEIRA, I. G. MAIA, A. E. VERCESI *et al.*, 2006 The plant energy-dissipating mitochondrial systems: depicting the genomic structure and the expression profiles of the gene families of uncoupling protein and alternative oxidase in monocots and dicots. J Exp Bot **57:** 849-864.

BORKOVICH, K. A., L. A. ALEX, O. YARDEN, M. FREITAG, G. E. TURNER *et al.*, 2004 Lessons from the genome sequence of Neurospora crassa: tracing the path from genomic blueprint to multicellular organism. Microbiol Mol Biol Rev **68:** 1-108.

BOXMA, B., R. M. DE GRAAF, G. W. VAN DER STAAY, T. A. VAN ALEN, G. RICARD *et al.*, 2005 An anaerobic mitochondrion that produces hydrogen. Nature **434:** 74-79.

BREIDENBACH, R. W., M. J. SAXTON, L. D. HANSEN and R. S. CRIDDLE, 1997 Heat generation and dissipation in plants: can the alternative oxidative phosphorylation pathway serve a thermoregulatory role in plant tissues other than specialized organs? Plant Physiol **114:** 1137-1140.

BRIX, J., S. RUDIGER, B. BUKAU, J. SCHNEIDER-MERGENER and N. PFANNER, 1999 Distribution of binding sequences for the mitochondrial import receptors Tom20, Tom22, and Tom70 in a presequence-carrying preprotein and a non-cleavable preprotein. J Biol Chem **274:** 16522-16530.

BRIX, J., G. A. ZIEGLER, K. DIETMEIER, J. SCHNEIDER-MERGENER, G. E. SCHULZ *et al.*, 2000 The mitochondrial import receptor Tom70: identification of a 25 kDa core domain with a specific binding site for preproteins. J Mol Biol **303:** 479-488.

BUCHANAN, B. B., and Y. BALMER, 2005 Redox regulation: a broadening horizon. Annu Rev Plant Biol **56:** 187-220.

BUI, E. T., P. J. BRADLEY and P. J. JOHNSON, 1996 A common evolutionary origin for mitochondria and hydrogenosomes. Proc Natl Acad Sci U S A **93:** 9651-9656.

BUTOW, R. A., and N. G. AVADHANI, 2004 Mitochondrial signaling: the retrograde response. Mol Cell **14:** 1-15.

CARLILE, M. J., and S. C. WATKINSON, 1997 *The Fungi* Academic Press, Harcourt Brace and

Company, London, Boston, San Diego, New York, Sydney, Tokyo.

CARNEIRO, P., M. DUARTE and A. VIDEIRA, 2004 The main external alternative NAD(P)H dehydrogenase of Neurospora crassa mitochondria. Biochim Biophys Acta **1608:** 45-52.

CHACINSKA, A., M. LIND, A. E. FRAZIER, J. DUDEK, C. MEISINGER *et al.*, 2005 Mitochondrial presequence translocase: switching between TOM tethering and motor recruitment involves Tim21 and Tim17. Cell **120:** 817-829.

CHACINSKA, A., S. PFANNSCHMIDT, N. WIEDEMANN, V. KOZJAK, L. K. SANJUAN SZKLARZ *et al.*, 2004 Essential role of Mia40 in import and assembly of mitochondrial intermembrane space proteins. Embo J **23:** 3735-3746.

CHAE, M. S., C. C. LIN, K. E. KESSLER, C. E. NARGANG, L. L. TANTON *et al.*, 2007a Identification of an alternative oxidase induction motif in the promoter region of the aod-1 gene in Neurospora crassa. Genetics **175:** 1597-1606.

CHAE, M. S., C. E. NARGANG, I. A. CLEARY, C. C. LIN, A. T. TODD *et al.*, 2007b Two zinc cluster transcription factors control induction of alternative oxidase in Neurospora crassa Genetics **177:** 1997-2006.

CHAN, D. C., 2006 Mitochondria: dynamic organelles in disease, aging, and development. Cell **125:** 1241-1252.

CHAPPLE, I. L., 1997 Reactive oxygen species and antioxidants in inflammatory diseases. J Clin Periodontol **24:** 287-296.

CHAUDHURI, M., W. AJAYI and G. C. HILL, 1998 Biochemical and molecular properties of the Trypanosoma brucei alternative oxidase. Mol Biochem Parasitol **95:** 53-68.

CHAUDHURI, M., R. D. OTT and G. C. HILL, 2006 Trypanosome alternative oxidase: from molecule to function. Trends Parasitol **22:** 484-491.

CHAUDHURI, M., R. SHARAN and G. C. HILL, 2002 Trypanosome alternative oxidase is regulated post-transcriptionally at the level of RNA stability. J Eukaryot Microbiol **49:** 263-269.

CHELSTOWSKA, A., and R. A. BUTOW, 1995 RTG genes in yeast that function in communication between mitochondria and the nucleus are also required for expression of genes encoding peroxisomal proteins. J Biol Chem **270:** 18141-18146.

CHEN, E. J., and C. A. KAISER, 2003 LST8 negatively regulates amino acid biosynthesis as a component of the TOR pathway. J Cell Biol **161:** 333-347.

CHIVASA, S., A. M. MURPHY, M. NAYLOR and J. P. CARR, 1997 Salicylic Acid Interferes with Tobacco Mosaic Virus Replication via a Novel Salicylhydroxamic Acid-Sensitive Mechanism. Plant Cell **9:** 547-557.

CLIFTON, R., A. H. MILLAR and J. WHELAN, 2006 Alternative oxidases in Arabidopsis: a comparative analysis of differential expression in the gene family provides new insights into function of non-phosphorylating bypasses. Biochim Biophys Acta **1757:** 730-741.

COLOT, H. V., G. PARK, G. E. TURNER, C. RINGELBERG, C. M. CREW *et al.*, 2006 A high-throughput gene knockout procedure for Neurospora reveals functions for multiple transcription factors. Proc Natl Acad Sci U S A **103:** 10352-10357.

CONSIDINE, M. J., R. C. HOLTZAPFFEL, D. A. DAY, J. WHELAN and A. H. MILLAR, 2002 Molecular distinction between alternative oxidase from monocots and dicots. Plant Physiol **129:** 949-953.

COSTANTINI, P., E. JACOTOT, D. DECAUDIN and G. KROEMER, 2000 Mitochondrion as a novel target of anticancer chemotherapy. J Natl Cancer Inst **92:** 1042-1053.

COVELLO, P. S., and M. W. GRAY, 1992 Silent mitochondrial and active nuclear genes for subunit 2 of cytochrome c oxidase (cox2) in soybean: evidence for RNA-mediated gene transfer. Embo J **11:** 3815-3820.

CROSSON, S., and K. MOFFAT, 2001 Structure of a flavin-binding plant photoreceptor domain: insights into light-mediated signal transduction. Proc Natl Acad Sci U S A **98:** 2995-3000.

CULLEN, K. J., Z. YANG, L. SCHUMAKER and Z. GUO, 2007 Mitochondria as a critical target of the chemotheraputic agent cisplatin in head and neck cancer. J Bioenerg Biomembr **39:** 43-50.

CURRAN, S. P., D. LEUENBERGER, W. OPPLIGER and C. M. KOEHLER, 2002a The Tim9p-Tim10p complex binds to the transmembrane domains of the ADP/ATP carrier. Embo J **21:** 942-953.

CURRAN, S. P., D. LEUENBERGER, E. SCHMIDT and C. M. KOEHLER, 2002b The role of the Tim8p-Tim13p complex in a conserved import pathway for mitochondrial polytopic inner membrane proteins. J Cell Biol **158:** 1017-1027.

DALEY, D. O., R. CLIFTON and J. WHELAN, 2002 Intracellular gene transfer: reduced hydrophobicity facilitates gene transfer for subunit 2 of cytochrome c oxidase. Proc Natl Acad Sci U S A **99:** 10510-10515.

DAVIS, A. J., N. B. SEPURI, J. HOLDER, A. E. JOHNSON and R. E. JENSEN, 2000 Two intermembrane space TIM complexes interact with different domains of Tim23p during its import into mitochondria. J Cell Biol **150:** 1271-1282.

DAVIS, R. H., and F. J. DE SERRES, 1970 Genetic and microbiological research techniques for *Neurospora crassa*. Methods Enzymol **17A:** 70-143.

DAY, D. A., A. H. MILLAR, J. T. WISKICH and J. WHELAN, 1994 Regulation of Alternative Oxidase Activity by Pyruvate in Soybean Mitochondria. Plant Physiol **106:** 1421-1427.

DEFRANOUX, N., M. GAISNE and J. VERDIERE, 1994 Functional analysis of the zinc cluster domain of the CYP1 (HAP1) complex regulator in heme-sufficient and heme-deficient yeast cells. Mol Gen Genet **242:** 699-707.

DENIAUD, A., J. HOEBEKE, J. P. BRIAND, S. MULLER, E. JACOTOT *et al.*, 2006 Peptido-targeting of the mitochondrial transition pore complex for therapeutic apoptosis induction. Curr Pharm Des **12:** 4501-4511.

DESCHENEAU, A. T., I. A. CLEARY and F. E. NARGANG, 2005 Genetic evidence for a regulatory pathway controlling alternative oxidase production in Neurospora crassa. Genetics **169:** 123-135.

DETMER, S. A., and D. C. CHAN, 2007 Functions and dysfunctions of mitochondrial dynamics. Nat Rev Mol Cell Biol **8:** 870-879.

DEYULIA, G. J., JR., J. M. CARCAMO, O. BORQUEZ-OJEDA, C. C. SHELTON and D. W. GOLDE, 2005 Hydrogen peroxide generated extracellularly by receptor-ligand interaction facilitates cell signaling. Proc Natl Acad Sci U S A **102:** 5044-5049.

DIETMEIER, K., A. HONLINGER, U. BOMER, P. J. DEKKER, C. ECKERSKORN *et al.*, 1997 Tom5 functionally links mitochondrial preprotein receptors to the general import pore. Nature **388:** 195-200.

DILOVA, I., S. ARONOVA, J. C. CHEN and T. POWERS, 2004 Tor signaling and nutrient-based signals converge on Mks1p phosphorylation to regulate expression of Rtg1.Rtg3p-dependent target genes. J Biol Chem **279:** 46527-46535.

DJAJANEGARA, I., P. M. FINNEGAN, C. MATHIEU, T. MCCABE, J. WHELAN *et al.*, 2002 Regulation of alternative oxidase gene expression in soybean. Plant Mol Biol **50:** 735-742.

DOJCINOVIC, D., J. KROSTING, A. J. HARRIS, D. J. WAGNER and D. M. RHOADS, 2005 Identification of a region of the Arabidopsis AtAOX1a promoter necessary for mitochondrial retrograde regulation of expression. Plant Mol Biol **58:** 159-175.

DOLEZAL, P., O. SMID, P. RADA, Z. ZUBACOVA, D. BURSAC *et al.*, 2005 Giardia mitosomes and trichomonad hydrogenosomes share a common mode of protein targeting. Proc Natl Acad Sci U S A **102:** 10924-10929.

DUARTE, M., M. PETERS, U. SCHULTE and A. VIDEIRA, 2003 The internal alternative NADH dehydrogenase of Neurospora crassa mitochondria. Biochem J **371:** 1005-1011.

ELTHON, T. E., R. L. NICKELS and L. MCINTOSH, 1989 Monoclonal Antibodies to the Alternative Oxidase of Higher Plant Mitochondria. Plant Physiol **89:** 1311-1317.

EMBLEY, T. M., M. VAN DER GIEZEN, D. S. HORNER, P. L. DYAL, S. BELL *et al.*, 2003 Hydrogenosomes, mitochondria and early eukaryotic evolution. IUBMB Life **55:** 387-395.

EPSTEIN, C. B., J. A. WADDLE, W. T. HALE, V. DAVE, J. THORNTON *et al.*, 2001 Genome-wide responses to mitochondrial dysfunction. Mol Biol Cell **12:** 297-308.

FANG, J., and D. S. BEATTIE, 2003 Alternative oxidase present in procyclic Trypanosoma brucei may act to lower the mitochondrial production of superoxide. Arch Biochem Biophys **414:** 294-302.

FINNEGAN, P. M., A. L. UMBACH and J. A. WILCE, 2003 Prokaryotic origins for the mitochondrial alternative oxidase and plastid terminal oxidase nuclear genes. FEBS Lett **555:** 425-430.

FINNEGAN, P. M., J. WHELAN, A. H. MILLAR, Q. ZHANG, M. K. SMITH *et al.*, 1997 Differential expression of the multigene family encoding the soybean mitochondrial alternative oxidase. Plant Physiol **114:** 455-466.

FIUMERA, H. L., S. A. BROADLEY and T. D. FOX, 2007 Translocation of mitochondrially synthesized Cox2 domains from the matrix to the intermembrane space. Mol Cell Biol **27:** 4664-4673.

FREY, T. G., C. W. RENKEN and G. A. PERKINS, 2002 Insight into mitochondrial structure and function from electron tomography. Biochim Biophys Acta **1555:** 196-203.

FRIEDRICH, T., K. STEINMULLER and H. WEISS, 1995 The proton-pumping respiratory complex I of bacteria and mitochondria and its homologue in chloroplasts. FEBS Lett **367:** 107-111.

FUKUDA, H., A. CASAS and A. BATLLE, 2005 Aminolevulinic acid: from its unique biological function to its star role in photodynamic therapy. Int J Biochem Cell Biol **37:** 272-276.

GABRIEL, K., D. MILENKOVIC, A. CHACINSKA, J. MULLER, B. GUIARD *et al.*, 2007 Novel mitochondrial intermembrane space proteins as substrates of the MIA import pathway. J Mol Biol **365:** 612-620.

GERBER, J., and R. LILL, 2002 Biogenesis of iron-sulfur proteins in eukaryotes: components, mechanism and pathology. Mitochondrion **2:** 71-86.

GERBER, J., U. MUHLENHOFF and R. LILL, 2003 An interaction between frataxin and Isu1/Nfs1 that is crucial for Fe/S cluster synthesis on Isu1. EMBO Rep **4:** 906-911.

GERMOT, A., H. PHILIPPE and H. LE GUYADER, 1996 Presence of a mitochondrial-type 70-kDa heat shock protein in Trichomonas vaginalis suggests a very early mitochondrial endosymbiosis in eukaryotes. Proc Natl Acad Sci U S A **93:** 14614-14617.

GIACOMELLO, M., I. DRAGO, P. PIZZO and T. POZZAN, 2007 Mitochondrial Ca2+ as a key regulator of cell life and death. Cell Death Differ **14:** 1267-1274.

GILLES-GONZALEZ, M. A., and G. GONZALEZ, 2004 Signal transduction by heme-containing PAS-domain proteins. J Appl Physiol **96:** 774-783.

GO, Y. M., T. R. ZIEGLER, J. M. JOHNSON, L. GU, J. M. HANSEN *et al.*, 2007 Selective protection of nuclear thioredoxin-1 and glutathione redox systems against oxidation during glucose and glutamine deficiency in human colonic epithelial cells. Free Radic Biol Med **42:** 363-370.

GOPALAKRISHNAN, A., and A. N. TONY KONG, 2007 Anticarcinogenesis by dietary phytochemicals: Cytoprotection by Nrf2 in normal cells and cytotoxicity by modulation of transcription factors NF-kappaB and AP-1 in abnormal cancer cells. Food Chem Toxicol.

GRAD, L. I., A. T. DESCHENEAU, W. NEUPERT, R. LILL and F. E. NARGANG, 1999 Inactivation of the Neurospora crassa mitochondrial outer membrane protein TOM70 by repeat-induced point mutation (RIP) causes defects in mitochondrial protein import and morphology. Curr Genet **36:** 137-146.

GRAY, M. W., G. BURGER and B. F. LANG, 1999 Mitochondrial evolution. Science **283:** 1476-1481.

GRAY, M. W., R. CEDERGREN, Y. ABEL and D. SANKOFF, 1989 On the evolutionary origin of the plant mitochondrion and its genome. Proc Natl Acad Sci U S A **86:** 2267-2271.

GREDILLA, R., G. BARJA and M. LOPEZ-TORRES, 2001a Effect of short-term caloric restriction on H2O2 production and oxidative DNA damage in rat liver mitochondria and location of the free radical source. J Bioenerg Biomembr **33:** 279-287.

GREDILLA, R., A. SANZ, M. LOPEZ-TORRES and G. BARJA, 2001b Caloric restriction decreases mitochondrial free radical generation at complex I and lowers oxidative damage to mitochondrial DNA in the rat heart. Faseb J **15:** 1589-1591.

GREEN, D. R., 2005 Apoptotic pathways: ten minutes to dead. Cell **121:** 671-674.

GRIFFITHS, A. J. F., R. A. COLLINS and F. E. NARGANG, 1995 Mitochondrial Genetics of *Neurospora*, pp. 93-105 in *The Mycota II, Genetics and Biotechnology*, edited by U. KUCK. Springer-Verlag, Berlin.

GRISWOLD, C. M., A. L. MATTHEWS, K. E. BEWLEY and J. W. MAHAFFEY, 1993 Molecular characterization and rescue of acatalasemic mutants of Drosophila melanogaster. Genetics **134:** 781-788.

GUPTA, R. S., 1995 Evolution of the chaperonin families (Hsp60, Hsp10 and Tcp-1) of proteins and the origin of eukaryotic cells. Mol Microbiol **15:** 1-11.

HACKSTEIN, J. H., J. TJADEN and M. HUYNEN, 2006 Mitochondria, hydrogenosomes and mitosomes: products of evolutionary tinkering! Curr Genet **50:** 225-245.

HANSEN, J. M., Y. M. GO and D. P. JONES, 2006 Nuclear and mitochondrial compartmentation of oxidative stress and redox signaling. Annu Rev Pharmacol Toxicol **46:** 215-234.

HASTY, P., J. CAMPISI, J. HOEIJMAKERS, H. VAN STEEG and J. VIJG, 2003 Aging and genome maintenance: lessons from the mouse? Science **299:** 1355-1359.

HATEFI, Y., 1985 The mitochondrial electron transport and oxidative phosphorylation system. Annu Rev Biochem **54:** 1015-1069.

HE, Q., H. SHU, P. CHENG, S. CHEN, L. WANG *et al.*, 2005 Light-independent phosphorylation of WHITE COLLAR-1 regulates its function in the Neurospora circadian negative feedback loop. J Biol Chem **280:** 17526-17532.

HEFTI, M. H., K. J. FRANCOIJS, S. C. DE VRIES, R. DIXON and J. VERVOORT, 2004 The PAS fold. A redefinition of the PAS domain based upon structural prediction. Eur J Biochem **271:** 1198-1208.

HEGARDT, F. G., 1999 Mitochondrial 3-hydroxy-3-methylglutaryl-CoA synthase: a control enzyme in ketogenesis. Biochem J **338 (Pt 3):** 569-582.

HENTZE, M. W., M. U. MUCKENTHALER and N. C. ANDREWS, 2004 Balancing acts: molecular control of mammalian iron metabolism. Cell **117:** 285-297.

HERRMANN, J. M., and N. BONNEFOY, 2004 Protein export across the inner membrane of mitochondria: the nature of translocated domains determines the dependence on the Oxa1 translocase. J Biol Chem **279:** 2507-2512.

HERRMANN, J. M., and W. NEUPERT, 2003 Protein insertion into the inner membrane of mitochondria. IUBMB Life **55:** 219-225.

HILL, K., K. MODEL, M. T. RYAN, K. DIETMEIER, F. MARTIN *et al.*, 1998 Tom40 forms the hydrophilic channel of the mitochondrial import pore for preproteins [see comment]. Nature **395:** 516-521.

HON, T., H. C. LEE, Z. HU, V. R. IYER and L. ZHANG, 2005 The heme activator protein Hap1 represses transcription by a heme-independent mechanism in Saccharomyces cerevisiae. Genetics **169:** 1343-1352.

HONLINGER, A., U. BOMER, A. ALCONADA, C. ECKERSKORN, F. LOTTSPEICH *et al.*, 1996 Tom7 modulates the dynamics of the mitochondrial outer membrane translocase and plays a pathway-related role in protein import. Embo J **15:** 2125-2137.

HOPPINS, S., L. LACKNER and J. NUNNARI, 2007 The machines that divide and fuse mitochondria. Annu Rev Biochem **76:** 751-780.

HUALA, E., P. W. OELLER, E. LISCUM, I. S. HAN, E. LARSEN *et al.*, 1997 Arabidopsis NPH1: a protein kinase with a putative redox-sensing domain. Science **278:** 2120-2123.

HUANG, X., U. VON RAD and J. DURNER, 2002 Nitric oxide induces transcriptional activation of the nitric oxide-tolerant alternative oxidase in Arabidopsis suspension cells. Planta **215:** 914-923.

HUH, W. K., and S. O. KANG, 2001 Characterization of the gene family encoding alternative oxidase from Candida albicans. Biochem J **356:** 595-604.

HUHNDORF, S. M., A. N. MILLER and F. A. FERNANDEZ, 2004 Molecular systematics of the Coronophorales and new species of Bertia, Lasiobertia and Nitschkia. Mycol Res **108:** 1384-1398.

HWANG, C. S., Y. U. BAEK, H. S. YIM and S. O. KANG, 2003 Protective roles of mitochondrial manganese-containing superoxide dismutase against various stresses in Candida albicans. Yeast **20:** 929-941.

ITO, T., T. CHIBA, R. OZAWA, M. YOSHIDA, M. HATTORI *et al.*, 2001 A comprehensive two-hybrid analysis to explore the yeast protein interactome. Proc Natl Acad Sci U S A **98:** 4569-4574.

ITO, Y., D. SAISHO, M. NAKAZONO, N. TSUTSUMI and A. HIRAI, 1997 Transcript levels of tandem-arranged alternative oxidase genes in rice are increased by low temperature. Gene **203:** 121-129.

JACINTO, E., and M. N. HALL, 2003 Tor signalling in bugs, brain and brawn. Nat Rev Mol Cell Biol **4:** 117-126.

JIA, Y., B. ROTHERMEL, J. THORNTON and R. A. BUTOW, 1997 A basic helix-loop-helix-leucine zipper transcription complex in yeast functions in a signaling pathway from mitochondria to the nucleus. Mol Cell Biol **17:** 1110-1117.

JITRAPAKDEE, S., A. VIDAL-PUIG and J. C. WALLACE, 2006 Anaplerotic roles of pyruvate carboxylase in mammalian tissues. Cell Mol Life Sci **63:** 843-854.

JOHNSTON, M., and J. DOVER, 1987 Mutations that inactivate a yeast transcriptional regulatory protein cluster in an evolutionarily conserved DNA binding domain. Proc Natl Acad Sci U S A **84:** 2401-2405.

JOSEPH-HORNE, T., D. W. HOLLOMON and P. M. WOOD, 2001 Fungal respiration: a fusion of standard and alternative components. Biochim Biophys Acta **1504:** 179-195.

JOZA, N., S. A. SUSIN, E. DAUGAS, W. L. STANFORD, S. K. CHO *et al.*, 2001 Essential role of the mitochondrial apoptosis-inducing factor in programmed cell death. Nature **410:** 549-554.

JUSZCZUK, I. M., and A. M. RYCHTER, 2003 Alternative oxidase in higher plants. Acta Biochim Pol **50:** 1257-1271.

KAKKAR, P., and B. K. SINGH, 2007 Mitochondria: a hub of redox activities and cellular distress control. Mol Cell Biochem **305:** 235-253.

KAPLAN, R. S., J. A. MAYOR, D. KAKHNIASHVILI, D. A. GREMSE, D. O. WOOD *et al.*, 1996 Deletion of the nuclear gene encoding the mitochondrial citrate transport protein from Saccharomyces cerevisiae. Biochem Biophys Res Commun **226:** 657-662.

KARPOVA, O. V., E. V. KUZMIN, T. E. ELTHON and K. J. NEWTON, 2002 Differential expression of alternative oxidase genes in maize mitochondrial mutants. Plant Cell **14:** 3271-3284.

KERSCHER, O., J. HOLDER, M. SRINIVASAN, R. S. LEUNG and R. E. JENSEN, 1997 The Tim54p-Tim22p complex mediates insertion of proteins into the mitochondrial inner membrane. J Cell Biol **139:** 1663-1675.

KERSCHER, O., N. B. SEPURI and R. E. JENSEN, 2000 Tim18p is a new component of the Tim54p-Tim22p translocon in the mitochondrial inner membrane. Mol Biol Cell **11:** 103-116.

KERSCHER, S., S. DROSE, V. ZICKERMANN and U. BRANDT, 2007 The Three Families of Respiratory NADH Dehydrogenases. Results Probl Cell Differ.

KERSCHER, S. J., 2000 Diversity and origin of alternative NADH:ubiquinone oxidoreductases. Biochim Biophys Acta **1459:** 274-283.

KHRAPKO, K., K. EBRALIDSE and Y. KRAYTSBERG, 2004 Where and when do somatic mtDNA mutations occur? Ann N Y Acad Sci **1019:** 240-244.

KHRAPKO, K., Y. KRAYTSBERG, A. D. DE GREY, J. VIJG and E. A. SCHON, 2006 Does premature aging of the mtDNA mutator mouse prove that mtDNA mutations are involved in natural aging? Aging Cell **5:** 279-282.

KHRAPKO, K., and J. VIJG, 2007 Mitochondrial DNA mutations and aging: a case closed? Nat Genet **39:** 445-446.

KIRCHMAN, P. A., S. KIM, C. Y. LAI and S. M. JAZWINSKI, 1999 Interorganelle signaling is a determinant of longevity in Saccharomyces cerevisiae. Genetics **152:** 179-190.

KISPAL, G., P. CSERE, C. PROHL and R. LILL, 1999 The mitochondrial proteins Atm1p and Nfs1p are essential for biogenesis of cytosolic Fe/S proteins. Embo J **18:** 3981-3989.

KISPAL, G., K. SIPOS, H. LANGE, Z. FEKETE, T. BEDEKOVICS *et al.*, 2005 Biogenesis of cytosolic ribosomes requires the essential iron-sulphur protein Rli1p and mitochondria. Embo J **24:** 589-598.

KOONIN, E. V., 1994 Yeast protein controlling inter-organelle communication is related to bacterial phosphatases containing the Hsp 70-type ATP-binding domain. Trends Biochem Sci **19:** 156-157.

KOVERMANN, P., K. N. TRUSCOTT, B. GUIARD, P. REHLING, N. B. SEPURI *et al.*, 2002 Tim22, the essential core of the mitochondrial protein insertion complex, forms a voltage-activated and signal-gated channel. Mol Cell **9:** 363-373.

KUJOTH, G. C., A. HIONA, T. D. PUGH, S. SOMEYA, K. PANZER *et al.*, 2005 Mitochondrial DNA mutations, oxidative stress, and apoptosis in mammalian aging. Science **309:** 481-484.

KURLAND, C. G., and S. G. ANDERSSON, 2000 Origin and evolution of the mitochondrial proteome. Microbiol Mol Biol Rev **64:** 786-820.

LAMBERS, H., 1982 Cyanide-resistant respiration: A non-phosphorylating electron transport pathway acting as an energy overflow. Physiol Plant **55:** 478-485.

LAMBOWITZ, A. M., J. R. SABOURIN, H. BERTRAND, R. NICKELS and L. MCINTOSH, 1989 Immunological identification of the alternative oxidase of Neurospora crassa mitochondria. Mol Cell Biol **9:** 1362-1364.

LAMBOWITZ, A. M., and C. W. SLAYMAN, 1971 Cyanide-resistant respiration in Neurospora crassa. J Bacteriol **108:** 1087-1096.

LAMBOWITZ, A. M., E. W. SMITH and C. W. SLAYMAN, 1972a Electron transport in Neurospora mitochondria. Studies on wild type and poky. J Biol Chem **247:** 4850-4858.

LAMBOWITZ, A. M., E. W. SMITH and C. W. SLAYMAN, 1972b Oxidative phosphorylation in Neurospora mitochondria. Studies on wild type, poky, and chloramphenicol-induced wild type. J Biol Chem **247:** 4859-4865.

LANG, B. F., G. BURGER, C. J. O'KELLY, R. CEDERGREN, G. B. GOLDING *et al.*, 1997 An ancestral mitochondrial DNA resembling a eubacterial genome in miniature. Nature **387:** 493-497.

LANG, B. F., M. W. GRAY and G. BURGER, 1999 Mitochondrial genome evolution and the origin of eukaryotes. Annu Rev Genet **33:** 351-397.

LANGE, H., A. KAUT, G. KISPAL and R. LILL, 2000 A mitochondrial ferredoxin is essential for biogenesis of cellular iron-sulfur proteins. Proc Natl Acad Sci U S A **97:** 1050-1055.

LANOUE, K. F., D. A. BERKICH, M. CONWAY, A. J. BARBER, L. Y. HU *et al.*, 2001 Role of specific aminotransferases in de novo glutamate synthesis and redox shuttling in the retina. J Neurosci Res **66:** 914-922.

LEE, H. C., and Y. H. WEI, 2007 Oxidative stress, mitochondrial DNA mutation, and apoptosis in aging. Exp Biol Med (Maywood) **232:** 592-606.

LENNON, A. M., U. H. NEUENSCHWANDER, M. RIBAS-CARBO, L. GILES, J. A. RYALS *et al.*, 1997 The Effects of Salicylic Acid and Tobacco Mosaic Virus Infection on the Alternative Oxidase of Tobacco. Plant Physiol **115:** 783-791.

LEON-AVILA, G., and J. TOVAR, 2004 Mitosomes of Entamoeba histolytica are abundant mitochondrion-related remnant organelles that lack a detectable organellar genome. Microbiology **150:** 1245-1250.

LI, J., S. SAXENA, D. PAIN and A. DANCIS, 2001a Adrenodoxin reductase homolog (Arh1p) of yeast mitochondria required for iron homeostasis. J Biol Chem **276:** 1503-1509.

LI, Q., R. G. RITZEL, L. L. MCLEAN, L. MCINTOSH, T. KO *et al.*, 1996 Cloning and analysis of the alternative oxidase gene of Neurospora crassa. Genetics **142:** 129-140.

LI, X., M. MARANI, R. MANNUCCI, B. KINSEY, F. ANDRIANI *et al.*, 2001b Overexpression of BCL-X(L) underlies the molecular basis for resistance to staurosporine-induced apoptosis in PC-3 cells. Cancer Res **61:** 1699-1706.

LIANG, H., and W. F. WARD, 2006 PGC-1alpha: a key regulator of energy metabolism. Adv Physiol Educ **30:** 145-151.

LIANG, S. D., R. MARMORSTEIN, S. C. HARRISON and M. PTASHNE, 1996 DNA sequence preferences of GAL4 and PPR1: how a subset of Zn2 Cys6 binuclear cluster proteins recognizes DNA. Mol Cell Biol **16:** 3773-3780.

LIAO, X., and R. A. BUTOW, 1993 RTG1 and RTG2: two yeast genes required for a novel path of communication from mitochondria to the nucleus. Cell **72:** 61-71.

LIAO, X. S., W. C. SMALL, P. A. SRERE and R. A. BUTOW, 1991 Intramitochondrial functions regulate nonmitochondrial citrate synthase (CIT2) expression in Saccharomyces cerevisiae. Mol Cell Biol **11:** 38-46.

LILL, R., and G. KISPAL, 2000 Maturation of cellular Fe-S proteins: an essential function of mitochondria. Trends Biochem Sci **25:** 352-356.

LILL, R., and U. MUHLENHOFF, 2005 Iron-sulfur-protein biogenesis in eukaryotes. Trends Biochem Sci **30:** 133-141.

LINDEBRO, M. C., L. POELLINGER and M. L. WHITELAW, 1995 Protein-protein interaction via PAS domains: role of the PAS domain in positive and negative regulation of the bHLH/PAS dioxin receptor-Arnt transcription factor complex. Embo J **14:** 3528-3539.

LIU, Z., and R. A. BUTOW, 2006 Mitochondrial retrograde signaling. Annu Rev Genet **40:** 159-185.

LIU, Z., T. SEKITO, C. B. EPSTEIN and R. A. BUTOW, 2001 RTG-dependent mitochondria to nucleus signaling is negatively regulated by the seven WD-repeat protein Lst8p. Embo J **20:** 7209-7219.

LIU, Z., T. SEKITO, M. SPIREK, J. THORNTON and R. A. BUTOW, 2003 Retrograde signaling is regulated by the dynamic interaction between Rtg2p and Mks1p. Mol Cell **12:** 401-411.

LIU, Z., M. SPIREK, J. THORNTON and R. A. BUTOW, 2005 A novel degron-mediated degradation of the RTG pathway regulator, Mks1p, by SCFGrr1. Mol Biol Cell **16:** 4893-4904.

LOGAN, D. C., 2006 The mitochondrial compartment. J Exp Bot **57:** 1225-1243.

LOMBARD, D. B., K. F. CHUA, R. MOSTOSLAVSKY, S. FRANCO, M. GOSTISSA *et al.*, 2005 DNA repair, genome stability, and aging. Cell **120:** 497-512.

LOPEZ-TORRES, M., R. GREDILLA, A. SANZ and G. BARJA, 2002 Influence of aging and long-term caloric restriction on oxygen radical generation and oxidative DNA damage in rat liver mitochondria. Free Radic Biol Med **32:** 882-889.

LUCIANO, P., and V. GELI, 1996 The mitochondrial processing peptidase: function and specificity. Experientia **52:** 1077-1082.

MAASSEN, J. A., L. M. T HART, G. M. JANSSEN, E. REILING, J. A. ROMIJN *et al.*, 2006 Mitochondrial diabetes and its lessons for common Type 2 diabetes. Biochem Soc Trans **34:** 819-823.

MACDONALD, M. J., 1995 Feasibility of a mitochondrial pyruvate malate shuttle in pancreatic islets. Further implication of cytosolic NADPH in insulin secretion. J Biol Chem **270:** 20051-20058.

MACPHERSON, S., M. LAROCHELLE and B. TURCOTTE, 2006 A fungal family of transcriptional regulators: the zinc cluster proteins. Microbiol Mol Biol Rev **70:** 583-604.

MAMANE, Y., K. HELLAUER, M. H. ROCHON and B. TURCOTTE, 1998 A linker region of the yeast zinc cluster protein leu3p specifies binding to everted repeat DNA. J Biol Chem **273:** 18556-18561.

MARGULIS, L., 1970 Origins of Eukaryotic Cells, pp. 349 in *Yale Univ. Press*, New Have, CT.

MARMORSTEIN, R., M. CAREY, M. PTASHNE and S. C. HARRISON, 1992 DNA recognition by GAL4: structure of a protein-DNA complex. Nature **356:** 408-414.

MARTIN, W., and R. G. HERRMANN, 1998 Gene transfer from organelles to the nucleus: how much, what happens, and Why? Plant Physiol **118:** 9-17.

MARTIN, W., and M. MULLER, 1998 The hydrogen hypothesis for the first eukaryote. Nature **392:** 37-41.

MARTINEZ-CABALLERO, S., S. M. GRIGORIEV, J. M. HERRMANN, M. L. CAMPO and K. W. KINNALLY, 2007 Tim17p regulates the twin pore structure and voltage gating of the mitochondrial protein import complex TIM23. J Biol Chem **282:** 3584-3593.

MARTINOU, J. C., and D. R. GREEN, 2001 Breaking the mitochondrial barrier. Nat Rev Mol Cell Biol **2:** 63-67.

MATAPURKAR, A., and Y. LAZEBNIK, 2006 Requirement of cytochrome c for apoptosis in human cells. Cell Death Differ **13:** 2062-2067.

MATHERS, J., J. A. FRASER, M. MCMAHON, R. D. SAUNDERS, J. D. HAYES *et al.*, 2004 Antioxidant and cytoprotective responses to redox stress. Biochem Soc Symp: 157-176.

MATHY, G., R. NAVET, P. GERKENS, P. LEPRINCE, E. DE PAUW *et al.*, 2006 Saccharomyces cerevisiae mitoproteome plasticity in response to recombinant alternative ubiquinol oxidase. J Proteome Res **5:** 339-348.

MATTHEWS, C. P., N. H. COLBURN and M. R. YOUNG, 2007 AP-1 a target for cancer prevention. Curr Cancer Drug Targets **7:** 317-324.

MAXWELL, D. P., R. NICKELS and L. MCINTOSH, 2002 Evidence of mitochondrial involvement in the transduction of signals required for the induction of genes associated with pathogen attack and senescence. Plant J **29:** 269-279.

MAXWELL, D. P., Y. WANG and L. MCINTOSH, 1999 The alternative oxidase lowers mitochondrial reactive oxygen production in plant cells. Proc Natl Acad Sci U S A **96:** 8271-8276.

McDONALD, A., and G. VANLERBERGHE, 2004 Branched mitochondrial electron transport in the Animalia: presence of alternative oxidase in several animal phyla. IUBMB Life **56:** 333-341.

McDONALD, A. E., S. AMIRSADEGHI and G. C. VANLERBERGHE, 2003 Prokaryotic orthologues of mitochondrial alternative oxidase and plastid terminal oxidase. Plant Mol Biol **53:** 865-876.

McDONALD, A. E., and G. C. VANLERBERGHE, 2005 Alternative oxidase and plastoquinol terminal oxidase in marine prokaryotes of the Sargasso Sea. Gene **349:** 15-24.

MEEUSE, B. J. D., 1975 Thermogenic Respiration in Aroids. Ann Rev Plant Physiol **26:** 117-126.

MEINECKE, M., R. WAGNER, P. KOVERMANN, B. GUIARD, D. U. MICK *et al.*, 2006 Tim50 maintains the permeability barrier of the mitochondrial inner membrane. Science **312:** 1523-1526.

MELOV, S., D. HINERFELD, L. ESPOSITO and D. C. WALLACE, 1997 Multi-organ characterization of mitochondrial genomic rearrangements in ad libitum and caloric restricted mice show striking somatic mitochondrial DNA rearrangements with age. Nucleic Acids Res **25:** 974-982.

MESECKE, N., N. TERZIYSKA, C. KOZANY, F. BAUMANN, W. NEUPERT *et al.*, 2005 A disulfide relay system in the intermembrane space of mitochondria that mediates protein import. Cell **121:** 1059-1069.

MICHEA-HAMZEHPOUR, M., and G. TURIAN, 1987 GMP-stimulation of the cyanide-insensitive mitochondrial respiration in heat-shocked conidia of Neurospora crassa. Experientia **43:** 439-440.

MILLAR, A. H., J. T. WISKICH, J. WHELAN and D. A. DAY, 1993 Organic acid activation of the alternative oxidase of plant mitochondria. FEBS Lett **329:** 259-262.

MILLENAAR, F. F., J. J. BENSCHOP, A. M. WAGNER and H. LAMBERS, 1998 The role of the alternative oxidase in stabilizing the in vivo reduction state of the ubiquinone pool and the activation state of the alternative oxidase. Plant Physiol **118:** 599-607.

MIZUNO, N., A. SUGIE, F. KOBAYASHI and S. TAKUMI, 2007 Mitochondrial alternative pathway is associated with development of freezing tolerance in common wheat. J Plant Physiol.

MODEL, K., C. MEISINGER, T. PRINZ, N. WIEDEMANN, K. N. TRUSCOTT *et al.*, 2001 Multistep assembly of the protein import channel of the mitochondrial outer membrane. Nat Struct Biol **8:** 361-370.

MOKRANJAC, D., and W. NEUPERT, 2005 Protein import into mitochondria. Biochem Soc Trans **33:** 1019-1023.

MOKRANJAC, D., S. A. PASCHEN, C. KOZANY, H. PROKISCH, S. C. HOPPINS *et al.*, 2003 Tim50, a novel component of the TIM23 preprotein translocase of mitochondria. Embo J **22:** 816-825.

MOREIRA, D., and P. LOPEZ-GARCIA, 1998 Symbiosis between methanogenic archaea and delta-proteobacteria as the origin of eukaryotes: the syntrophic hypothesis. J Mol Evol **47:** 517-530.

MOYNIHAN, M. R., A. ORDENTLICH and I. RASKIN, 1995 Chilling-Induced Heat Evolution in Plants. Plant Physiol **108:** 995-999.

MUHLENHOFF, U., J. GERBER, N. RICHHARDT and R. LILL, 2003 Components involved in assembly and dislocation of iron-sulfur clusters on the scaffold protein Isu1p. Embo J **22:** 4815-4825.

MULLER, J. M., D. MILENKOVIC, B. GUIARD, N. PFANNER and A. CHACINSKA, 2007 Precursor Oxidation by Mia40 and Erv1 Promotes Vectorial Transport of Proteins into the Mitochondrial Intermembrane Space. Mol Biol Cell.

MULLER, M., 1993 The hydrogenosome. J Gen Microbiol **139:** 2879-2889.

MURPHY, A. M., S. CHIVASA, D. P. SINGH and J. P. CARR, 1999 Salicylic acid-induced resistance to viruses and other pathogens: a parting of the ways? Trends Plant Sci **4:** 155-160.

NADEAU, P. J., S. J. CHARETTE, M. B. TOLEDANO and J. LANDRY, 2007 Disulfide Bond-mediated multimerization of Ask1 and its reduction by thioredoxin-1 regulate H(2)O(2)-induced c-Jun NH(2)-terminal kinase activation and apoptosis. Mol Biol Cell **18:** 3903-3913.

NAKAMURA, K., K. SAKAMOTO, Y. KIDO, Y. FUJIMOTO, T. SUZUKI *et al.*, 2005 Mutational analysis of the Trypanosoma vivax alternative oxidase: the E(X)6Y motif is conserved in both mitochondrial alternative oxidase and plastid terminal oxidase and is indispensable for enzyme activity. Biochem Biophys Res Commun **334:** 593-600.

NARGANG, F. E., M. PREUSS, W. NEUPERT and J. M. HERRMANN, 2002 The Oxa1 protein forms a homooligomeric complex and is an essential part of the mitochondrial export translocase in Neurospora crassa. J Biol Chem **277:** 12846-12853.

NARGANG, F. E., D. RAPAPORT, R. G. RITZEL, W. NEUPERT and R. LILL, 1998 Role of the negative charges in the cytosolic domain of TOM22 in the import of precursor proteins into mitochondria. Mol Cell Biol **18:** 3173-3181.

NASSOGNE, M. C., B. HERON, G. TOUATI, D. RABIER and J. M. SAUDUBRAY, 2005 Urea cycle defects: management and outcome. J Inherit Metab Dis **28:** 407-414.

NINOMIYA, Y., K. SUZUKI, C. ISHII and H. INOUE, 2004 Highly efficient gene replacements in Neurospora strains deficient for nonhomologous end-joining. Proc Natl Acad Sci U S A **101:** 12248-12253.

NISSIM, I., O. HORYN, B. LUHOVYY, A. LAZAROW, Y. DAIKHIN *et al.*, 2003 Role of the glutamate dehydrogenase reaction in furnishing aspartate nitrogen for urea synthesis: studies in perfused rat liver with 15N. Biochem J **376:** 179-188.

ORANGE, J. S., O. LEVY and R. S. GEHA, 2005 Human disease resulting from gene mutations that interfere with appropriate nuclear factor-kappaB activation. Immunol Rev **203:** 21-37.

ORBACH, M. J., 1994 A cosmid with a HyR marker for fungal library construction and screening. Gene **150:** 159-162.

ORDOG, S. H., V. J. HIGGINS and G. C. VANLERBERGHE, 2002 Mitochondrial alternative oxidase is not a critical component of plant viral resistance but may play a role in the hypersensitive response. Plant Physiol **129:** 1858-1865.

ORR, W. C., and R. S. SOHAL, 1993 Effects of Cu-Zn superoxide dismutase overexpression of life span and resistance to oxidative stress in transgenic Drosophila melanogaster. Arch Biochem Biophys **301:** 34-40.

ORR, W. C., and R. S. SOHAL, 1994 Extension of life-span by overexpression of superoxide dismutase and catalase in Drosophila melanogaster. Science **263:** 1128-1130.

ORRENIUS, S., 2007 Reactive oxygen species in mitochondria-mediated cell death. Drug Metab Rev **39:** 443-455.

OWEN, O. E., S. C. KALHAN and R. W. HANSON, 2002 The key role of anaplerosis and cataplerosis for citric acid cycle function. J Biol Chem **277:** 30409-30412.

OZAWA, T., 1999 Mitochondrial genome mutation in cell death and aging. J Bioenerg Biomembr **31:** 377-390.

PALMER, J. D., 1997 Organelle genomes: going, going, gone! Science **275:** 790-791.

PAPA, S., M. TUENA DE GOMEZ-PUYOU and A. GOMEZ-PUYOU, 1975 On the mechanism of action of alkylguanidines on oxidative phosphorylation in mitochondria. Eur J Biochem **55:** 1-8.

PARSONS, H. L., J. Y. YIP and G. C. VANLERBERGHE, 1999 Increased respiratory restriction during phosphate-limited growth in transgenic tobacco cells lacking alternative oxidase. Plant Physiol **121:** 1309-1320.

PASCHEN, S. A., U. ROTHBAUER, K. KALDI, M. F. BAUER, W. NEUPERT *et al.*, 2000 The role of the TIM8-13 complex in the import of Tim23 into mitochondria. Embo J **19:** 6392-6400.

PASTORE, D., D. TRONO, M. N. LAUS, N. DI FONZO and Z. FLAGELLA, 2007 Possible plant mitochondria involvement in cell adaptation to drought stress. A case study: durum wheat mitochondria. J Exp Bot **58:** 195-210.

PETROZZI, L., G. RICCI, N. J. GIGLIOLI, G. SICILIANO and M. MANCUSO, 2007 Mitochondria and neurodegeneration. Biosci Rep **27:** 87-104.

PFEIFER, K., K. S. KIM, S. KOGAN and L. GUARENTE, 1989 Functional dissection and sequence of yeast HAP1 activator. Cell **56:** 291-301.

PHILLIPS, J. P., S. D. CAMPBELL, D. MICHAUD, M. CHARBONNEAU and A. J. HILLIKER, 1989 Null mutation of copper/zinc superoxide dismutase in Drosophila confers hypersensitivity to paraquat and reduced longevity. Proc Natl Acad Sci U S A **86:** 2761-2765.

PIECZENIK, S. R., and J. NEUSTADT, 2007 Mitochondrial dysfunction and molecular pathways of disease. Exp Mol Pathol **83:** 84-92.

PITHUKPAKORN, M., 2005 Disorders of pyruvate metabolism and the tricarboxylic acid cycle. Mol Genet Metab **85:** 243-246.

PLAXTON, W. C., 1996 The Organization and Regulation of Plant Glycolysis. Annu Rev Plant Physiol Plant Mol Biol **47:** 185-214.

POLIDOROS, A. N., P. V. MYLONA, K. PASENTSIS, J. G. SCANDALIOS and A. S. TSAFTARIS, 2005 The maize alternative oxidase 1a (Aox1a) gene is regulated by signals related to oxidative stress. Redox Rep **10:** 71-78.

PONGRATZ, I., C. ANTONSSON, M. L. WHITELAW and L. POELLINGER, 1998 Role of the PAS domain in regulation of dimerization and DNA binding specificity of the dioxin receptor. Mol Cell Biol **18:** 4079-4088.

PUCCIO, H., and M. KOENIG, 2000 Recent advances in the molecular pathogenesis of Friedreich ataxia. Hum Mol Genet **9:** 887-892.

REECE, R. J., and M. PTASHNE, 1993 Determinants of binding-site specificity among yeast C6 zinc cluster proteins. Science **261:** 909-911.

REGOES, A., D. ZOURMPANOU, G. LEON-AVILA, M. VAN DER GIEZEN, J. TOVAR *et al.*, 2005 Protein import, replication, and inheritance of a vestigial mitochondrion. J Biol Chem **280:** 30557-30563.

REHLING, P., K. MODEL, K. BRANDNER, P. KOVERMANN, A. SICKMANN *et al.*, 2003 Protein insertion into the mitochondrial inner membrane by a twin-pore translocase. Science **299:** 1747-1751.

RERNGSAMRAN, P., M. B. MURPHY, S. A. DOYLE and D. J. EBBOLE, 2005 Fluffy, the major regulator of conidiation in Neurospora crassa, directly activates a developmentally regulated hydrophobin gene. Mol Microbiol **56:** 282-297.

RHEE, S. G., S. W. KANG, W. JEONG, T. S. CHANG, K. S. YANG *et al.*, 2005 Intracellular messenger function of hydrogen peroxide and its regulation by peroxiredoxins. Curr Opin Cell Biol **17:** 183-189.

RHOADS, D. M., and L. MCINTOSH, 1992 Salicylic Acid Regulation of Respiration in Higher Plants: Alternative Oxidase Expression. Plant Cell **4:** 1131-1139.

RHOADS, D. M., and L. MCINTOSH, 1993a Cytochrome and Alternative Pathway Respiration in Tobacco (Effects of Salicylic Acid). Plant Physiol **103:** 877-883.

RHOADS, D. M., and L. MCINTOSH, 1993b The salicylic acid-inducible alternative oxidase gene aox1 and genes encoding pathogenesis-related proteins share regions of sequence similarity in their promoters. Plant Mol Biol **21:** 615-624.

RHOADS, D. M., A. L. UMBACH, C. R. SWEET, A. M. LENNON, G. S. RAUCH *et al.*, 1998 Regulation of the cyanide-resistant alternative oxidase of plant mitochondria. Identification of the cysteine residue involved in alpha-keto acid stimulation and intersubunit disulfide bond formation. J Biol Chem **273:** 30750-30756.

RIBAS-CARBO, M., N. L. TAYLOR, L. GILES, S. BUSQUETS, P. M. FINNEGAN *et al.*, 2005 Effects of water stress on respiration in soybean leaves. Plant Physiol **139:** 466-473.

RISSLER, M., N. WIEDEMANN, S. PFANNSCHMIDT, K. GABRIEL, B. GUIARD *et al.*, 2005 The essential mitochondrial protein Erv1 cooperates with Mia40 in biogenesis of intermembrane space proteins. J Mol Biol **353:** 485-492.

ROBSON, C. A., and G. C. VANLERBERGHE, 2002 Transgenic plant cells lacking mitochondrial alternative oxidase have increased susceptibility to mitochondria-dependent and -independent pathways of programmed cell death. Plant Physiol **129:** 1908-1920.

RODGERS, K. R., and G. S. LUKAT-RODGERS, 2005 Insights into heme-based O2 sensing from structure-function relationships in the FixL proteins. J Inorg Biochem **99:** 963-977.

RODRIGUEZ-MANZANEQUE, M. T., J. TAMARIT, G. BELLI, J. ROS and E. HERRERO, 2002 Grx5 is a mitochondrial glutaredoxin required for the activity of iron/sulfur enzymes. Mol Biol Cell **13:** 1109-1121.

ROTHERMEL, B. A., J. L. THORNTON and R. A. BUTOW, 1997 Rtg3p, a basic helix-loop-helix/leucine zipper protein that functions in mitochondrial-induced changes in gene expression, contains independent activation domains. J Biol Chem **272:** 19801-19807.

ROUAULT, T. A., and W. H. TONG, 2005 Iron-sulphur cluster biogenesis and mitochondrial iron homeostasis. Nat Rev Mol Cell Biol **6:** 345-351.

SAISHO, D., E. NAMBARA, S. NAITO, N. TSUTSUMI, A. HIRAI *et al.*, 1997 Characterization of the gene family for alternative oxidase from Arabidopsis thaliana. Plant Mol Biol **35:** 585-596.

SAKAJO, S., N. MINAGAWA and A. YOSHIMOTO, 1997 Effects of nucleotides on cyanide-resistant respiratory activity in mitochondria isolated from antimycin A-treated yeast Hansenula anomala. Biosci Biotechnol Biochem **61:** 396-399.

SAKAMOTO, W., N. SPIELEWOY, G. BONNARD, M. MURATA and H. WINTZ, 2000 Mitochondrial localization of AtOXA1, an arabidopsis homologue of yeast Oxa1p involved in the insertion and assembly of protein complexes in mitochondrial inner membrane. Plant Cell Physiol **41:** 1157-1163.

SAMBROOK, J., and D. W. RUSSELL, 2001 *Molecular cloning. A laboratory manual.* Cold Spring Harbor Laboratory Press, Cold Spring Harbor, New York.

SANZ, A., P. CARO, V. AYALA, M. PORTERO-OTIN, R. PAMPLONA *et al.*, 2006 Methionine restriction decreases mitochondrial oxygen radical generation and leak as well as oxidative damage to mitochondrial DNA and proteins. Faseb J **20:** 1064-1073.

SANZ, A., P. CARO and G. BARJA, 2004 Protein restriction without strong caloric restriction decreases mitochondrial oxygen radical production and oxidative DNA damage in rat liver. J Bioenerg Biomembr **36:** 545-552.

SCHILKE, B., C. VOISINE, H. BEINERT and E. CRAIG, 1999 Evidence for a conserved system for iron metabolism in the mitochondria of Saccharomyces cerevisiae. Proc Natl Acad Sci U S A **96:** 10206-10211.

SCHJERLING, P., and S. HOLMBERG, 1996 Comparative amino acid sequence analysis of the C6 zinc cluster family of transcriptional regulators. Nucleic Acids Res **24:** 4599-4607.

SCHLUNZEN, F., R. ZARIVACH, J. HARMS, A. BASHAN, A. TOCILJ *et al.*, 2001 Structural basis for the interaction of antibiotics with the peptidyl transferase centre in eubacteria. Nature **413:** 814-821.

SCHONBAUM, G. R., W. D. BONNER, JR., B. T. STOREY and J. T. BAHR, 1971 Specific inhibition of the cyanide-insensitive respiratory pathway in plant mitochondria by hydroxamic acids. Plant Physiol **47:** 124-128.

SCHRINER, S. E., N. J. LINFORD, G. M. MARTIN, P. TREUTING, C. E. OGBURN *et al.*, 2005 Extension of murine life span by overexpression of catalase targeted to mitochondria. Science **308:** 1909-1911.

SCHWAB, A. J., 1973 Mitochondrial protein synthesis and cyanide-resistant respiration in copper-depleted, cytochrome oxidase-deficient Neurospora crassa. FEBS Lett **35:** 63-66.

SEKITO, T., J. THORNTON and R. A. BUTOW, 2000 Mitochondria-to-nuclear signaling is regulated by the subcellular localization of the transcription factors Rtg1p and Rtg3p. Mol Biol Cell **11:** 2103-2115.

SEYMOUR, R. S., 2001 Biophysics and physiology of temperature regulation in thermogenic flowers. Biosci Rep **21:** 223-236.

SHAW, J. M., and J. NUNNARI, 2002 Mitochondrial dynamics and division in budding yeast. Trends Cell Biol **12:** 178-184.

SHERMAN, E. L., N. E. GO and F. E. NARGANG, 2005 Functions of the small proteins in the TOM complex of Neurospora crasssa. Mol Biol Cell **16:** 4172-4182.

SHIMIZU, S., Y. EGUCHI, W. KAMIIKE, Y. FUNAHASHI, A. MIGNON *et al.*, 1998 Bcl-2 prevents apoptotic mitochondrial dysfunction by regulating proton flux. Proc Natl Acad Sci U S A **95:** 1455-1459.

SIEDOW, J. N., A. L. UMBACH and A. L. MOORE, 1995 The active site of the cyanide-resistant oxidase from plant mitochondria contains a binuclear iron center. FEBS Lett **362:** 10-14.

SIEGER, S. M., B. K. KRISTENSEN, C. A. ROBSON, S. AMIRSADEGHI, E. W. ENG *et al.*, 2005 The role of alternative oxidase in modulating carbon use efficiency and growth during macronutrient stress in tobacco cells. J Exp Bot **56:** 1499-1515.

SIKORSKI, R. S., and P. HIETER, 1989 A system of shuttle vectors and yeast host strains designed for efficient manipulation of DNA in Saccharomyces cerevisiae. Genetics **122:** 19-27.

SIMONS, B. H., F. F. MILLENAAR, L. MULDER, L. C. VAN LOON and H. LAMBERS, 1999 Enhanced expression and activation of the alternative oxidase during infection of Arabidopsis with Pseudomonas syringae pv tomato. Plant Physiol **120:** 529-538.

SINGER, T. P., and R. R. RAMSAY, 1994 The reaction sites of rotenone and ubiquinone with mitochondrial NADH dehydrogenase. Biochim Biophys Acta **1187:** 198-202.

SIRRENBERG, C., M. F. BAUER, B. GUIARD, W. NEUPERT and M. BRUNNER, 1996 Import of carrier proteins into the mitochondrial inner membrane mediated by Tim22. Nature **384:** 582-585.

SLUSE, F. E., and W. JARMUSZKIEWICZ, 1998 Alternative oxidase in the branched mitochondrial respiratory network: an overview on structure, function, regulation, and role. Braz J Med Biol Res **31:** 733-747.

ST-PIERRE, J., S. DRORI, M. ULDRY, J. M. SILVAGGI, J. RHEE *et al.*, 2006 Suppression of reactive oxygen species and neurodegeneration by the PGC-1 transcriptional coactivators. Cell **127:** 397-408.

STABEN, C., B. JENSEN, M. SINGER, J. POLLOCK, M. SCHECHTMAN *et al.*, 1989 Use of a bacterial Hygromycin B resistance gene as a dominant selectable marker in Neurospora crassa transformation. Fungal Genetics Newsl. **36:** 79-81.

STENMARK, P., and P. NORDLUND, 2003 A prokaryotic alternative oxidase present in the bacterium Novosphingobium aromaticivorans. FEBS Lett **552:** 189-192.

STOJANOVSKI, D., M. RISSLER, N. PFANNER and C. MEISINGER, 2006 Mitochondrial morphology and protein import--a tight connection? Biochim Biophys Acta **1763:** 414-421.

STONE, G., and I. SADOWSKI, 1993 GAL4 is regulated by a glucose-responsive functional domain. Embo J **12:** 1375-1385.

STUART, R., 2002 Insertion of proteins into the inner membrane of mitochondria: the role of the Oxa1 complex. Biochim Biophys Acta **1592:** 79-87.

SUNDARESAN, M., Z. X. YU, V. J. FERRANS, D. J. SULCINER, J. S. GUTKIND *et al.*, 1996 Regulation of reactive-oxygen-species generation in fibroblasts by Rac1. Biochem J **318 (Pt 2):** 379-382.

SUSIN, S. A., H. K. LORENZO, N. ZAMZAMI, I. MARZO, B. E. SNOW *et al.*, 1999 Molecular characterization of mitochondrial apoptosis-inducing factor. Nature **397:** 441-446.

SZABADKAI, G., A. M. SIMONI, K. BIANCHI, D. DE STEFANI, S. LEO *et al.*, 2006 Mitochondrial dynamics and Ca2+ signaling. Biochim Biophys Acta **1763:** 442-449.

TANTON, L. L., C. E. NARGANG, K. E. KESSLER, Q. LI and F. E. NARGANG, 2003 Alternative oxidase expression in Neurospora crassa. Fungal Genet Biol **39:** 176-190.

TAYLOR, B. L., and I. B. ZHULIN, 1999 PAS domains: internal sensors of oxygen, redox potential, and light. Microbiol Mol Biol Rev **63:** 479-506.

TERZIYSKA, N., B. GRUMBT, M. BIEN, W. NEUPERT, J. M. HERRMANN *et al.*, 2007 The sulfhydryl oxidase Erv1 is a substrate of the Mia40-dependent protein translocation pathway. FEBS Lett **581:** 1098-1102.

THANNICKAL, V. J., R. M. DAY, S. G. KLINZ, M. C. BASTIEN, J. M. LARIOS *et al.*, 2000 Ras-dependent and -independent regulation of reactive oxygen species by mitogenic growth factors and TGF-beta1. Faseb J **14:** 1741-1748.

THANNICKAL, V. J., and B. L. FANBURG, 1995 Activation of an H2O2-generating NADH oxidase in human lung fibroblasts by transforming growth factor beta 1. J Biol Chem **270:** 30334-30338.

THANNICKAL, V. J., and B. L. FANBURG, 2000 Reactive oxygen species in cell signaling. Am J Physiol Lung Cell Mol Physiol **279:** L1005-1028.

THIRKETTLE-WATTS, D., T. C. MCCABE, R. CLIFTON, C. MOORE, P. M. FINNEGAN *et al.*, 2003 Analysis of the alternative oxidase promoters from soybean. Plant Physiol **133:** 1158-1169.

THORSNESS, P. E., and T. D. FOX, 1990 Escape of DNA from mitochondria to the nucleus in Saccharomyces cerevisiae. Nature **346:** 376-379.

TODD, R. B., and A. ANDRIANOPOULOS, 1997 Evolution of a fungal regulatory gene family: the Zn(II)2Cys6 binuclear cluster DNA binding motif. Fungal Genet Biol **21:** 388-405.

TOLBERT, N. E., 1981 Metabolic pathways in peroxisomes and glyoxysomes. Annu Rev Biochem **50:** 133-157.

TOVAR-MENDEZ, A., J. A. MIERNYK and D. D. RANDALL, 2003 Regulation of pyruvate dehydrogenase complex activity in plant cells. Eur J Biochem **270:** 1043-1049.

TOVAR, J., A. FISCHER and C. G. CLARK, 1999 The mitosome, a novel organelle related to mitochondria in the amitochondrial parasite Entamoeba histolytica. Mol Microbiol **32:** 1013-1021.

TOVAR, J., G. LEON-AVILA, L. B. SANCHEZ, R. SUTAK, J. TACHEZY *et al.*, 2003 Mitochondrial remnant organelles of Giardia function in iron-sulphur protein maturation. Nature **426:** 172-176.

TRAVEN, A., J. M. WONG, D. XU, M. SOPTA and C. J. INGLES, 2001 Interorganellar communication. Altered nuclear gene expression profiles in a yeast mitochondrial dna mutant. J Biol Chem **276:** 4020-4027.

TRIFUNOVIC, A., A. WREDENBERG, M. FALKENBERG, J. N. SPELBRINK, A. T. ROVIO *et al.*, 2004 Premature ageing in mice expressing defective mitochondrial DNA polymerase. Nature **429:** 417-423.

TRUSCOTT, K. N., K. BRANDNER and N. PFANNER, 2003 Mechanisms of protein import into mitochondria. Curr Biol **13:** R326-337.

TSUDA, A., W. H. WITOLA, S. KONNAI, K. OHASHI and M. ONUMA, 2006 The effect of TAO expression on PCD-like phenomenon development and drug resistance in Trypanosoma brucei. Parasitol Int **55:** 135-142.

TSUDA, A., W. H. WITOLA, K. OHASHI and M. ONUMA, 2005 Expression of alternative oxidase inhibits programmed cell death-like phenomenon in bloodstream form of Trypanosoma brucei rhodesiense. Parasitol Int **54:** 243-251.

TSUJIMOTO, Y., and S. SHIMIZU, 2007 Role of the mitochondrial membrane permeability transition in cell death. Apoptosis **12:** 835-840.

TUCKERMAN, J. R., G. GONZALEZ and M. A. GILLES-GONZALEZ, 2001 Complexation precedes phosphorylation for two-component regulatory system FixL/FixJ of Sinorhizobium meliloti. J Mol Biol **308:** 449-455.

TURPAEV, K. T., 2002 Reactive oxygen species and regulation of gene expression. Biochemistry (Mosc) **67:** 281-292.

TURPIN, D. H., F. C. BOTHA, R. G. SMITH, R. FEIL, A. K. HORSEY *et al.*, 1990 Regulation of Carbon Partitioning to Respiration during Dark Ammonium Assimilation by the Green Alga Selenastrum minutum. Plant Physiol **93:** 166-175.

UMBACH, A. L., M. A. GONZALEZ-MELER, C. R. SWEET and J. N. SIEDOW, 2002 Activation of the plant mitochondrial alternative oxidase: insights from site-directed mutagenesis. Biochim Biophys Acta **1554:** 118-128.

UMBACH, A. L., V. S. NG and J. N. SIEDOW, 2006 Regulation of plant alternative oxidase activity: a tale of two cysteines. Biochim Biophys Acta **1757:** 135-142.

UMBACH, A. L., and J. N. SIEDOW, 1993 Covalent and Noncovalent Dimers of the Cyanide-Resistant Alternative Oxidase Protein in Higher Plant Mitochondria and Their Relationship to Enzyme Activity. Plant Physiol **103:** 845-854.

UMBACH, A. L., and J. N. SIEDOW, 1996 The reaction of the soybean cotyledon mitochondrial cyanide-resistant oxidase with sulfhydryl reagents suggests that alpha-keto acid activation involves the formation of a thiohemiacetal. J Biol Chem **271:** 25019-25026.

UMBACH, A. L., and J. N. SIEDOW, 2000 The cyanide-resistant alternative oxidases from the fungi Pichia stipitis and Neurospora crassa are monomeric and lack regulatory features of the plant enzyme. Arch Biochem Biophys **378:** 234-245.

UMBACH, A. L., J. T. WISKICH and J. N. SIEDOW, 1994 Regulation of alternative oxidase kinetics by pyruvate and intermolecular disulfide bond redox status in soybean seedling mitochondria. FEBS Lett **348:** 181-184.

UNSELD, M., J. R. MARIENFELD, P. BRANDT and A. BRENNICKE, 1997 The mitochondrial genome of Arabidopsis thaliana contains 57 genes in 366,924 nucleotides. Nat Genet **15:** 57-61.

VALKO, M., C. J. RHODES, J. MONCOL, M. IZAKOVIC and M. MAZUR, 2006 Free radicals, metals and antioxidants in oxidative stress-induced cancer. Chem Biol Interact **160:** 1-40.

VALLE, I., A. ALVAREZ-BARRIENTOS, E. ARZA, S. LAMAS and M. MONSALVE, 2005 PGC-1alpha regulates the mitochondrial antioxidant defense system in vascular endothelial cells. Cardiovasc Res **66:** 562-573.

VAN BUUREN, K. J., P. F. ZUURENDONK, B. F. VAN GELDER and A. O. MUIJSERS, 1972 Biochemical and biophysical studies on cytochrome aa 3 . V. Binding of cyanide to cytochrome aa 3. Biochim Biophys Acta **256:** 243-257.

VAN DER LAAN, M., N. WIEDEMANN, D. U. MICK, B. GUIARD, P. REHLING *et al.*, 2006 A role for Tim21 in membrane-potential-dependent preprotein sorting in mitochondria. Curr Biol **16:** 2271-2276.

VAN HELLEMOND, J. J., F. R. OPPERDOES and A. G. TIELENS, 2005 The extraordinary mitochondrion and unusual citric acid cycle in Trypanosoma brucei. Biochem Soc Trans **33:** 967-971.

VANDERLEYDEN, J., C. PEETERS, H. VERACHTERT and H. BERTRAND, 1980 Stimulation of the alternative oxidase of Neurospora crassa by Nucleoside phosphates. Biochem J **188:** 141-144.

VANLERBERGHE, G. C., and L. MCINTOSH, 1992a Coordinate Regulation of Cytochrome and Alternative Pathway Respiration in Tobacco. Plant Physiol **100:** 1846-1851.

VANLERBERGHE, G. C., and L. MCINTOSH, 1992b Lower Growth Temperature Increases Alternative Pathway Capacity and Alternative Oxidase Protein in Tobacco. Plant Physiol **100:** 115-119.

VANLERBERGHE, G. C., and L. MCINTOSH, 1994 Mitochondrial electron transport regulation of nuclear gene expression. Studies with the alternative oxidase gene of tobacco. Plant Physiol **105:** 867-874.

VANLERBERGHE, G. C., and L. MCINTOSH, 1997 ALTERNATIVE OXIDASE: From Gene to Function. Annu Rev Plant Physiol Plant Mol Biol **48:** 703-734.

VANLERBERGHE, G. C., L. MCINTOSH and J. Y. YIP, 1998 Molecular localization of a redox-modulated process regulating plant mitochondrial electron transport. Plant Cell **10:** 1551-1560.

VANLERBERGHE, G. C., and L. MCLNTOSH, 1996 Signals Regulating the Expression of the Nuclear Gene Encoding Alternative Oxidase of Plant Mitochondria. Plant Physiol **111:** 589-595.

VANLERBERGHE, G. C., and S. H. ORDOG, 2002 Alternative Oxidase: integrating carbon metabolism and electron transport in plant respiration, pp. 173-191 in *Photosynthetic Nitrogen Assimilation and Associated Carbon and Respiratory Metabolism*, edited by C. H. FOYER and G. NOCTOR. Kluwer Academic, The Netherlands.

VANLERBERGHE, G. C., C. A. ROBSON and J. Y. YIP, 2002 Induction of mitochondrial alternative oxidase in response to a cell signal pathway down-regulating the cytochrome pathway prevents programmed cell death. Plant Physiol **129:** 1829-1842.

VANLERBERGHE, G. C., J. Y. YIP and H. L. PARSONS, 1999 In Organello and in Vivo Evidence of the Importance of the Regulatory Sulfhydryl/Disulfide System and Pyruvate for Alternative Oxidase Activity in Tobacco. Plant Physiol **121:** 793-803.

VASHEE, S., H. XU, S. A. JOHNSTON and T. KODADEK, 1993 How do "Zn2 cys6" proteins distinguish between similar upstream activation sites? Comparison of the DNA-binding specificity of the GAL4 protein in vitro and in vivo. J Biol Chem **268:** 24699-24706.

VEIGA, A., J. D. ARRABACA, F. SANSONETTY, P. LUDOVICO, M. CORTE-REAL *et al.*, 2003 Energy conversion coupled to cyanide-resistant respiration in the yeasts Pichia membranifaciens and Debaryomyces hansenii. FEMS Yeast Res **3:** 141-148.

VERHAGEN, A. M., and D. L. VAUX, 2002 Cell death regulation by the mammalian IAP antagonist Diablo/Smac. Apoptosis **7:** 163-166.

VERMULST, M., J. H. BIELAS, G. C. KUJOTH, W. C. LADIGES, P. S. RABINOVITCH *et al.*, 2007 Mitochondrial point mutations do not limit the natural lifespan of mice. Nat Genet **39:** 540-543.

VITALINI, M. W., R. M. DE PAULA, W. D. PARK and D. BELL-PEDERSEN, 2006 The rhythms of life: circadian output pathways in Neurospora. J Biol Rhythms **21:** 432-444.

VOGEL, F., C. BORNHOVD, W. NEUPERT and A. S. REICHERT, 2006 Dynamic subcompartmentalization of the mitochondrial inner membrane. J Cell Biol **175:** 237-247.

VON HEIJNE, G., 1986 Why mitochondria need a genome. FEBS Lett **198:** 1-4.

VON HEIJNE, G., 1989 Control of topology and mode of assembly of a polytopic membrane protein by positively charged residues. Nature **341:** 456-458.

WAGHRAY, M., Z. CUI, J. C. HOROWITZ, I. M. SUBRAMANIAN, F. J. MARTINEZ *et al.*, 2005 Hydrogen peroxide is a diffusible paracrine signal for the induction of epithelial cell death by activated myofibroblasts. Faseb J **19:** 854-856.

WAGNER, A. M., 1995 A role for active oxygen species as second messengers in the induction of alternative oxidase gene expression in Petunia hybrida cells. FEBS Lett **368:** 339-342.

WANG, D., F. ZHENG, S. HOLMBERG and G. B. KOHLHAW, 1999 Yeast transcriptional regulator Leu3p. Self-masking, specificity of masking, and evidence for regulation by the intracellular level of Leu3p. J Biol Chem **274:** 19017-19024.

WANG, G. Y., and J. D. KEASLING, 2002 Amplification of HMG-CoA reductase production enhances carotenoid accumulation in Neurospora crassa. Metab Eng **4:** 193-201.

WATLING, J. R., S. A. ROBINSON and R. S. SEYMOUR, 2006 Contribution of the alternative pathway to respiration during thermogenesis in flowers of the sacred lotus. Plant Physiol **140:** 1367-1373.

WESTERMANN, B., and H. PROKISCH, 2002 Mitochondrial dynamics in filamentous fungi. Fungal Genet Biol **36:** 91-97.

WIEDEMANN, N., A. E. FRAZIER and N. PFANNER, 2004 The protein import machinery of mitochondria. J Biol Chem **279:** 14473-14476.

WIEDEMANN, N., N. PFANNER and M. T. RYAN, 2001 The three modules of ADP/ATP carrier cooperate in receptor recruitment and translocation into mitochondria. Embo J **20:** 951-960.

WIEDEMANN, N., M. VAN DER LAAN, D. P. HUTU, P. REHLING and N. PFANNER, 2007 Sorting switch of mitochondrial presequence translocase involves coupling of motor module to respiratory chain. J Cell Biol **179:** 1115-1122.

WOOD, M. J., G. STORZ and N. TJANDRA, 2004 Structural basis for redox regulation of Yap1 transcription factor localization. Nature **430:** 917-921.

WOODRUFF, R. C., J. P. PHILLIPS and A. J. HILLIKER, 2004 Increased spontaneous DNA damage in Cu/Zn superoxide dismutase (SOD1) deficient Drosophila. Genome **47:** 1029-1035.

WU, G., and S. M. MORRIS, JR., 1998 Arginine metabolism: nitric oxide and beyond. Biochem J **336 (Pt 1):** 1-17.

WU, W. S., 2006 The signaling mechanism of ROS in tumor progression. Cancer Metastasis Rev **25:** 695-705.

WU, Z., P. PUIGSERVER, U. ANDERSSON, C. ZHANG, G. ADELMANT *et al.*, 1999 Mechanisms controlling mitochondrial biogenesis and respiration through the thermogenic coactivator PGC-1. Cell **98:** 115-124.

XU, G., and Y. SHI, 2007 Apoptosis signaling pathways and lymphocyte homeostasis. Cell Res **17:** 759-771.

YAFFE, M. P., 1999 Dynamic mitochondria. Nat Cell Biol **1:** E149-150.

YAMAMOTO, H., M. ESAKI, T. KANAMORI, Y. TAMURA, S. NISHIKAWA *et al.*, 2002 Tim50 is a subunit of the TIM23 complex that links protein translocation across the outer and inner mitochondrial membranes. Cell **111:** 519-528.

YANG, D., Y. OYAIZU, H. OYAIZU, G. J. OLSEN and C. R. WOESE, 1985 Mitochondrial origins. Proc Natl Acad Sci U S A **82:** 4443-4447.

YARUNIN, A., V. G. PANSE, E. PETFALSKI, C. DEZ, D. TOLLERVEY *et al.*, 2005 Functional link between ribosome formation and biogenesis of iron-sulfur proteins. Embo J **24:** 580-588.

YILDIZ, O., M. DOI, I. YUJNOVSKY, L. CARDONE, A. BERNDT *et al.*, 2005 Crystal structure and interactions of the PAS repeat region of the Drosophila clock protein PERIOD. Mol Cell **17:** 69-82.

YIP, J. Y., and G. C. VANLERBERGHE, 2001 Mitochondrial alternative oxidase acts to dampen the generation of active oxygen species during a period of rapid respiration induced to support a high rate of nutrient uptake. Physiol Plant **112:** 327-333.

YOON, T., and J. A. COWAN, 2003 Iron-sulfur cluster biosynthesis. Characterization of frataxin as an iron donor for assembly of [2Fe-2S] clusters in ISU-type proteins. J Am Chem Soc **125:** 6078-6084.

YUKIOKA, H., S. INAGAKI, R. TANAKA, K. KATOH, N. MIKI *et al.*, 1998 Transcriptional activation of the alternative oxidase gene of the fungus Magnaporthe grisea by a respiratory-inhibiting fungicide and hydrogen peroxide. Biochim Biophys Acta **1442:** 161-169.

YUVANIYAMA, P., J. N. AGAR, V. L. CASH, M. K. JOHNSON and D. R. DEAN, 2000 NifS-directed assembly of a transient [2Fe-2S] cluster within the NifU protein. Proc Natl Acad Sci U S A **97:** 599-604.

ZHANG, L., and L. GUARENTE, 1994 The yeast activator HAP1--a GAL4 family member--binds DNA in a directly repeated orientation. Genes Dev **8:** 2110-2119.

ZHANG, Z., L. HUANG, V. M. SHULMEISTER, Y. I. CHI, K. K. KIM *et al.*, 1998 Electron transfer by domain movement in cytochrome bc1. Nature **392:** 677-684.

ZHAO, G., and X. WANG, 2006 Advance in antitumor agents targeting glutathione-S-transferase. Curr Med Chem **13:** 1461-1471.

ZHENG, L., V. L. CASH, D. H. FLINT and D. R. DEAN, 1998 Assembly of iron-sulfur clusters. Identification of an iscSUA-hscBA-fdx gene cluster from Azotobacter vinelandii. J Biol Chem **273:** 13264-13272.

ZHOU, K. M., and G. B. KOHLHAW, 1990 Transcriptional activator LEU3 of yeast. Mapping of the transcriptional activation function and significance of activation domain tryptophans. J Biol Chem **265:** 17409-17412.